BOREAL SHIELD PEATLAND CO_2 EXCHANGE: A MULTI-YEAR ANALYSIS AND POST-WILDFIRE RECOVERY ASSESSMENT

BOREAL SHIELD PEATLAND CO_2 EXCHANGE: A MULTI-YEAR ANALYSIS AND POST-WILDFIRE RECOVERY ASSESSMENT

By RENÉE M. MCDONALD, B. Sc.

A Thesis Submitted to the School of Graduate Studies in Partial Fulfillment of the Requirements

for the Degree of Master of Science

McMaster University

MASTER OF SCIENCE (2021)

McMaster University

School of Earth, Environment & Society

Hamilton, Ontario, Canada

TITLE: Boreal shield peatland CO_2 exchange: A multi-year analysis and post-wildfire recovery assessment

AUTHOR: Renée McDonald, B.Sc. (St. Francis Xavier University)

SUPERVISOR: Dr. James M. Waddington

NUMBER OF PAGES: xvii + 117

Abstract

Peatland ecosystems are important as natural climate regulators for their capacity to store carbon over long-time scales. Carbon cycling in peatlands in the boreal ecozone of Canada has been more widely studied than the boreal shield of Ontario, where peat depths are thinner and peatlands spatially smaller. The reliance on fill and spill hydrologic connectivity makes the water table dynamics of peatlands in Ontario's Eastern Georgian Bay (EGB) region of the Ontario shield ecozone sensitive to rain and drought periods. The drying of wetlands in the EGB region decreases moss productivity and increases the ecosystem's vulnerability to wildfire through an increase in the water table depth. In an effort to understand how peatlands respond to interannual climate variability and wildfire, we examined the role of regional climate patterns on growing season CO_2 exchange from an Ontario shield peatland and completed a post-wildfire assessment of CO_2 exchange patterns in a recently burned peatland for the first and second year post-wildfire. Using the eddy covariance technique, we analyzed 5-years of growing season CO_2 exchange data from 2016 to 2020 from an unburned peatland and 2-years of growing season CO_2 exchange data from a burned peatland (2019-2020) in EGB. Plot-scale CO_2 exchange measurements were also completed within the burned peatland jointly with abiotic variables and vegetation community surveys. Water table depth was identified as an important variable to explain total summer CO_2 uptake (GPP) and net ecosystem exchange (NEE), where years of considerable rainfall maintained a water table near the peat surface and perpetuated high vegetation productivity. Summer total ecosystem respiration (ER) was greatly influenced by preceding winter and spring air temperature, with warmer winter air temperatures leading to summers of increased total ER. Warmer winter air temperatures also initiated water flow across the landscape, thus reviving plant and microbial activity following snow cover. These findings have important implications for the function of these

shallow Ontario shield peatlands in a warming climate, where decreased water availability with projected increased temperatures and evapotranspiration leaves peatlands at risk of a net loss of C over the summer with lower water table.

In the burned landscape, there was lower GPP in the summer (2019) compared to the wet summer of 2020, however the burned landscape continued to act as a net CO_2 sink for the summer season of both years. The rapid recovery of vegetation across the wildfire-disturbed landscape has important implications for the function of these peatlands over time, with the ability for continued carbon uptake and reinstating peat accumulation processes.

Acknowledgements

First I'd like to thank my supervisor, Dr. Mike Waddington, for the opportunity to join the McMaster Ecohydrology Lab. Thank you for your positivity, always supporting my ideas, and for your leadership throughout the uncertainty of the pandemic. I am appreciative of your flexibility and ongoing support, always highlighting the need for a work life balance, and the chance to grow and become a better scientist.

Thanks to all of our lab's postdocs for their ongoing help throughout the stages of my thesis. To Paul, thanks for the introduction to Matlab, for your upkeep of the EC stations, and all of the technical help along with Manu. Thanks to Colin, Chantel, and Sophie for your feedback throughout the design, fieldwork, and analysis of my thesis.

Dr. Dave Risk gave me my first opportunity to delve into the world of research straight out of the first year of my undergrad, and believed in me through and through. I will be forever grateful for the incredible opportunities I had the privilege of partaking in over my three years in the Flux Lab at St.FX, sparking my curiosity and love for research, including many days elbow deep in peat in northern Norway, driving around Saskatchewan and the Cape Breton Highlands, and growing an array of technical skills. Thank you Dave for your leadership, support, and encouragement to pursue a master's degree.

To all of my ecohydrology lab mates, thank you for the warm welcome the first summer I joined the lab, for making me feel so welcome, and for all of the fun trips to Killbear, Island Queen, Trestle, and Country Gourmet. Thanks to Maddy, Emma, and Hope for standing in peatlands with me for days last summer to collect as many gas samples as we could. To Danielle, Greg, and Taylor - thank you for being the best officemates and friends one could ask for, for our incredibly fun,

relaxing, and tropical "work trip" of winter 2019, and for always being ready with a smile and a laugh.

Thanks to my friends, near and far, for always filling my heart and finding ways to connect, including countless long zoom calls, over the past few years. To Nicole and Jasmine, our neighbourhood walks at home are my favourite to catch up right where we left off and I have loved spending the first summer in the same place as you both again for the first time in 6 years! To Fiona and Brandon, I will always look forward to our 6-month (+) reunions and loved adventuring around Quebec City, Toronto, and Frontenac with you both. Thanks to the McMaster Rowing team and my pals, the Mighty Lighties, for so kindly welcoming me onto your team and into your boat for the 2019 season. It was a pleasure to row alongside such talented, smart, kind, strong, and incredible people, and I would love to rip down the course one more time with you!

To my family, for their endless support and love throughout my degree, the pandemic, and in life. I may not have been close to home, but I am always thankful for your encouragement to live life, try new things, and meet new people. Thanks Allison and Nick for keeping my spirits high and belly full with our weekly virtual baking nights this year.

Last, but certainly not least, to Joe - thank you for your constant support, laughter, and sense of adventure. Thanks for always being keen for my (sometimes ridiculous) spontaneous plans, especially our pre-covid trip to Toronto for brunch and I look forward to many more Fritter Fridays. I am so thankful for all of our Ontario adventures, and look forward to exploring many more beautiful places together. Every day is a joy to spend with you.

Table of Contents

List of Figures

Figure 2.6: (A) Cumulative summer (JJA) net ecosystem exchange (NEE) (g C m^{-2}), (B) gross primary production (GPP), and (C) ecosystem respiration (ER) for 2016 to 2020. Colours indicate year as follows: 2016 – *red*, 2017 – *blue*, 2018 – *orange*, 2019 – *purple*, 2020 – *green.*

Figure 2.7: Cumulative flux (g C m^{-2}) of (A) net ecosystem exchange (NEE), (B) gross primary productivity (GPP), and (C) ecosystem respiration (ER) for the summer period (months: JJA) as a function of mean water table depth (m) for the time period. Regression line fit using ordinary least squares linear model. Colours indicate year as follows: 2016 – *red*, 2017 – *blue*, 2018 – *orange*, 2019 – *purple*, 2020 – *green.*

Figure 2.8: Light response relationship between half-hourly NEE (µmol m^{-2} s^{-1}) and PPFD (µmol m^{-2} s^{-1}) using Frolking et al. (1998) equation for summer (JJA). Colours indicate year as follows: 2016 – red, 2017 – blue, 2018 – orange, 2019 – purple, 2020 – green.

Figure 3.1: (A, B) Mean growing season daily air temperature (^{o}C), (C, D) mean growing season daily water table depth (m), (E, F) daily rainfall (mm), (g, h) daily NEE (g C m^{-2} d^{-1}), and (I, J) daily diurnal cycle of photosynthetic photon flux density (PPFD, µmol m^{-2} s^{-1}) for a typical week of the growing season (July 1-7). Left column shows unburned site, right column shows burned site. Years are represented by colours: 2019 - *purple*, 2020 – *green*.

Figure 3.2: Vegetation community composition from general vegetation surveys and flux plots, indicating the proportional cover of bare peat (light blue), litter (dark blue), moss and lichen (light green), and vascular species (dark green). Surveys were completed in July and August 2020.

Figure 3.3: Daily net ecosystem exchange (NEE), gross primary production (GPP), and ecosystem respiration (ER) in 2019 (purple) and 2020 (green) sites, for the unburned (light grey) and burned

sites (black). Data included is from summed half hourly fluxes for May 1 to October 31 of each year (Data starts July 2019 for the burned site).

Figure 3.4: Cumulative CO_2 flux (g C m^{-2}) from July 2019 to October 2020 for the burned site using daily flux data. Line type shows CO_2 flux type: *solid* - NEE, *dotted* - GPP, *dashed* - ER.

Figure 3.5: Ecosystem-scale light response relationship between half-hourly summer (months: JJA) net ecosystem exchange (NEE, µmol m^{-2} s^{-1}) and photosynthetic photon flux density (PPFD, µmol m^{-2} s^{-1}) for each site (left – unburned, right – burned) and year (*purple* - 2019, *green* - 2020).

Figure 3.6: Plot-scale mean CO_2 flux (g C m^{-2} d^{-1}) by peat depth category: shallow peat within the peatland margins and deep peat in the middle of the unburned and burned peatland. Colours representing sites: *blue* – unburned, *red* – burned. Error bars showing ± standard error.

Figure 3.7: Plot-scale light response relationship from chamber-based flux measurements, showing the relationship between net ecosystem exchange (NEE, µmol m^{-2} s^{-1}) and photosynthetic photon flux density (PPFD, µmol m^{-2} s^{-1}) for the (left, blue) unburned and (right, red) burned sites in August and September 2020.

Figure 3.8: Plot-scale relationship between ecosystem respiration (ER, g C m^{-2} d^{-1}) and peat temperature (^{o}C), from chamber-based flux measurements in August and September 2020. Colours represent sites (unburned, *blue*; burned, *red).*

List of Tables

List of Abbreviations and Symbols

$\propto$	Initial slope of light response relationship
AIC	Akaike's information criterion
ANOVA	Analysis of variance
^{o}C	Degrees Celsius
C	Carbon
CH_4	Methane
CO_2	Carbon Dioxide
CUP	Carbon uptake period
DIC	Dissolved inorganic carbon
DOC	Dissolved organic carbon
DOY	Day of year
EC	Eddy covariance
EGB	Eastern Georgian Bay
ER	Ecosystem respiration
ET	Evapotranspiration
GLMM	Generalized linear mixed effects model
GPP	Gross primary production
GPP_{max}	Maximum gross primary production
GS	Growing season
Hz	Hertz
JJA	Months of June, July, August
LAI	Leaf area index

LE	Latent heat
N	Nitrogen
NEE	Net ecosystem exchange
nls	Nonlinear least-squares regression
P	Phosphorus
PAR	Photosynthetically active radiation
POC	Particulate organic carbon
PPFD	Photosynthetic photon flux density
Precip	Precipitation
PS33	Parry Sound 33 wildfire
PVC	Polyvinyl chloride
R_g	Incoming solar radiation
Spp.	Species
T_{air}	Air temperature
VIF	Variance inflation factorr
VPD	Vapour pressure deficit
VWC	Volumetric water content
WT	Water table
WTD	Water table depth

Declaration of Academic Achievement

This thesis has been prepared in the "sandwich thesis" format, with written material prepared solely by this author. Chapters one and four provide a general introduction and conclusion, respectively. Chapters two and three are independent manuscripts. Dr. Paul Moore was instrumental in the installation and management of the eddy covariance towers, and eddy covariance data processing. Dr. Chantel Markle and Dr. Sophie Wilkinson were instrumental in the application of generalized linear mixed models. Dr. Mike Waddington was instrumental in directing research design, and additional input on research design from Dr. Manuel Helbig and Dr. Paul Moore was received. Emma Sherwood, Hope Freeman, and Madeleine Hayes were assistants with installation of field equipment, greenhouse gas sample collection, and vegetation surveys.

Chapter 1 - General Introduction

1.1 Northern peatlands

Northern peatlands are important ecosystems for long term carbon storage (Blodau et al., 2004; Clymo, 1987) storing an estimated 545 Pg of carbon (C) (Nichols and Peteet, 2019) globally, while covering only 2.8% of the global land area (Xu et al., 2018). The accumulation of large peat deposits in the northern hemisphere has occurred throughout the Holocene (Yu et al., 2010), where peat formation is facilitated by cool and permanently saturated peat allowing plant productivity to exceed ecosystem respiration and combustion (Clymo, 1987). This peat accumulation ecosystem function and peatland resilience to climate change and climate-mediated disturbances (*e.g.* drought, wildfire) are facilitated by a suite of hydrological, biogeochemical, and ecological processes and feedbacks (Clymo, 1987; Gorham, 1991; Waddington et al., 2015).

The vertical structure of peatlands is largely controlled by water table position, separating the aerobic acrotelm zone from the anoxic, fully saturated catotelm layer (Clymo, 1984; Gorham, 1991; Hilbert et al., 2000). Water table position is therefore a first order control on differential rates of decomposition, where saturation decreases decomposition (Benscoter, Vitt, et al., 2005; Clymo, 1984). On the surface of peatlands, vegetation community composition and their varying decay rates, acrotelm thickness, and in turn water table depth control the formation of microtopography (Belyea & Clymo, 2001; Belyea, 1996). Differences in the decomposability of *Sphagnum* species leads to an undulating formation of hummocks and hollows, where easily decomposable *Sphagnum* species results in greater decay rates creating low-lying hollows, and other *Sphagnum* species with lower decomposability creating elevated hummocks (Belyea, 1996).

This microtopography is responsive to changes in surface moisture content, where precipitation and changes in water storage often shifts the relative size of hummocks and hollows, adding to the self-regulatory feedbacks between carbon cycling and hydrology in peatlands (Waddington et al., 2015).

1.2 Peatland carbon cycling

In peatland ecosystems, the primary carbon storage reservoirs are in peat and vegetation (Gorham, 1991). As mentioned earlier, peatlands tend to be net sinks for atmospheric CO_2, through primary productivity of the moss and vascular plant community, which then locks in C into the peatland through the process of peat formation (Clymo, 1984). Fluxes of CO_2 from peatlands are a major component of the carbon cycle, and can be measured as net ecosystem exchange (NEE), which is the difference between gross primary productivity (GPP) from vegetation, and ecosystem respiration (ER) from autotrophic and heterotrophic respiration (Bubier et al., 2003; Lafleur et al., 2001; Moore et al., 1998; Ryan and Law, 2005). NEE is the largest component of the net ecosystem carbon balance and has been the focus of studies to characterize peatland C exchange (*e.g.* Limpens et al., 2008; Lindroth et al., 2009; Lund et al., 2010). Fluxes of CH_4 from peatlands tend to be several orders of magnitude smaller than NEE, therefore many studies focus on NEE to determine a net CO_2 source or sink status for peatlands (Koehler et al., 2011; Moore et al., 1998). Fluvial carbon fluxes (DOC, DIC, POC, CH_4) can also be important for a peatland carbon balance, and the exchange of fluvial C fluxes with the atmosphere and surrounding ecosystem is largely controlled by hydrology of the peatland (Waddington and Roulet, 1997). Net CO_2 flux from peatlands to the atmosphere is dictated by a suite of abiotic factors (i.e. temperature, moisture, photosynthetically active radiation) and biotic factors (i.e. moss and vascular vegetation cover)

(Frolking et al., 1998; Lloyd and Taylor, 1994; Orchard and Cook, 1983; Ryan and Law, 2005; Waddington et al., 2010) and will be discussed in detail below.

Daily fluxes, growing season budgets, and annual budgets of CO_2 for peatlands in the boreal region have been shown to range between sites and interannually (Lund et al., 2010; Roulet et al., 2007; Strachan et al., 2016; Sulman et al., 2010; Teklemariam et al., 2010). Climatic variables affect C cycling in peatlands from daily (Peichl et al., 2014) to decadal time scales (Chimner et al., 2017). Interannual variability in CO_2 exchange is reflected in the range of cumulative NEE measured over multiple years at sites, where Koehler et al. (2011) measured an annual net uptake range of 12.5 g CO_2 m^{-2} to 84 g CO_2 m^{-2} with the summer season having the greatest variation across years in an Atlantic blanket bog. Similarly, Roulet et al. (2007) estimated an annual NEE of – 2 g C m^{-2} to -112 g C m^{-2} at Mer Bleue peatland, and in the Hudson Bay lowlands, mean annual NEE was -52 g C m^{-2} and -80 g C m^{-2} for 5- years of monitoring at a fen and bog, respectively (Helbig et al., 2019). Daily CO_2 fluxes from boreal peatlands tend to show net uptake over the summer, and zero or net emission in the winter, with early spring and late fall fluxes fluctuating, and annual CO_2 balances depending on both winter and growing season meteorological conditions (Aurela et al., 2004; Peichl et al., 2014). Summer daily NEE is variable between sites and years. For example, Humphreys et al. (2006) measured a range in daily NEE across seven northern peatlands from -1.0 g C m^{-2} d^{-1} to -2.8 g C m^{-2} d^{-1} (net uptake), while Lund et al. (2010) measured mean daily NEE in July of -1.2 g C m^{-2} d^{-1}. Budgets of CO_2 have been shown to be significantly related to peatland water table depth, where a shallow water table allows for greater cumulative CO_2 uptake (Peichl et al., 2014; Strachan et al., 2016).

There are several key abiotic ecohydrological factors that have been identified as controlling peatland C cycling including air and peat temperature (Lafleur et al., 2005; Lloyd and Taylor, 1994), soil moisture (Waddington & Roulet, 2000, Bubier et al. 2003), water table depth (Sonnentag et al., 2010; Strachan et al., 2016; Teklemariam et al., 2010), and light availability (Frolking et al., 1998), as well as interactive effects between them. Ecosystem respiration is a function of autotrophic and heterotrophic respiration, and an exponential increase in ecosystem respiration with increasing temperatures has been characterized by Lloyd & Taylor (1994). Enhanced C sequestration under increased temperatures has also been observed (Järveoja et al., 2018), while conversely there may be increased respiration and decreased primary production from moisture limitations under warmer growing season conditions, contributing to decreased annual net CO_2 uptake (Helbig et al., 2019). As mentioned earlier, water table depth is a key driver of peatland C fluxes, as peatland structure is highly dependent on saturated conditions to limit decomposition rates, and the composition of peatland vegetation is connected to water table dynamics (Limpens et al., 2008). Connection to the water table is important for the productivity of *Sphagnum* species, where photosynthetic capacity is greater with higher water table, in turn affecting peat accumulation rates (Bubier et al., 2003; Rydin and McDonald, 1985). The response of peatland CO_2 exchange to the combination of warm and dry conditions has been widely documented and is highly variable, where changes in temperature and moisture have stimulated increased GPP (Roulet et al., 2007), decreased GPP (Aurela et al., 2007), increased ER (Cai et al., 2010; Lund et al., 2010; Riutta et al., 2007), increased GPP and ER (Flanagan and Syed, 2011), as well as differential responses between bogs and fens (Adkinson et al., 2011). As mentioned earlier, light availability controls ecosystem productivity and it often does so through a rectangular-hyperbola relationship, where plant productivity increases nonlinearly with increasing light levels

to a point of saturation (Frolking et al., 1998; Waddington and Roulet, 1996). This light response relationship varies seasonally and geographically (Frolking et al., 1998). Changes to light availability as a result of rainfall events may also be a contributing factor to creating decreased CO_2 sink strength of a peatland (Nijp et al., 2015). These abiotic ecohydrological controls influence CO_2 exchange collectively with vegetation composition and phenology being the key biotic controls in peatland C cycling.

A recent emphasis on the biological drivers of peatland CO_2 exchange has highlighted the role of vegetation community and phenology as controls on net ecosystem exchange, with abiotic factors acting secondarily (Armstrong et al., 2015; Järveoja et al., 2018; Koebsch et al., 2020; Peichl et al., 2018). The use of phenological indices have been identified as a key indicator of peatland CO_2 exchange, in both natural and wildfire-disturbed peatlands (Humphreys et al., 2006; Järveoja et al., 2018; Morison et al., 2021). The seasonality of plant development over the warm season closely resembles the seasonal trend of NEE, where CO_2 fluxes increase with air temperature trends and decrease following the onset of fall senescence (Järveoja et al., 2018). Plant functional traits are also an important component to consider in peatland ecosystems, where different plant functional types have differing biochemical and phenological traits contributing to the C cycle from photosynthetic capacity, C turnover in soils, and root exudates used for heterotrophic respiration (Ward et al., 2009). Moss-dominated areas may have lower ER and GPP than areas with high vascular vegetation cover (Armstrong et al., 2015; Humphreys et al., 2014; Riutta et al., 2007). *Sphagnum* moss communities photosynthesize at greater capacity when connected to the water table, within the top 30 cm of peat (Rydin and McDonald, 1985), indicating there is an inherent connection between biotic and abiotic ecohydrological controls on peatland

CO_2 exchange. The role of peatland vegetation and interactions with abiotic controls is important to delineate how climate change will affect the essential carbon storage function of peatlands in different geographic regions.

1.3 Peatland wildfires

Wildfire is considered a major natural or anthropogenic disturbance that affects carbon cycling in northern peatlands (Turetsky et al., 2002, 2015). Increased frequency of wildland fire, intensity, and extent of affected areas are expected with future climate change (Bergeron and Flannigan, 1995; Flannigan et al., 2005; Kasischke and Turetsky, 2006). Peatland wildfires typically burn through smouldering combustion (Rein, 2009), which pose several challenges for fire management, human and ecosystem health (Bowman and Johnston, 2005; Flannigan et al., 2013). With climate change and changes in wildfire frequency, there is concern peatlands may transition from net C sinks to net C sources in the near future (Bradshaw and Warkentin, 2015). Indeed wildfire in peatland ecosystems has the potential to release portions of the 'legacy' carbon stored in the peat to the atmosphere, converting peatlands from net C sinks to net C sources for a period of time following wildfire (Ingram et al., 2019; Turetsky et al., 2002, 2015; Wieder et al., 2009; Zoltai et al., 1998). Carbon is lost directly to the atmosphere through combustion of biomass during wildfire (Turetsky et al., 2002) and in the years following wildfire due to the loss of above ground biomass, changes in evapotranspiration, vegetation, and peat accumulation (Kettridge et al., 2019; Wieder et al., 2009; Zoltai et al., 1998).

Burn severity and carbon loss has been associated with peat depth and moss species composition across a peatland (Benscoter and Wieder, 2003; Hokanson et al., 2016; Wilkinson et

al., 2020). Ecohydrological characteristics of *Sphagnum* moss may create differential burn severity across a peatland, where hummock-forming species with greater water retention are less vulnerable to burning, and there is greater C loss from hollows (Benscoter and Wieder, 2003; Hayward and Clymo, 1982; Rydin and McDonald, 1985). Singed fragments of the pre-fire vegetation community help with recovery and regeneration of microtopography (Benscoter et al., 2005; Wieder et al., 2009). A higher water table following wildfire promotes *Sphagnum* colonization in low lying areas where surface conditions are saturated and sufficient light is available (Thompson et al., 2014), reestablishing the carbon sequestration from atmosphere to ecosystem (Gray et al., 2020; Morison et al., 2021). Peat depth has also been identified as a control on peat burn severity across peatlands, where shallower peat is more vulnerable to deeper, and more severe burning (Wilkinson et al., 2020), as is the case for shallow peatland margins versus the middle areas of peatlands with deeper peat (Hokanson et al., 2016).

Post-fire carbon cycling has also been connected to peat burn severity (Morison et al., 2021), water table position (Kettridge et al., 2015), changes in nutrient availability (van Beest et al., 2019), and vegetation recolonization (Gray et al., 2020). Burn severity and post-fire hydrological conditions influence post-fire successional trajectories (Benscoter and Vitt, 2008; Kettridge et al., 2015; Lukenbach et al., 2015). Burn severity is highly heterogeneous on small spatial scales, influencing differential rates in vegetation colonization and the restoration of photosynthetic processes (Grau-Andrés et al., 2017). Changes in the vegetation community composition are greatest in the first 10 years following wildfire (Benscoter and Vitt, 2008), contributing to the recovery of peat accumulation (Benscoter et al., 2005) and long term carbon sequestration capacity of peatland ecosystems (Wieder et al., 2009; Zoltai et al., 1998). Vegetation community

complexity increases continuously due to interspecific competition (Benscoter and Vitt, 2008) until complete vegetation cover is recovered within approximately 20 years post-fire (Wieder et al., 2009; Zoltai et al., 1998).

Post-wildfire CO_2 exchange

The post-wildfire trajectory of peatlands is critical to examine in order to predict the resiliency of peatland ecosystems to future climate change, which in turn brings about changes in the fire regime. Previous studies have evaluated the return of northern peatlands to C sinks following wildfire, however this has been estimated to occur more than 12 years following wildfire (Wieder et al., 2009). For a peatland to return to a C sink therefore relies on the re-establishment of moss species (Waddington et al., 2010; Waddington and Warner, 2001), which has been shown to be connected to burn severity and nutrient availability following wildfire (Morison et al., 2021; van Beest et al., 2019). Morison et al. (2021) found deeper burned areas to have rapid moss recolonization and greater mean GPP and ER than moderate and low severity areas, although NEE was comparable between the burned and unburned sites. Similarly, NEE between burned and unburned sites were attributed to vegetation recovery following wildfire in a temperate peatland (Gray et al., 2020). At the ecosystem-scale, a reduction in GPP and greater reduction to ER in a burned peatland still allowed for net carbon uptake, although of smaller magnitude than the unburned control site (Morison et al., 2020).

Effects of wildfire on peatland structure

The recovery of peatland microtopographic features following wildfire depends highly on burn severity (Benscoter et al., 2005; Benscoter and Wieder, 2003; Lukenbach et al., 2015). Burn severity may vary within a single peatland, owing to differences in pre-fire hydrogeological setting

(Lukenbach et al., 2015) and peat depth (Wilkinson et al., 2020). Differential burning of hummocks and hollows changes post-fire microtopographic development by promoting standing water in newly created hollows close to the water table, thereby favouring colonization of *Sphagnum* and other hollow species in the short term and more rapid peat accumulation in the long term (Benscoter et al., 2005; Benscoter and Vitt, 2008; Lukenbach et al., 2015). In cases where hummocks do not burn severely and remnant microtopographic features are present following wildfire, hummock species are often favoured to recolonize due to dry surface conditions (Benscoter and Vitt, 2008). Differences in the vegetation community composition between hollows, hummocks, and lawns will also likely create distinctly different peat properties and may affect CO_2 fluxes (Benscoter et al., 2005; Thompson et al., 2014; Waddington et al., 2015).

1.4 Boreal shield landscape

The ecohydrological characteristics of peatlands in the Ontario shield region differ greatly from the boreal plains where many of the aforementioned depressions in the granitic bedrock facilitate the development of moss cushions and lichen mats on bedrock outcrops (Hudson et al., 2021), moss dominated ephemeral wetlands, and *Sphagnum*-dominated peatlands (Devito et al., 1989), interspersed with upland forest areas (Catling and Brownell, 1999). Peat depressions across the Ontario shield region vary in size, due to the controls on hydrologic conditions imposed by underlying bedrock (Didemus, 2016; Moore et al., 2021; Vu, 2019), facilitating differential peat accumulation rates and heterogeneous land-atmosphere exchange patterns throughout peatlands in the region (Catling and Brownell, 1999; Devito et al., 1989; Didemus, 2016; Waddington and Roulet, 2000). These boreal shield ecosystems are highly sensitive to water availability due to hydrologic connectivity between landscape units primarily through fill and spill dynamics (Spence

and Woo, 2003), relying on precipitation events to maintain water table levels. Moreover, given the boreal shield has less groundwater storage and groundwater flow than the boreal plains, the impact of wildfire burn severity is likely greater in the boreal shield. However, Wilkinson et al. (2020) estimated average C loss from an Ontario shield wildfire to be 1.61 kg C m^{-2}, similar to other boreal plains wildfires (Benscoter and Wieder, 2003; Hokanson et al., 2016), and up to 98% of the peat profile burned in shallow peatlands (< 66 cm), suggesting peatlands of the Ontario shield may have similar post-wildfire recovery trajectories. There is limited further research surrounding boreal shield wildfire, and post-wildfire recovery in the rock barrens, which is where this study aims to fill the knowledge gap.

1.5 Thesis objectives

The objectives of this thesis are to (i) quantify growing season CO_2 exchange in a peatland in the Canadian Shield rock barrens landscape, (ii) identify key controlling variables on the interannual variability of summer CO_2 fluxes, (iii) investigate ecosystem recovery of CO_2 exchange processes post-wildfire, and (iv) identify key ecohydrological controls on plot-scale CO_2 exchange in an unburned and burned landscape. To address the first two objectives, we use 5-years of growing season CO_2 exchange measurements using the eddy covariance technique from an undisturbed peatland in the Canadian Shield rock barrens region. Statistical analyses were used to identify key environmental variables contributing to interannual variability in total summer CO_2 exchange budgets (cumulative fluxes). To address the third and fourth objectives, we use ecosystem-scale CO_2 measurements from a recently burned area of the rock barrens landscape for the growing season 1- and 2- years post-wildfire, and plot-scale measurements from the 2nd year

post-wildfire which were then used to determine the measured ecohydrological variables that may exhibit the greatest control on plot-scale NEE, GPP, and ER in a burned and unburned peatland using statistical analyses.

There has been an increasing number of long-term datasets quantifying peatland CO_2 exchange, and this research extends the existing geographical range by providing a new long-term dataset for a peatland in the Canadian boreal shield region. We have captured the important first few years following a major wildfire disturbance in the Canadian boreal shield region, from which we can estimate the trajectory of ecosystem recovery.

1.6 Literature cited

Adkinson, A. C., Syed, K. H., & Flanagan, L. B. (2011). Contrasting responses of growing season ecosystem CO_2 exchange to variation in temperature and water table depth in two peatlands in northern Alberta. Canada, J. Geophys. Res., 116, G01004. https://doi.org/10.1029/2010JG001512.

Armstrong, A., Waldron, S., Ostle, N. J., Richardson, H., & Whitaker, J. (2015). Biotic and Abiotic Factors Interact to Regulate Northern Peatland Carbon Cycling. *Ecosystems,* 18, 1395-1409. https://doi.org/10.1007/s10021-015-9907-4.

Aurela, M., Laurila, T., & Tuovinen, J. (2004). The timing of snow melt controls the annual Co2 balance in a subarctic fen. *Geophysical Research Letters,* 31, L16119, 1-4. https://doi.org/10.1029/2004GL020315.

Aurela, M., Riutta, T., Laurila, T., Tuovinen, J., Vesala, T., Tuittila, E., Rinne, J., Haapanala, S., & Laine, J. (2007). CO_2 exchange of a sedge fen in southern Finland-the impact of a drought period. *Tellus B: Chemical and Physical Meteorology*, 59:5, 826-837. https://doi.org/10.1111/j.1600-0889.2007.00309.x.

Belyea, L. (1996). Separating the Effects of Litter Quality and Microenvironment on Decomposition Rates in a Patterned Peatland. *Oikos*, 77:3, 529-539.

Belyea, L., & Clymo, R. S. (2001). Feedback Control of the Rate of Peat Formation. *Proceedings: Biological Sciences*, 268:1473, 1315-1321. https://doi.org/10.1098/rspb.2001.1665.

Benscoter, B. W., Vitt, D. H., & Wieder, R. K. (2005). Association of postfire peat accumulation and microtopography in boreal bogs. *Canadian Journal of Forest Research*, 35, 2188-2193. https://doi.org/10.1139/x05-115.

Benscoter, B. W., & Wieder, R. K. (2003). Variability in organic matter lost by combustion in a boreal bog during the 2001 Chisholm fire. *Canadian Journal of Forest Research,* 33, 2509-2513. https://doi.org/10.1139/x03-162.

Benscoter, B. W., & Vitt, D. H. (2008). Spatial Patterns and Temporal Trajectories of the Bog Ground Layer Along a Post-Fire Chronosequence. *Ecosystems*, 11, 1054-1064. https://doi.org/10.1007/s10021-008-9178-4.

Bergeron, Y., & Flannigan, M. D. (1995). Predicting the effects of climate change on fire frequency in the southeastern Canadian boreal forest. *Water, Air, & Soil Pollution,* 82, 437-444. https://doi.org/10.1007/BF01182853.

Blodau, C., Basiliko, N., & Moore, T. R. (2004). Carbon turnover in peatland mesocosms exposed to different water table levels. *Biogeochemistry,* 67, 331-351. https://doi.org/10.1023/B:BIOG.0000015788.30164.e2.

Bowman, D. M. J. S., & Johnston, F. H. (2005). Wildfire Smoke, Fire Management, and Human Health. *EcoHealth*, 2, 76-80. https://doi.org/10.1007/s10393-004-0149-8.

Bradshaw, C. J. A., & Warkentin, I. G. (2015). Global estimates of boreal forest carbon stocks and flux. *Global and Planetary Change,* 128, 24-30. https://doi.org/10.1016/j.gloplacha.2015.02.004.

Bubier, J. L., Crill, P. M., Moore, T. R., Savage, K., & Varner, R. K. (1998). Seasonal patterns and controls on net ecosystem CO_2 exchange in a boreal peatland complex. *Global Biogeochem. Cycles*, 12(4), 703-714. https://doi.org/10.1029/98GB02426.

Bubier, J. L., Bhatia, G., Moore, T. R., Roulet, N. T., & Lafleur, P. M. (2003). Spatial and Temporal Variability in Growing-Season Net Ecosystem Carbon Dioxide Exchange at a Large Peatland in Ontario, Canada. *Ecosystems*, 6, 353-367. https://doi.org/10.1007/s10021-003-0125-0.

Cai, T., Flanagan, L. B., & Syed, K. H. (2010). Warmer and drier conditions stimulate respiration more than photosynthesis in a boreal peatland ecosystem: Analysis of automatic chambers and eddy covariance measurements. *Plant, Cell and Environment*, 33, 394-407. https://doi.org/10.1111/j.1365-3040.2009.02089.x.

Catling, P. M., & Brownell, V. R. (1999). The Flora and Ecology of Southern Ontario Granite Barrens. In R. C. Anderson, J. S. Fralish, & J. M. Baskin (Eds.) *Savannas, Barrens, and Rock Outcrop Plant Communities of North America* (pp. 392-405). Cambridge University Press.

Chimner, R. A., Pypker, T. G., Hribljan, J. A., Moore, P. A., & Waddington, J. M. (2017). Multi-decadal Changes in Water Table Levels Alter Peatland Carbon Cycling. *Ecosystems*, 20(5), 1042-1057. https://doi.org/10.1007/s10021-016-0092-x.

Clymo, R. S. (1984). The Limits to Peat Bog Growth. *Philosophical Transactions of the Royal Society B: Biological Sciences,* 303 (1117), 605-654. https://doi.org/10.1098/rstb.1984.0002.

Clymo, R. S. (1987). The ecology of peatlands. *Science Progress (1933-)*, 71, 593-614.

Devito, K. J., Dillon, P. J., & Lazerte, B. D. (1989). Phosphorus and nitrogen retention in five Precambrian shield wetlands. *Biogeochemistry*, 8, 185-204. https://doi.org/10.1007/BF00002888.

Didemus, B. (2016). Water storage dynamics in peat-filled depressions of Canadian shield rock barrens: implications for primary peat formation [Unpublished MSc thesis]. McMaster University.

Flanagan, L. B., & Syed, K. H. (2011). Stimulation of both photosynthesis and respiration in response to warmer and drier conditions in a boreal peatland ecosystem. *Global Change Biology,* 17, 2271-2287. https://doi.org/10.1111/j.1365-2486.2010.02378.x.

Flannigan, M. D., Logan, K. A., Amiro, B. D., Skinner, W. R., & Stocks, B. J. (2005). Future area burned in Canada. *Climate Change,* 72, 1-16. https://doi.org/10.1007/s10584-005-5935-y.

Flannigan, M., Cantin, A. S., de Groot, W. J., Wotton, M., Newbury, A., & Gowman, L. M. (2013). Global wildland fire season severity in the 21st century. *Forest Ecology and Management,* 294, 54-61. https://doi.org/10.1016/j.foreco.2012.10.022.

Frolking, S. E., Bubier, J. L., Moore, T. R., Ball, T., Bellisario, L. M., Bhardwaj, A., Carroll, P., Crill, P. M., Lafleur, P. M., McCaughey, J. H., Roulet, N. T., Suyker, A. E., Verma, S. B., Waddington, J. M., & Whiting, G. J. (1998). Relationship between ecosystem productivity and photosynthetically active radiation for northern peatlands. *Global Biogeochem. Cycles,* 12(1), 115-126. https://doi.org/10.1029/97GB03367.

Grau-Andrés, R., Gray, A., & Davies, G. M. (2017). Sphagnum abundance and photosynthetic capacity show rapid short-term recovery following managed burning. *Plant Ecology & Diversity*, 10(4), 353-359. https://doi.org/10.1080/17550874.2017.1394394.

Gray, A., Davies, G. M., Domènech, R., Taylor, E., & Levy, P. E. (2021). Peatland Wildfire Severity & Post-fire Gaseous Carbon Fluxes. *Ecosystems,* 24, 713-725. https://doi.org/10.1007/s10021-020-00545-0.

Gorham, E. (1991). Northern Peatlands: Role in the Carbon Cycle and Probably Response to Climatic Warming. *Ecological Applications,* 1(2), 182-195.

Hayward, P., & Clymo, R. (1982). Profiles of water content and pore size in *Sphagnum* and peat, and their relation to peat bog ecology. *Proceedings of the Royal Society of London – Biological Sciences,* 215, 299-325. https://doi.org/10.1098/rspb.1982.0044.

Helbig, M., Humphreys, E. R., & Todd, A. (2019). Contrasting Temperature Sensitivities of CO_2 Exchange in Peatlands of the Hudson Bay Lowlands, Canada. *JGR: Biogeosciences,* 124, 2126-2143. https://doi.org/10.1029/2019JG005090.

Hilbert, D. W., Roulet, N., & Moore, T. (2000). Modelling and analysis of peatlands as dynamical systems. *Journal of Ecology,* 88, 230-242. https://doi.org/10.1046/j.1365-2745.2000.00438.x.

Hokanson, K. J., Lukenbach, M. C., Devito, K. J., Kettridge, N., Petrone, R. M., & Waddington, J. M. (2016). Groundwater connectivity controls peat burn severity in the boreal plains. *Ecohydrology*, 9, 574-584. https://doi.org/10.1002/eco.1657.

Hudson, D. T., Markle, C. E., Harris, L. I., Moore, P. A., & Waddington, J. M. (2021). Ecohydrological controls on lichen and moss CO_2 exchange in rock barrens turtle nesting habitat. *Ecohydrology*, 14, 1-11, https://doi.org/10.1002/eco.2255.

Humphreys, E. R., Lafleur, P. M., Flanagan, L. B., Hedstrom, N., Syed, K. H., Glenn, A. J., & Granger, R. (2006). Summer carbon dioxide and water vapour fluxes across a range of northern peatlands. *Journal of Geophysical Research,* 111, G04011. https://doi.org/10.1029/2005JG000111.

Humphreys, E. R., Charron, C., Brown, M. & Jones, R. (2014). Two Bogs in the Canadian Hudson Bay Lowlands and a Temperate Bog Reveal Similar Annual Net Ecosystem Exchange of CO_2. *Arctic, Antarctic, and Alpine Research*, 46:1, 103-113. https://doi.org/10.1657/1938-4246.46.1.103.

Ingram, R. C., Moore, P. A., Wilkinson, S., Petrone, R. M., & Waddington, J. M. (2019). Postfire soil carbon accumulation does not recover boreal peatland combustion loss in some hydrogeological settings. *Journal of Geophysical Research: Biogeosciences*, 124, 775–788. https://doi.org/10.1029/ 2018JG004716.

Järveoja, J., Nilsson, M. B., Gažovič, M., Crill, P. M., & Peichl, M. (2018). Partitioning of net CO_2 exchange using an automated chamber system reveals plant phenology as key control of production and respiration fluxes in a boreal peatland. *Global Change Biology*, 24, 3436-3451. https://doi.org/10.1111/gcb.14292.

Kasischke, E. S., & Turetsky, M. R. (2006). Recent changes in the fire regime across the North American boreal region – Spatial and temporal patterns of burning across Canada and Alaska. *Geophysical Research Letters,* 33, L09703. https://doi.org/10.1029/2006GL025677.

Kettridge, N., Lukenbach, M. C., Hokanson, K. J., Devito, K. J., Petron, R. M., Mendoza, C. A., & Waddington, J. M. (2019). Severe wildfire exposes remnant peat carbon stocks to increased post-fire drying. *Scientific Reports,* 9, 5-10. https://doi.org/10.1038/s41598-019-40033-7.

Kettridge, N., Turetsky, M. R., Sherwood, J. H., Thompson, D. K., Miller, C. A., Benscoter, B. W., Flannigan, M. D., Wotton, B. M., & Waddington, J. M. (2015). Moderate drop in water

table increases peatland vulnerability to post-fire regime shift. *Scientific Reports*, 5, 8063. https://doi.org/10.1038/srep08063.

Koehler, A., Sottocornola, M., & Kiely, G. (2011). How strong is the current carbon sequestration of an Atlantic blanket bog?. *Global Change Biology,* 17, 309-319. https://doi.org/10.1111/j.1365-2486.2010.02180.x.

Lafleur, P. M., Roulet, N. T., & Admiral, S. W. (2001). Annual cycle of CO_2 exchange at a bog peatland. *Journal of Geophysical Research,* 106(D3), 3071-3081. https://doi.org/10.1029/2000JD900588.

Lafleur, P. M., Moore, T. R., Roulet, N. T., & Frolking, S. (2005). Ecosystem Respiration in a Cool Temperate Bog Depends on Peat Temperature But Not Water Table. *Ecosystems,* 8, 619-629. https://doi.org/10.1007/s10021-003-0131-2.

Limpens, J., Berendse, F., Blodau, C., Canadell, J. G., Freeman, C., Holden, J., Roulet, N., Rydin, H., & Schaepman-Strub, G. (2008). Peatlands and the carbon cycle: from local processes to global implications – a synthesis. *Biogeosciences,* 5, 1475-1491. https://doi.org/10.5194/bg-5-1739-2008.

Lindroth, A., Lund, M., Nilsson, M., Aurela, M., Röjle Christensen, T., Laurila, T., Rinne, J., Riutta, T., Sagerfors, J., StröM, L., Tuovinen, J., & Vesala, T. (2007). Environmental controls on the CO_2 exchange in northern European mires. *Tellus B: Chemical and Physical Meteorology*, 59(5), 812-825. https://doi.org/10.1111/j.1600-0889.2007.00310.x.

Lloyd, J., & Taylor, J. A. (1994). On the Temperature Dependence of Soil Respiration. *Functional Ecology,* 8(3), 315-323.

Lukenbach, M. C., Devito, K. J., Kettridge, N., Petrone, R. M., & Waddington, J. M. (2015). Hydrogeolocial controls on post-fire moss recovery in peatlands. *Journal of Hydrology*, 530, 405-418. https://doi.org/10.1016/j.jhydrol.2015.09.075.

Lund, M., Lafleur, P. M., Roulet, N. T., Lindroth, A., Christensen, T. R., Aurela, M., Chojnicki, B. H., et al. (2010). Variability in exchange of CO_2 across 12 northern peatland and tundra sites. *Global Change Biology*, 16, 2436-2448. https://doi.org/10.1111/j.1365-2486.2009.02104.x.

Markle, C. E., North, T. D., Harris, L. I., Moore, P. A., & Waddington, J. M. (2020). Spatial Heterogeneity of Surface Topography in Peatlands: Assessing Overwintering Habitat Availability for the Eastern Massasauga Rattlesnake. *Wetlands*, 40, 2337-2349. https://doi.org/10.1007/s13157-020-01378-2.

Moore, T. R., Roulet, N. T., & Waddington, J. M. (1998). Uncertainty in Predicting the Effect of Climatic Change on the Carbon Cycling of Canadian Peatlands. *Climatic Change,* 40, 229-245. https://doi.org/10.1023/A:1005408719297.

Moore, P. A., Smolarz, A. G., Markle, C. E., & Waddington, J. M. (2019). Hydrological and thermal properties of moss and lichen species on rock barrens: Implications for turtle nesting habitat. *Ecohydrology,* 12, e2057. https://doi.org/10.1002/eco.2057.

Moore, P. A., Didemus, B. D., Furukawa, A. K., & Waddington, J. M. (2021). Peat depth as a control on Sphagnum moisture stress during seasonal drought. *Hydrological Processes*, 35, e14117. https://doi.org/10.1002/hyp.14117.

Morison, M., van Beest, C., Macrae, M., Nwaishi, F., & Petrone, R. (2021). Deeper burning in a boreal fen peatland 1-year post-wildfire accelerates recovery trajectory of carbon dioxide uptake. *Ecohydrology,* 14(3), e2277. https://doi.org/10.1002/eco.2277.

Morison, M. Q., Petrone, R. M., Wilkinson, S. L., Green, A., & Waddington, J. M. (2020). Ecosystem scale evapotranspiration and CO_2 exchange in burned and unburned peatlands: Implications for the ecohydrological resilience of carbon stocks to wildfire. *Ecohydrology,* 13(2), e2189. https://doi.org/10.1002/eco.2189.

Nichols, J. E, & Peteet, D. M. (2019). Rapid expansion of northern peatlands and doubled estimate of carbon storage. *Nature Geoscience,* 12(11), 917-921. https://doi.org/10.1038/s41561-019-0454-z

Nijp, J. J., Limpens, J., Metselaar, K., Peichl, M., Nilsson, M. B., van der Zee, S. E. A. T. M., & Berendse, F. (2015). Rain events decrease boreal peatland net CO_2 uptake through reduced light availability. *Global Change Biology*, 21, 2309-2320. https://doi.org/10.1111/gcb.12864.

Orchard, V. A., & Cook, F. J. (1983). Relationship between soil respiration and soil moisture. *Soil Biology and Biogeochemistry,* 15(4), 447-453.

Peichl, M., Öquist, M., Löfvenius, M. O., Ilstedt, U., Sagerfors, J., Grelle, A., Lindroth, A., & Nilsson, M. B. (2014). A 12-year record reveals pre-growing season temperature and water table level threshold effects on the net carbon dioxide exchange in a boreal fen. *Environmental Research Letters,* 9(5). https://doi.org/10.1088/1748-9326/9/5/055006.

Rein, G. (2009). Smouldering Combustion Phenomena in Science and Technology. *International Review of Chemical Engineering,* 1, 3-18.

Riutta, T., Laine, J., Aurela, M., Rinne, J., Vesala, T., Laurila, T., Haapanala, S., Pihlatie, M., & Tuittila, E. S. (2007). Spatial variation in plant community functions regulates carbon gas dynamics in a boreal fen ecosystem. *Tellus B: Chemical and Physical Meteorology*, 59(5), 838-852. https://doi.org/10.1111/j.1600-0889.2007.00302.x.

Ryan, M. G., & Law, B. E. (2005). Interpreting, measuring, and modeling soil respiration. *Biogeochemistry,* 73, 3-27. https://doi.org/10.1007/s10533-004-5167-7.

Rydin, H., & McDonald, A. J. S. (1985). Tolerance of Sphagnum to water level. *Journal of Bryology,* 13, 572-578. https://doi.org/10.1179/jbr.1985.13.4.571.

Roulet, N. T., Lafleur, P. M., Richard, P. J. H., Moore, T. R., Humphreys, E. R., & Bubier, J. (2007). Contemporary carbon balance and late Holocene carbon accumulation in a northern peatland. *Global Change Biology*, 13(2), 397-411. https://doi.org/10.1111/j.1365-2486.2006.01292.x.

Smolarz, A. G., Moore, P. A., Markle, C. E., & Waddington, J. M. (2018). Identifying resilient Eastern Massasauga Rattlesnake (Sistrurus catenatus) peatland hummock hibernacula. *Canadian Journal of Zoology,* 96(6), 1024-1031. https://doi.org/10.1139/cjz-2017-0334.

Sonnentag, O., van der Kamp, G., Barr, A. G., & Chen, J. M. (2010). On the relationship between water table depth and water vapour and carbon dioxide fluxes in a minerotrophic fen. *Global Change Biology*, 16(6), 1762-1776. https://doi.org/10.1111/j.1365-2486.2009.02032.x.

Spence, C., & Woo, M. (2003). Hydrology of subarctic Canadian shield: soil-filled valleys. *Journal of Hydrology*, 279, 151-166. https://doi.org/10.1016/S0022-1694(03)00175-6.

Strachan, I. B., Pelletier, L., & Bonneville, M. (2016). Inter-annual variability in water table depth controls net ecosystem carbon dioxide exchange in a boreal bog. *Biogeochemistry,* 127, 99-111. https://doi.org/10.1007/s10533-015-0170-8.

Sulman, B. N., Desai, A. R., Saliendra, N. Z., Lafleur, P. M., Flanagan, L. B., Sonnentag, O., Mackay, D. S., Barr, A. G., & van der Kamp, G. (2010). CO_2 fluxes at northern fens and bogs have opposite responses to inter-annual fluctuations in water table. *Geophysical Research Letters,* 37, LI9702. https://doi.org/10.1029/2010GL044018.

Teklemariam, T. A., Lafleur, P. M., Moore, T. R., Roulet, N. T., & Humphreys, E. R. (2010). The direct and indirect effects of inter-annual meteorological variability on ecosystem carbon dioxide exchange at a temperate ombrotrophic bog. *Agricultural and Forest Meteorology*, 150, 1402-1411. https://doi.org/10.1016/j.agrformet.2010.07.002.

Thompson, D. K., Benscoter, B. W., & Waddington, J. M. (2014). Water balance of a burned and unburned forested boreal peatland. *Hydrological Processes,* 28, 5954-5964. https://doi.org/10.1002/hyp.10074.

Turetsky, M., Wieder, K., Halsey, L., & Vitt, D. (2002). Current disturbance and the diminishing peatland carbon sink. *Geophysical Research Letters,* 29(11). https://doi.org/10.1029/2001GL014000.

Turetsky, M. R., Benscoter, B., Page, S., Rein, G., van der Werf, G. R., & Watts, A. (2015). Global vulnerability of peatlands to fire and carbon loss. *Nature Geoscience,* 8(1), 11-14. https://doi.org/10.1038/ngeo2325.

Van Beest, C., Petrone, R., Nwaishi, F., Waddington, J. M., & Macrae, M. (2019). Increased Peatland Nutrient Availability Following the Fort McMurray Horse River Wildfire. *Diversity*, 11(9), 1-17. https://doi.org/10.3390/d11090142.

Vu, J. (2019). The Effect of Access Road Construction on the Hydrology of Wetlands in Rock Barren Landscapes [Unpublished MSc thesis]. McMaster University.

Waddington, J .M., Morris, P. J., Kettridge, N., Granath, G., Thompson, D. K., & Moore, P. A. (2015). Hydrological feedbacks in northern peatlands. *Ecohydrology*, 8, 113-127. https://doi.org/10.1002/eco.1493.

Waddington, J. M., & Roulet, N. T. (1997). Groundwater flow and dissolved carbon movement in a boreal peatland. *Journal of Hydrology*, 191, 122-138. https://doi.org/10.1016/S0022-1694(96)03075-2.

Waddington, J. M., & Roulet, N. T. (2000). Carbon balance of a boreal patterned peatland. *Global Change Biology*, 6, 87-97. https://doi.org/10.1046/j.1365-2486.2000.00283.x.

Waddington, J. M., & Roulet, N. T. (1996). Atmosphere-wetland carbon exchanges: Scale dependency of CO_2 and CH_4 exchange on the developmental topography of a peatland. *Global Biogeochemical Cycles,* 10(2), 233-245. https://doi.org/10.1029/95GB03871.

Waddington, J. M., Strack, M., & Greenwood, M. J. (2010). Toward restoring the net carbon sink function of degraded peatlands: Short-term response in CO_2 exchange to ecosystem-scale restoration. *Journal of Geophysical Research,* 115, G01008. https://doi.org/10.1029/2009jg001090.

Waddington, J. M., & Warner, K. D. (2001). Atmospheric CO_2 sequestration in restored mined peatlands. *Ecoscience,* 8(3), 359-368. https://doi.org/10.1080/11956860.2001.11682664.

Ward, S., Bardgett, R. D., McNamara, N. P., & Ostle, N. J. (2009). Plant functional group identity influences short-term peatland ecosystem carbon flux: evidence from a plant removal experiment. *Functional Ecology,* 23(2), 454-462. https://doi.org/10.1111/j.1365-2435.2008.01521.x.

Wieder, R. K., Scott, K. D., Kamminga, K., Vile, M. A., Vitt, D. H., Bone, T., Xu, B., Benscoter, B. W., & Bhatti, J. S. (2009). Postfire carbon balance in boreal bogs of Alberta, Canada. *Global Change Biology,* 25(1), 63-81. https://doi.org/10.1111/j.1365-2486.2008.01756.x.

Wilkinson, S. L., Tekatch, A. M., Markle, C. E., Moore, P. A., & Waddington, J. M. (2020). Shallow peat is most vulnerable to high peat burn severity during wildfire. *Environmental Research Letters,* 15(10), 104032. https://doi.org/10.1088/1748-9326/aba7e8.

Xu, J., Morris, P. J., Liu, J., & Holden, J. (2018). PEATMAP: Refining estimates of global peatland distribution based on a meta-analysis. *Catena*, 160, 134-140. https://doi.org/10.1016/j.catena.2017.09.010.

Yu, Z., Loisel, J., Brosseau, D. P., Beilman, D. W., & Hunt, S. J. (2010). Global peatland dynamics since the Last Glacial Maximum. *Geophysical Research Letters,* 37, LI3402. https://doi.org/10.1029/2010GL043584.

Zoltai, S. C., Morrissey, L. A., Livingston, G. P., & de Groot, W. J. (1998). Effects of fires on carbon cycling in North American boreal peatlands. *Environmental Reviews,* 6, 13-24. https://doi.org/10.1139/a98-002.

Chapter 2 – Multi-year CO_2 exchange in a boreal shield peatland, Ontario, Canada

2.1 Abstract

Peatlands in northern regions, including the Ontario boreal shield, are important ecosystems with a range of ecosystem functions and values, including being key carbon storage reservoirs and natural climate solutions. However, there is concern this long-term carbon storage is at risk due to climate change mediated drought as peatland CO_2 fluxes have shown notable connections to ecohydrological variables, including water table depth. For example, while most peatland CO_2 exchange studies have focused on deep peatlands that have been shown to be more resilient to drought, shallower peatlands may be more sensitive to interannual variability in micrometeorological conditions. The high hydrological connectivity of shallow peatlands in the Eastern Georgian Bay (EGB) Ontario shield to other components of the landscape are sensitive to fluctuating water tables throughout the growing season, closely following precipitation patterns. In order to better understand the response of boreal shield peatlands to meteorological conditions, we examined ecohydrological controls on CO_2 fluxes with a focus on the summer season for five years, 2016 to 2020. We found GPP to be more variable from year to year compared to ER, and lower GPP fluxes in dry summer years. Daily water table depth was found to be a significant control on summer total NEE and GPP, where summers with substantial rainfall sequestered more total CO_2 than dry summer years as the water table is maintained near the peat surface. These findings indicate meteorological trends around EGB play a key role in carbon uptake rates in peatlands throughout the landscape. For the region, warm and dry conditions are expected to

increase, with the possibility peatlands may become net carbon sources in the summer season of very dry years.

2.2 Introduction

Peatlands in northern regions are globally important ecosystems for long-term carbon storage (Blodau et al., 2004; Clymo, 1987), and have been identified as natural climate solutions through protection and restoration policies (Drever et al., 2021). While only covering 2.8% of the global land area and 17% of Canada, peatlands store approximately one-third of the global organic soil carbon pool (Gorham, 1991; Xu et al., 2018; Yu et al., 2010). The accumulation of large peat deposits in the northern hemisphere has occurred throughout the Holocene (Nichols and Peteet, 2019; Yu et al., 2010), where peat formation is facilitated by permanently saturated conditions allowing for long-term storage of carbon (Clymo, 1987). The net carbon sink function of peatlands is a result of primary production exceeding decomposition and combustion C loss (Clymo, 1987; Gorham, 1991). With climate change and changes in the wildfire disturbance regime (Flannigan et al., 2009), there is concern peatlands may transition from net carbon sinks to net carbon sources due to resulting changes in environmental conditions controlling primary production and ecosystem respiration in the near future (Turetsky et al., 2002, 2015).

Annual, growing season, and daily fluxes of CO_2 have been shown to be controlled by a range of climatic and environmental factors including temperature (Lund et al., 2010), water table depth (Sonnentag et al., 2010; Strachan et al., 2016), light availability (Frolking et al., 1998), and phenology (Kross et al., 2014; Peichl et al., 2015). These environmental and climatic variables affect carbon cycling on varying time scales, from decadal changes (Chimner et al., 2017) to

interannual (Fortuniak et al., 2021; Helbig et al., 2019; Roulet et al., 2007; Strachan et al., 2016), and daily (Peichl et al., 2014), as well as between sites (Humphreys et al., 2006; Lund et al., 2010).

Water table depth controls several aspects of peatland structure and function. Water table depth and water availability are an important moderator to regulate the C balance of a peatland through the connection between water table depth, vegetation productivity, and decomposition rates (Rydin and McDonald, 1985; Waddington et al., 2015). A water table level near the peatland surface is important to maintaining saturated conditions that limit decomposition rates (Benscoter et al., 2005b; Clymo, 1984), and controls the volume of aerated peat, thereby limiting plant size and productivity (Gorham, 1991). The photosynthetic capacity of *Sphagnum* species depends strongly on water content, requiring a connection to the water table or frequent rain events (Bubier et al., 2003; Robroek et al., 2009), as desiccation may become a threat to *Sphagnum* species as the distance to water table increases (Rydin and McDonald, 1985). Vascular species have a lower dependency on water table depth, as rooting structures can extend deeper to a lower water table (Murphy and Moore, 2010). However, long-term changes in water table position may promote a change in peatland species distribution (Breeuwer et al., 2009; Moore et al., 2002). Water table depth has been established as a dominant control on growing season and summer CO_2 budgets, where dry summers with a low water table have reduced cumulative net CO_2 uptake (Aurela et al., 2007; Bubier et al., 2003; Fortuniak et al., 2021; Moore and Knowles, 1989; Strachan et al., 2016). However, the response of peatland CO_2 exchange to changes in water table depth have been found to be varied, where short-term changes in water table depth may stimulate greater ecosystem respiration (Bubier et al., 2003), while at the seasonal scale lower mean summer water table had lower GPP rates (Lund et al., 2012; Strachan et al., 2016) and increased ER (Aurela et al., 2007;

Lund et al., 2012). Given that climate change is expected to increase the frequency and length of summer droughts, peatlands are vulnerable to transition from net CO_2 sinks to net CO_2 sources given the previously mentioned ecohydrological controls (Fortuniak et al., 2021; Strachan et al., 2016).

Peatlands on the boreal shield landscape form in bedrock depressions on the landscape and are present at varying spatial scales interspersed within upland forest area (Catling and Brownell, 1999). Peatlands on this landscape are especially prone to a fluctuating water table position, as these ecosystems rely on fill and spill connectivity and the water table within the peatland is therefore dependent on lateral inflow from adjacent upland areas (Spence and Woo, 2003). Robust autogenic feedbacks are amplified in deeper peatlands, resulting in intensified wet and dry periods on this landscape compared to peatlands in other hydrogeological settings (Devito et al., 1989; Waddington et al., 2015), and therefore may be more sensitive to climatic interannual variability. In the boreal shield, peatlands tend to be shallower than those in the boreal plains region, these shallower boreal shield peatlands may be more susceptible to drought conditions from water table drawdown below the peat profile and limited water storage (Dixon et al., 2017). Shallow peatlands in the boreal shield region therefore are more vulnerable to moisture stress from the disconnect between surface mosses and a sufficient water supply, with the potential to limit CO_2 uptake from inhibited productivity by *Sphagnum* sp. during drought (Moore et al., 2021; Strack and Price, 2009). As climate change is expected to bring increased temperatures and frequency of drought conditions, long-term CO_2 uptake capacity of shallow boreal shield peatlands are not only at risk but may act as sentinels for change as their interannual CO_2 exchange budgets are likely more extreme than the deeper and more expansive peatlands that have been more widely studied.

However, the response of peatland CO_2 exchange to climatic interannual variability has not been widely studied in the boreal shield, as such, there is a need to estimate the growing season CO_2 exchange budget from relatively shallow boreal shield peatlands and evaluate the effects of meteorological interannual variability CO_2 exchange processes in the boreal shield.

In this study, we examine the inter-annual variability of NEE and its components (GPP and ER) throughout the growing season in a relatively shallow boreal shield peatland from 2016 to 2020. By using five years of growing season data (May to October), we have captured a range of environmental conditions which has allowed for the investigation of environmental drivers of daily and total summer CO_2 flux. Investigating the interannual variability in CO_2 exchange for the growing season also comes with implications for vegetation community of the peatland with climate change and the indirect impacts on essential habitat for species at risk (Markle et al., 2020a; Smolarz et al., 2018). This work covers a new geographic range for studying interannual variability of peatland CO_2 exchange, and will increase our understanding in how wetlands in the boreal shield region will respond to climate change.

2.3 Methods

2.3.1 Study area

The study site is located in a peatland within the open rock barrens landscape of the eastern Georgian Bay (EGB) region in Ontario, Canada and is in the Georgian Bay Biosphere, Mnidoo Gamii, a UNESCO biosphere situated within the Robinson-Huron Treaty of 1850 and the Williams Treaty of 1923, and located on Anishinabek territory. Ontario's EGB region is located in the Ontario shield ecozone and is composed of a mosaic of moss cushions and lichen mats, moss-dominated ephemeral wetlands, *Sphagnum*-dominated peatlands, and forested uplands of exposed granitic bedrock on the Canadian Boreal Shield (Markle et al., 2020b; Moore et al., 2019). The growing season is from May to September, inclusive, for this region. The regional 19-year (2002-2019) mean (± s.d.) annual temperature is 6.6 ± 11.3 ºC, with mean monthly air temperature in January of -8.5 ºC and a mean monthly air temperature in July of 20.5 ºC. Long-term annual cumulative precipitation totals 853 ± 251 mm, and the growing season rainfall long-term mean is 452 ± 148 mm.

The peatland area is 4800 m^2 with a mean peat depth of 59 cm (Moore et al., 2021), and has hummock-hollow-lawn microtopography in some areas of the peatland. The vegetation community is comprised of mosses *(Polytrichum strictum, Sphagnum palustre, Sphagnum fallax, Sphagnum cuspidatum),* a variety of shrubs (*Rhododendrom groenlandicum, Chamaedaphne calyculata),* and a few scattered jack pine *(Pinus banksiana)*.

2.3.2 Instrumentation

The standard eddy covariance (EC) technique was used to measure CO_2 fluxes. Continuous fluxes of CO_2 were measured simultaneously with wind velocity by an integrated three-

dimensional sonic anemometer and open-path infrared gas analyzer (IRGASON, Campbell Scientific, Canada), along with fine wire thermocouple (FW10 Type E, Campbell Scientific, Canada). Instruments were mounted 7.8 m above the land surface and oriented at 285^{o}. All measurements were recorded with a datalogger and data retrieved by telemetry (CR5000, Campbell Scientific, Canada). Wind direction measurements were corrected to align with cardinal directions.

Supporting meteorological variables were measured at the tower. Incoming solar radiation was measured by a pyranometer (SP-Lite2, Kipp & Zonen, Netherlands) and net radiation was recorded by a net radiometer (CNR1, Kipp & Zonen, Netherlands). Photosynthetic photon flux density (PPFD) was calculated from incoming shortwave radiation using a conversion factor of 2.3, the product of the fraction of incoming radiation that is photosynthetically active radiation (approx. 0.5) and a unit conversion factor. Air temperature and relative humidity were measured with a temperature and relative humidity probe (HMP60, Vaisala, Finland), while rainfall was measured using a tipping bucket rain gauge at the base of the tower (TE525M, Texus Electronics Inc., USA) and soil temperatures were measured in hummock and hollow microtopography at depths of 0.01, 0.05, 0.10, 0.15, 0.20, 0.50 m using copper-constantin thermocouples attached a rod inserted into the peat. Water table depth was measured every 15 minutes in the deepest part of the peatland to bedrock using Solinst levelogger pressure transducer (Solinst, Georgetown, ON) in 0.05 m diameter PVC wells. Photosynthetic photon flux density was calculated from incoming shortwave radiation

2.3.3 Eddy covariance data

Using the eddy covariance technique, NEE data were collected from one peatland over 5 years of the growing season, from May 1 to October 31 of 2016 to 2020. Net ecosystem exchange (NEE) of CO_2 was derived from the sum of turbulent CO_2 flux and the storage term at 10 Hz. Coordinate rotation, frequency response correction, density correction for temperature and humidity compensation (Webb et al., 1980), spike removal, and calculation of half-hourly fluxes were completed in an in-house Matlab script (Mathworks, USA).

Flux data were further processed using the *REddyProc* package in R (R Core Team, 2020) for gap-filling, u* filtering, and flux partitioning (Wutzler et al., 2018). Vapour pressure deficit (VPD) was calculated from relative humidity and air temperature. Calculated NEE were filtered by a friction velocity threshold of 0.14 m s^{-1}, derived according to Papale et al. (2006) representing the limit of turbulent conditions whereby below the threshold flux data may have large uncertainties due to low surface wind speed (Papale et al., 2006; Wutzler et al., 2018). This threshold was selected as this was the minimal velocity when the correlation with temperature from nighttime data, selected when the global radiation is below 20 W m^{-2}, became weak or absent (Reichstein et al., 2005). Calculated NEE was gap filled using the marginal distribution sampling method and look up tables for incoming solar radiation (R_g), VPD, T_{air}, and mean diurnal course, whereby the number of days used in the algorithm increases until a window of more than 2 datapoints is identified (Reichstein et al., 2005; Wutzler et al., 2018). The proportion of each year's dataset identified as gaps prior to filling were 45% (2016), 48% (2017), 48% (2018), 43% (2019), 45% (2020). The marginal distribution sampling method was then used to gap fill environmental conditions: R_g, T_{air}, and VPD.

Flux partitioning of NEE into GPP and ER was completed using daytime-based methods where a modified light-response curve that incorporates the temperature-respiration relationship is used to model NEE (Falge et al., 2001; Lasslop et al., 2010; Lloyd and Taylor, 1994). NEE is the difference between gross primary productivity (GPP) and ecosystem respiration (ER) (Eq 2.1):

$$NEE = GPP - ER \quad (2.1)$$

A detailed flux footprint analysis was completed using the Kljun et al. (2015) flux footprint prediction model in R. The footprint was overlain on the land classification map to determine the proportions of land classes within each half-hour flux footprint. A simple linear regression analysis was completed to determine the percent of the 'peat' land cover class within each half-hour footprint as a significant predictor of flux.

Daily fluxes were calculated by converting the units of each half hourly measurement from μmol CO_2 m^{-2} s^{-1} to g C m^{-2} d^{-1}, fluxes were then summed for each day. Cumulative fluxes were calculated by adding successive daily flux together for a continuous period of time, for example from June 1 to August 31 for the summer season. For all measurements a negative flux indicates uptake by the ecosystem, and positive measurements indicate exchange from ecosystem to atmosphere. Uncertainty estimates from half hour and daily gap-filled data were used to quantify uncertainty in the cumulative flux estimates for the summer season (Liu et al., 2009; Moncrieff et al., 1996; Richardson et al., 2012). For this analysis, growing season is from May 1 to October 31, and the summer season is classified as June 1 to August 31.

2.3.4 Analyses

2.3.4.1 Growing season length and carbon uptake period

The growing season period was identified as the first day of seven consecutive days when T_{air} was above 5°C (Lund et al., 2010). The end of the growing season was defined as the first of seven consecutive days where T_{air} was below 5°C. To define the end of the carbon uptake period (CUP), a 10-day moving average on daily NEE was calculated (Fu et al., 2017). The moving average was then used to manually define the transition day from sink to source, whereby the end day of the CUP was selected if the moving average was a positive value (NEE changing from negative to positive, indicating net release to atmosphere) for more than 3 consecutive days.

2.3.4.2 Multiple linear regressions

We performed a similar multiple linear regression analysis to determine the main environmental variables contributing to cumulative flux for the summer season (June 1 to August 31). The variables used in the analysis include: mean water table depth (m), mean summer air temperature (°C), cumulative precipitation (mm), total PPFD (μmol m^{-2}), winter antecedent mean air temperature (January to April) (°C). Data for each year were modelled with a full model including all four variables as predictors. We identified variables from the significance in the full model (t-test, $p<0.05$). Following a backward elimination procedure, selected variables were included in a 'reduced model' which was compared to the full model using F-test statistic and AIC. The reduced model was further evaluated if results were not significant therefore the null hypothesis would be rejected (indicating the addition of extra variables did not improve model fit). Partial F-test on the selected model was conducted to evaluate whether specific variables included improved model fit ($p>0.05$). Multicollinearity within each selected model was evaluated using the variance inflation factor (VIF).

2.3.4.3 Light response

Light response curves were estimated from the relationship between measured NEE (µmol m^{-2} s^{-1}) and incoming PPFD (µmol m^{-2} s^{-1}) using the nonlinear least squares analysis in R. The light response relationship was evaluated based on the rectangular hyperbola equation from Frolking et al. (1998) (Eq 2.2):

$$NEE = \frac{\propto PPFD\ GPP_{max}}{\propto PPFD + GPP_{max}} + \mathrm{R} \quad (2.2)$$

where $\propto$ represents the quantum yield (initial slope), R is the y-intercept (or nighttime respiration value; µmol m^{-2} s^{-1}), GPP_{max} is the maximum gross photosynthesis (µmol m^{-2} s^{-1}). All variable parameters ($\propto$, GPP_{max}) were determined through nonlinear least-square regression (*nls*) in R.

2.4 Results

2.4.1 Environmental variables

Mean daily air temperature from May to October for 2016 to 2020 ranged from 14.9 (2019) to 16.2 ^{o}C (2020) (Table 2.1). The region's 19-year long-term mean air temperature for the growing season months is 15.7 ± 4.5 ^{o}C (Environment Canada, 2021). Mean monthly air temperatures varied, with the lowest peak summer air temperature occurring in July 2017, and greatest in July 2018 (Figure 2.1). Cumulative rainfall for May 1 to September 30 exceeded the regional long-term average of 400.5 mm in 2017, 2019, and 2020 (Environment Canada, 2021). The greatest cumulative rainfall was 529.2 mm in 2017, with the lowest occurring in 2016 (373.5 mm) (Table 2.1). Monthly rainfall varied between years, with the three years experiencing a dry summer from lower cumulative rainfall (2016, 2018, 2019) also having a substantial summer drought where water table position decreased continuously throughout summer months (Figure 2.1). Air temperature and rainfall anomalies calculated from the 18-year long term mean for each month did not often fall in the warmer and wetter category (Figure 2.2). Air temperature anomalies in all months of the 2016 growing season were low with all months experiencing drier than average rainfall, except August. All months in 2017 were colder and wetter than average, although a later fall onset is reflected in a warmer and drier October. In contrast, an early fall onset occurred in 2020 with greater precipitation and cooler temperatures in August and September. In 2018, the growing season began warm and dry, becoming wetter in late summer and in early fall was colder and wetter than the average. All months of 2019 experienced cooler than average temperatures. The growing season water table position closely followed rainfall anomalies, with months of numerous rain events not experiencing large water table drawdown (Figure 2.1).

Mean daily water table depth reflects cumulative precipitation for each year (Figure 2.1b, c). For all years the trends in water table position follow a similar pattern in early spring until early June, where mean daily water table depth is less than 20 cm below the surface. Water table depth diverges after the beginning of June, with 2016, 2018, and 2019 experiencing a greater more rapid drying than other years. Water table position remaining in the surface 20 cm reflects years of greater cumulative rainfall than the long-term average and a greater rainfall rate in the summer months (2017 and 2020).

Mean growing season PPFD varied between study years, with lowest incoming PPFD in 2017 and greatest in 2019 (Table 2.1). Peak PPFD occurred in June for 2016 and 2020, and in July for 2017, 2018, and 2019 (Figure 2.3).

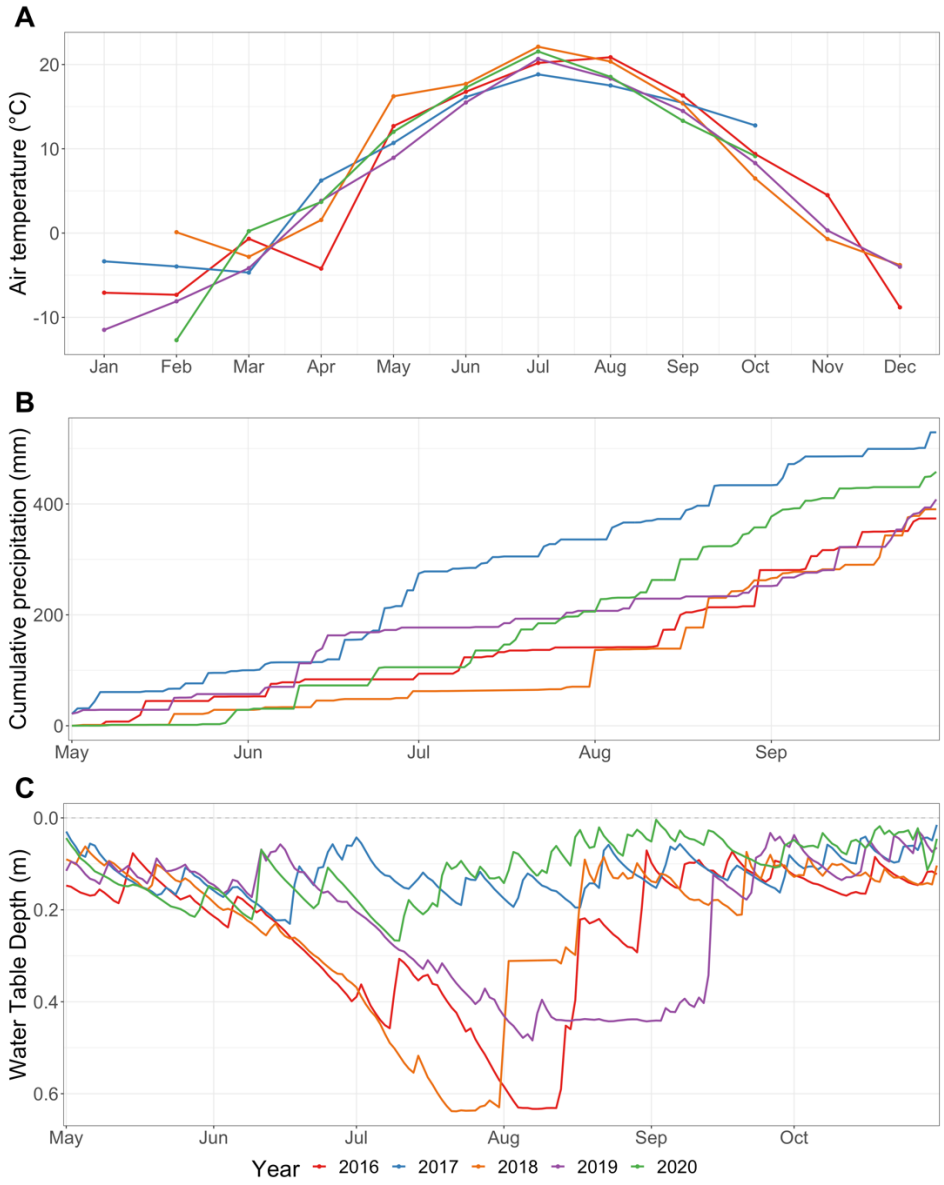

Figure 2.1: (A) Mean monthly air temperature (ºC) from January to December, (B) cumulative precipitation (mm) from May to late September, (C) mean daily water table depth (m) for May to late October. Date for July 25 to August 13, 2018 were gap-filled using mean WT drawdown rate for 2018 growing season and the linear relationship between WT rise and rainfall event for the year. The colour of the line indicates the year as follows: *2016* – red*, 2017* – blue*, 2018* – orange*, 2019* – purple*, 2020* – green.

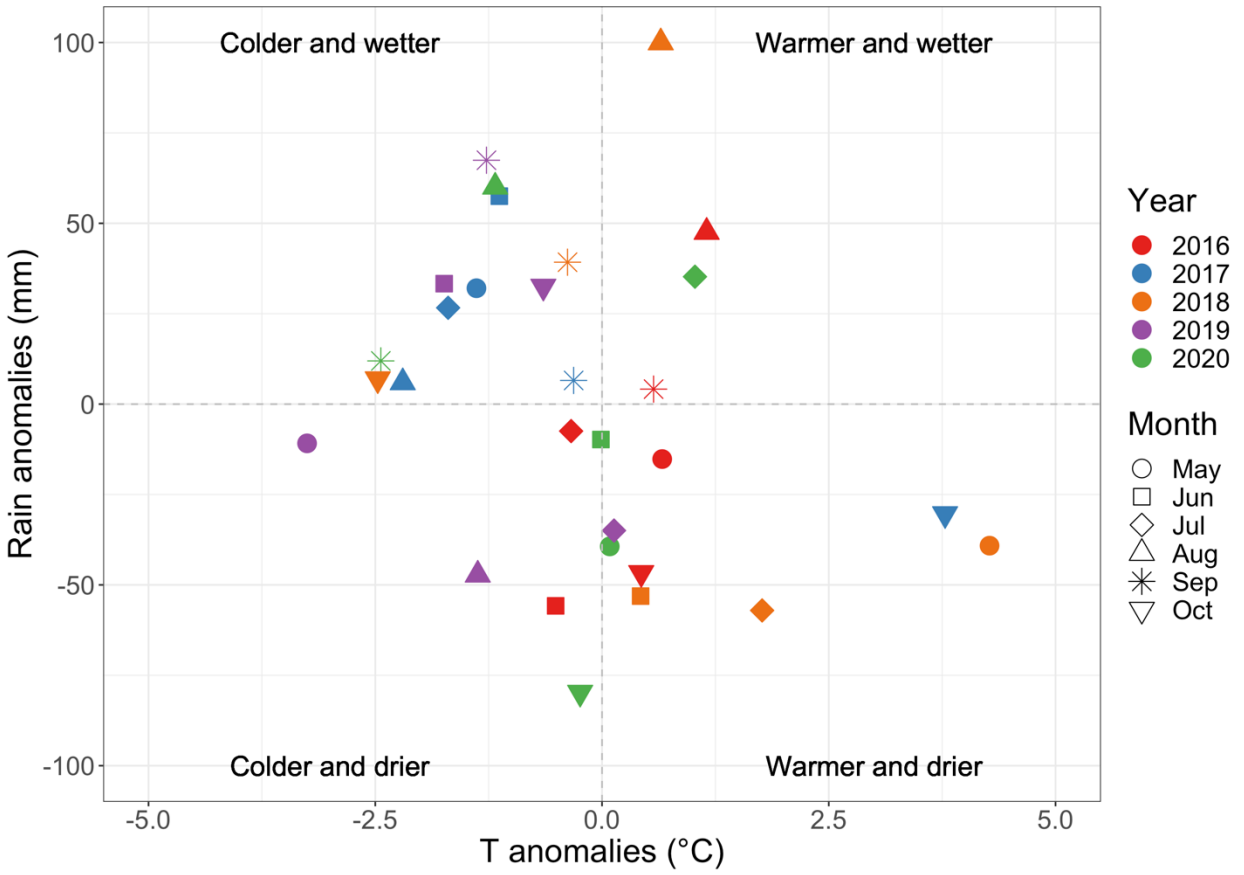

Figure 2.2: Air temperature (°C) and rainfall (mm) anomalies (May-October) for 2016-2020 compared to the 18-year average for the region (Environment Canada, 2021). Symbols denote months of the growing season and colours distinguish between years – 2016 – *red*, 2017 – *blue*, 2018 – *orange*, 2019 – *purple*, 2020 – *green.*

Table 2.1: Mean air temperature, cumulative precipitation, mean daily water table depth, mean and maximum daily NEE for growing season, total summer NEE, CUP end day, mean PPFD for growing season, and growing season length for each year of the study.

	2016	2017	2018	2019	2020
Air temperature (°C)	16.1	15.4	15.8	14.9	16.2
Cumulative rainfall (mm)	373.8	529.2	390.4	408.2	458.0
Daily WTD (m)	-0.274	-0.131	-0.236	-0.251	-0.121
Mean daily NEE (g C m^{-2} d^{-1})	-0.12	-0.84	-0.36	-0.45	-0.54
Max daily NEE (g C m^{-2} d^{-1})	-2.47	-3.10	-2.58	-2.58	-2.77
Total summer NEE (g C m^{-2}) (± s.d.)	-10.8 (55)	-110.5 (76)	-27.6 (55)	-55.7 (52)	-99.0 (58)
End day of carbon uptake period (Julian day)	190	258	194	226	240
Mean PPFD (µmol m^{-2} s^{-1})	894	757	845	952	839
Growing season length (days of T_{air} > 5°C)	187	171	174	181	171

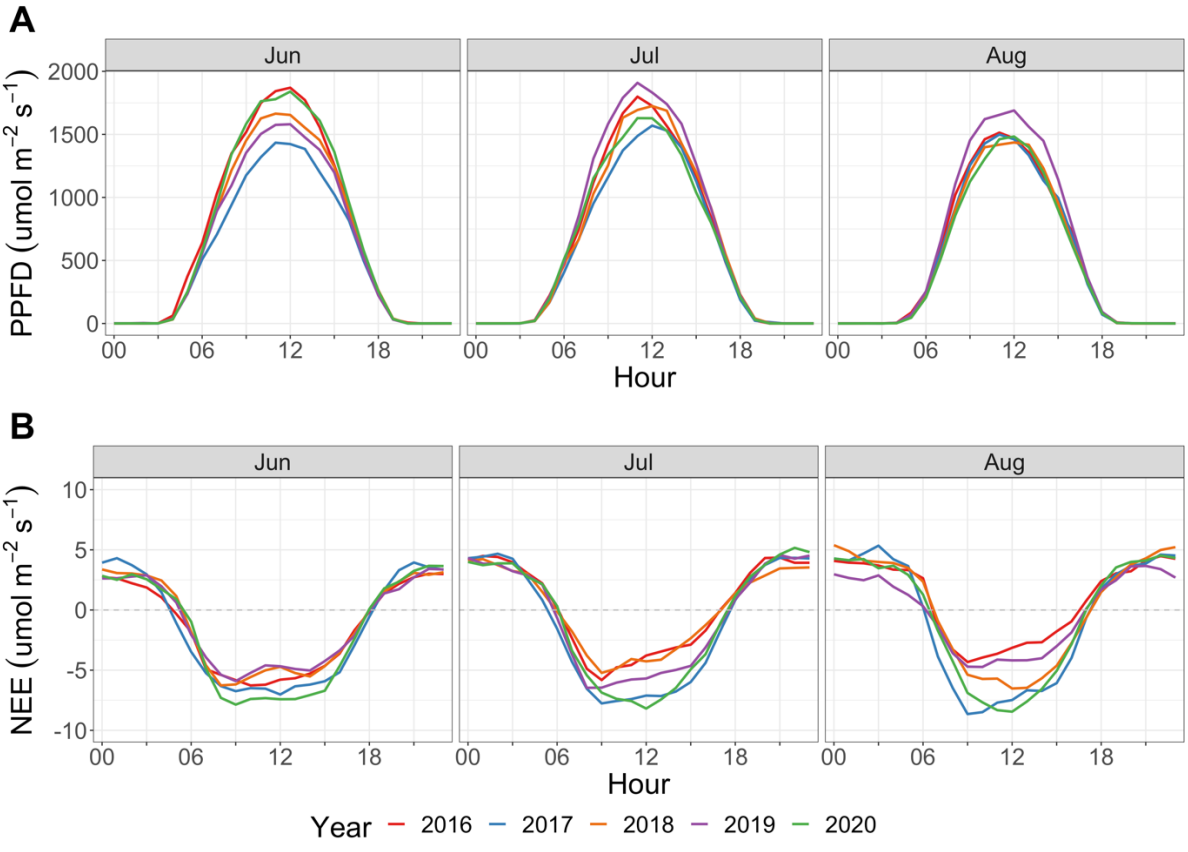

Figure 2.3: (A) Mean diurnal cycle of PPFD (µmol m^{-2} s^{-1}), (B) mean diurnal cycle of NEE (µmol m^{-2} s^{-1}) for June, July, August, September of 2016-2020.

2.4.2 Growing season length and carbon uptake period

Growing season length ranged from 171 days in 2017 and 2020, to 187 days in 2016, and the mean growing season length was 177 days (± 7 days). The growing season start days for 2016-2020 were May 17 (2016, DOY: 138), April 22 (2017, DOY: 112), April 30 (2018, DOY: 120), May 3 (2019, DOY: 123), and April 25 (2020, DOY: 116) (Figure 2.4). The end of the growing season occurred on November 20 (2016, DOY: 325), October 10 (2017, DOY: 283), October 21 (2018, DOY: 264), October 31 (2019, DOY: 304), and October 13 (2020, DOY: 287). Years with an early transition to daily source of CO_2 coincided with longer growing season length.

The transition from daily CO_2 uptake to daily CO_2 emission is described as the end of the carbon uptake period (CUP) (Fu et al., 2017), occurring on different days for each year of the study period from early July in 2016 to mid-September in 2017. The earliest transition to daily CO_2 emission occurred on July 8 (DOY: 190) in 2016, which was also the year with the latest start of the growing season and longest growing season length (Figure 2.4). In 2017, the year with longest growing season length was also the year with latest CUP end. In 2018, 2019 and 2020 the CUP end occurred on June 13 (DOY: 164), August 14 (DOY: 226), and August 27 (DOY: 240), respectively.

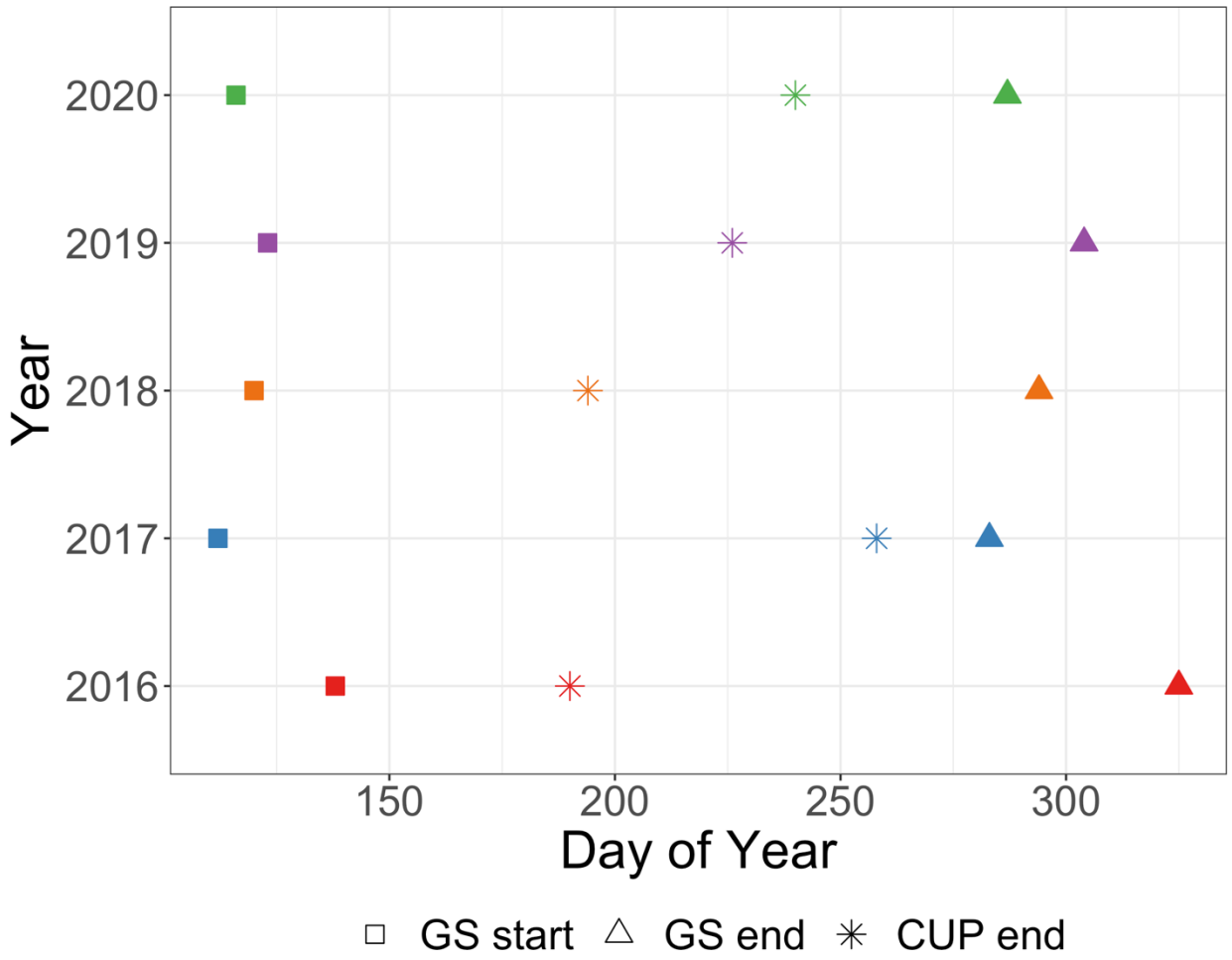

Figure 2.4: Growing season start (GS start), growing season end (GS end), and carbon uptake period end (CUP end) dates for 2016 to 2020. Growing season is defined as the period of time when air temperature is above 5°C. Carbon uptake period end day is the day of transition from net daily sink of CO_2 to net daily source of CO_2.

2.4.3 CO_2 exchange

2.4.3.1 Daily flux

Mean (± s.d.) daily growing season net uptake ranged from -0.12 (± 1.11) g C m^{-2} d^{-1} (2016) to -0.87 (± 1.04) g C m^{-2} d^{-1} (2017) and highest summer (JJA) net uptake ranged from -2.47 g C m^{-2} d^{-1} (2016) to -3.10 g C m^{-2} d^{-1} (2017) (Figure 2.5, Table 2.2). Maximum summer NEE occurred in June for all years, with the earliest peak NEE in 2018 on June 6 (DOY: 157) and latest occurring in 2017 on June 27 (DOY: 178). Mean daily growing season GPP ranged from -2.99 (± 1.41) g C m^{-2} d^{-1} (2019) to -3.65 (± 1.88) g C m^{-2} d^{-1} (2017). Maximum summer GPP was -8.25 g C m^{-2} d^{-1} in June 2018, and lowest summer GPP_{max} of -6.00 g C m^{-2} d^{-1} in July 2018. Summer GPP_{max} occurred latest in 2018 (August 8, DOY: 220), while summer GPP_{max} occurred in June for 2017, 2019 and 2020, and in July for 2016. Greatest summer ER_{max} occurred in 2016 of 7.24 g C m^{-2} d^{-1}, and lowest in 2018 of 5.50 g C m^{-2} d^{-1}. ER_{max} occurred in latest in the year in August of 2017, 2018 and 2020, July in 2016 and 2019. The transition day from net uptake to net release (negative to positive NEE) occurred earliest in the year in 2016 (July 8, DOY: 190) and 2018 (July 13, DOY: 194), and latest in 2017 (September 15, DOY: 258) (Figure 2.5).

Table 2.2: Mean and maximum NEE, GPP, ER (g C m^{-2} d^{-1} ± s.d.) for each year from 2016 to 2020 for growing season (May to October) and the summer season (June to August).

	2016	2017	2018	2019	2020
$NEE_{GS,mean}$	-0.12 (1.11)	-0.84 (1.04)	-0.36 (0.85)	-0.45 (1.05)	-0.54 (1.13)
$GPP_{GS,mean}$	-3.21 (1.15)	-3.65 (1.88)	-3.27 (1.34)	-2.99 (1.41)	-3.39 (1.85)
$ER_{GS,mean}$	3.00 (1.46)	2.58 (1.44)	2.78 (1.23)	2.22 (1.16)	2.65 (1.56)
$NEE_{JJA,mean}$	-0.12 (1.31)	-1.20 (0.92)	-0.30 (0.98)	-0.61 (0.96)	-1.08 (1.19)
$GPP_{JJA,mean}$	-3.47 (1.16)	-5.03 (1.35)	-3.95 (1.01)	-3.97 (1.14)	-4.66 (1.13)
$ER_{JJA,mean}$	3.12 (1.30)	3.36 (1.16)	3.15 (1.03)	2.77 (1.02)	3.37 (1.28)
$NEE_{JJA,max}$	-2.47	-3.10	-2.58	-2.58	-2.77
$GPP_{JJA,max}$	-6.42	-8.25	-6.00	-6.64	-7.25
$ER_{JJA,max}$	7.24	5.66	5.50	5.91	6.25
Transition to source (DOY)	July 8 (190)	Sept 15 (258)	July 13 (194)	August 14 (226)	August 27 (240)

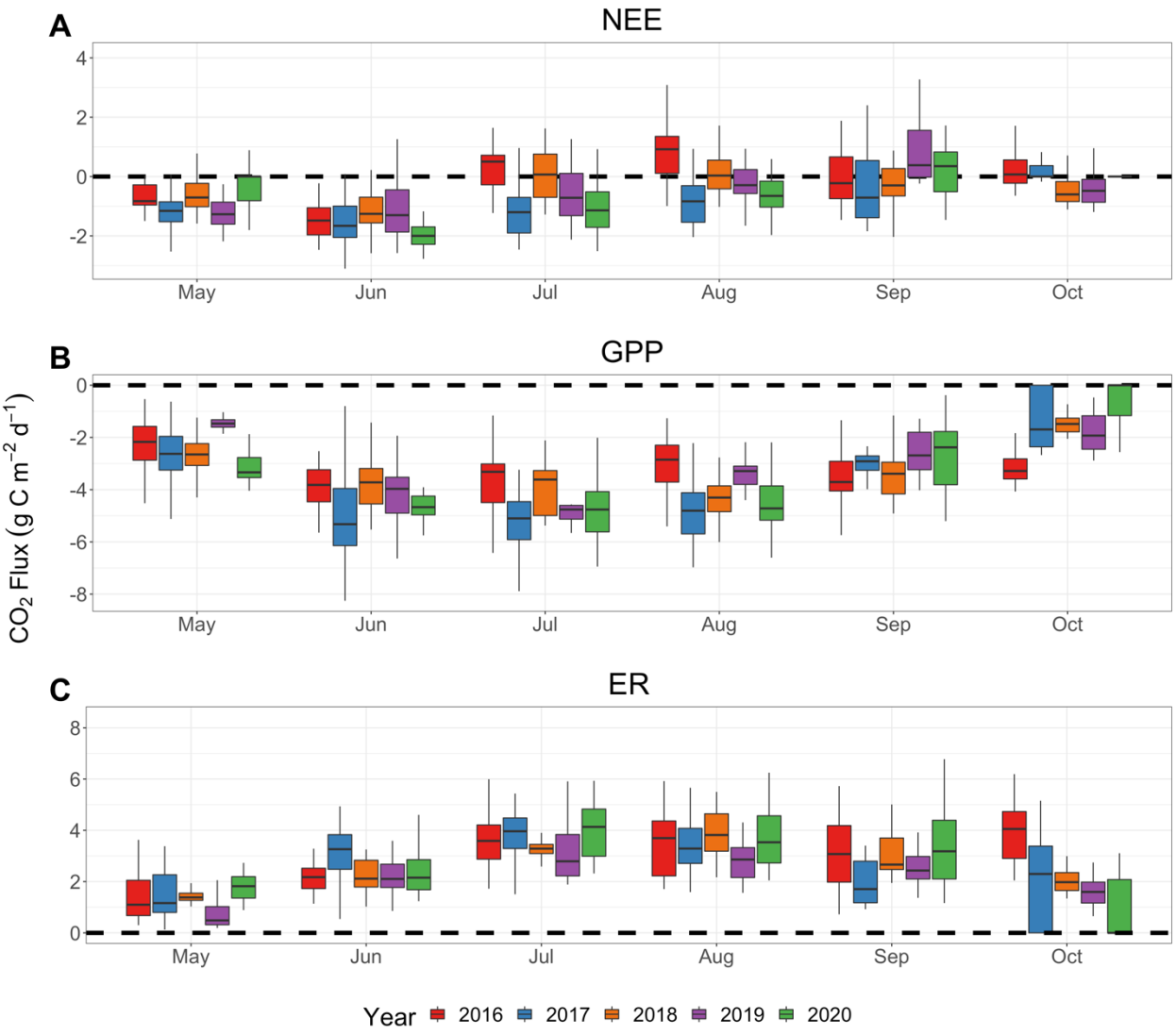

Figure 2.5: Daily (A) net ecosystem exchange (NEE), (B) gross primary productivity (GPP), and (C) ecosystem respiration (ER) (g C m^{-2} d^{-1}) from May to October for 2016 (red), 2017 (blue), 2018 (orange), 2019 (purple), and 2020 (green). Boxes show the 25th and 75th percentiles; lines inside the boxes show the median.

2.4.3.2 Seasonal diurnal cycle

Daytime maximum NEE was generally greater in 2017 and 2020 wet summers (Figure 2.3). The early transition to a net daily CO_2 source is reflected in a lower magnitude of daytime NEE in July of 2016 and 2018, while daytime net uptake remained greatest (most negative) and relatively constant for June to August in 2017 and 2020. Maximum daytime PPFD was observed in June for 2016 and 2020, and July for all other years, however the magnitude of maximum daytime PPFD was lower in 2017 than all other years. The more frequent rain events and possibility of greater cloud cover throughout the growing season of 2017 is reflected in a lower magnitude of daytime maximum PPFD for June and July. The differences in the diurnal cycle of NEE between years does not fully reflect the daily cycle of incoming light, and in combination with the light response relationship there are other environmental variables playing an important role in the CO_2 exchange.

2.4.3.3 Summer CO_2 budget and environmental controls

The interannual variability of cumulative summer fluxes (NEE, GPP, ER) were explained by a combination of environmental conditions including mean summer water table depth, summer air temperature, winter air temperatures (Jan-Apr), and summer cumulative rainfall. Average cumulative summer NEE was variable between years ranging from -10.8 g C m^{-2} in 2016 to -110.5 g C m^{-2} in 2017, with a mean cumulative NEE flux of -60.7 ± 43 g C m^{-2} (Table 2.1; Figure 2.6). The site was a CO_2 sink for all years for the summer period. Cumulative summer NEE and GPP were strongly related to average WTD ($R^2 = 0.76$, $p < 0.05$; $R^2 = 0.9$, $p < 0.05$) (Figure 2.7). Greatest cumulative summer NEE and GPP occurred in 2017, and lowest cumulative NEE and GPP were in 2016. Adding mean winter air temperatures to WTD as a predictor of NEE improved

the correlation (R^2 = 0.92, p = 0.038, F: 25.06). Lowest air temperatures for the preceding winter occurred in 2016 and 2019, while similarly 2016 had the lowest cumulative summer NEE. The warmest winter air temperatures occurred in 2020, the same year is on the higher end of cumulative summer NEE range. Low winter air temperatures may sustain the snow pack longer, pushing the start of spring vegetation growth later into the year indicated by a later start to the growing season (Table 2.3).

Cumulative summer GPP ranged from -319.5 g C m^{-2} in 2016 to -462.8 g C m^{-2} in 2017, with a mean cumulative GPP of -388.1 ± 57 g C m^{-2} for the five years (Figure 2.6) There was a strong, significant relationship between cumulative summer GPP and summer WTD (R^2_{adj} = 0.9, p = 0.009) (Figure 4.7), and the addition of summer air temperature, through multiple linear regression, increased predictive capacity of cumulative GPP (R^2_{adj} = 0.99, p = 0.003).

Cumulative summer GPP ranged from 255.2 g C m^{-2} in 2019 to 310.2 g C m^{-2} in 2020, with a mean cumulative flux of 290.3 ± 22 g C m^{-2} for the five years (Figure 2.6). While no strong relationship between WTD with ER was found (Figure 2.7), there were relationships between cumulative ER, total summer rainfall, and winter air temperatures although not statistically significant (R^2_{adj} = 0.53, p = 0.236, F: 3.24) (Table 2.3). The absence of a relationship between WTD and ER may indicate a dominance of autotrophic respiration in total ER (Strachan et al., 2016).

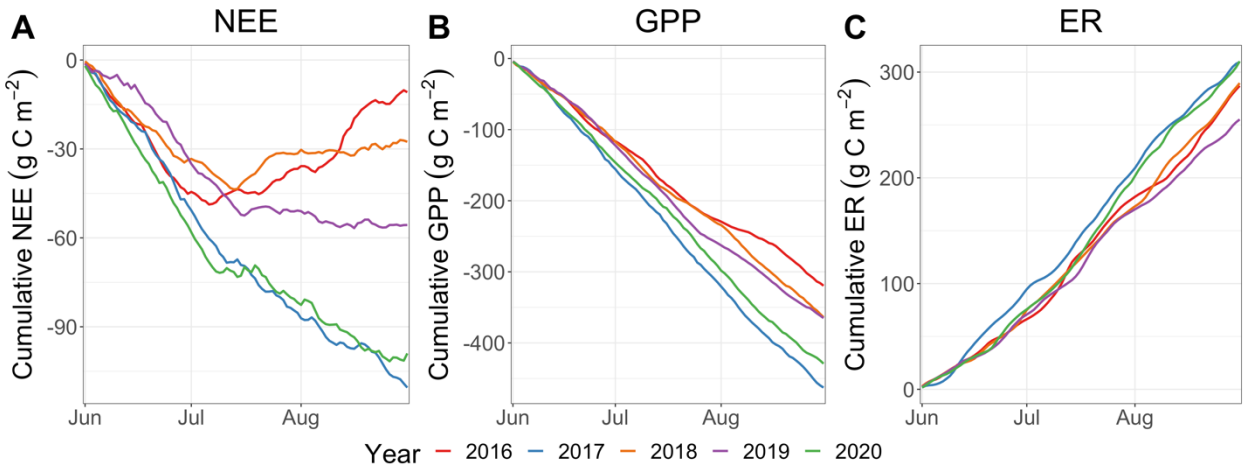

Figure 2.6: (A) Cumulative summer (JJA) net ecosystem exchange (NEE) (g C m^{-2}), (B) gross primary production (GPP), and (C) ecosystem respiration (ER) for 2016 to 2020. Colours indicate year as follows: 2016 – *red*, 2017 – *blue*, 2018 – *orange*, 2019 – *purple*, 2020 – *green.*

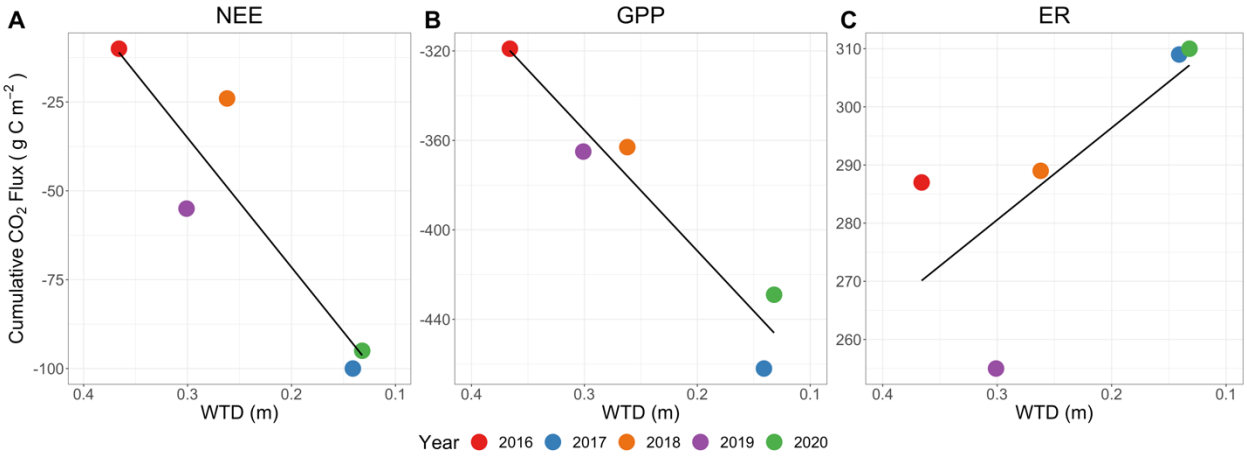

Figure 2.7: Cumulative flux (g C m^{-2}) of (A) net ecosystem exchange (NEE), (B) gross primary productivity (GPP), and (C) ecosystem respiration (ER) for the summer period (months: JJA) as a function of mean water table depth (m) for the time period. Regression line fit using ordinary least squares linear model. Colours indicate year as follows: 2016 – *red*, 2017 – *blue*, 2018 – *orange*, 2019 – *purple*, 2020 – *green.*

Table 2.3: Results of multiple linear regression modelling for cumulative summer (JJA) net ecosystem exchange (NEE), gross primary production (GPP), and ecosystem respiration (ER), showing the estimate, ± s.e., p-value of environmental variable tested and model parameters.

	NEE			GPP			ER		
Intercept	-179.20	± 19.65	(0.012)	-895.43	±55.36	(0.004)	263.37	±31.99	(0.014)
Summer WTD	581.03	± 101.01	(0.029)	471.08	±24.18	(0.003)			
Winter T_{air}	8.98	± 3.50	(0.13)				3.98	±3.01	(0.317)
Summer T_{air}				21.12	±3.08	(0.021)			
Summer rain							0.14	±0.11	(0.345)
n	5			5			5		
R^2_{adj}	0.923			0.994			0.528		
F-statistic	25.060			322.483			3.239		
p-value	0.038			0.003			0.236		
df	2.000			2.000			2.000		
AIC	41.810			32.637			44.915		
deviance	253.063			40.408			470.859		

**p-value in brackets*.

2.4.3.4 Light response relationship

The initial slope of the light response relationship, quantum yield (∝), was greatest in the wet summer year of 2017 (0.034 (± 0.0008)), and lowest in the dry summer of 2016 (0.016 (± 0.0005)) (Table 2.4, Figure 2.8). In 2017, the steeper slope indicates measured NEE is greater in that year at comparable light levels (Figure 2.8). This may be an indication that more accessible water from the higher water table has allowed for vegetation to photosynthesize more efficiently. This is reflected in a greater GPP_{max} for the 'wet' summer years of 2017 and 2020, -14.4 (± 0.14) µmol m^{-2} s^{-1} and -16.7 (± 0.23) µmol m^{-2} s^{-1}, respectively (Table 2.4). In years where water table depth was below 60 cm over the summer, there was a similar summer GPP_{max} of -11.4 (± 0.21) µmol m^{-2} s^{-1} and -11.8 (± 0.18) µmol m^{-2} s^{-1} for 2016 and 2018, respectively.

Table 2.4: Net CO_2 exchange model parameters for the summer (JJA) light response curve relationship (Frolking et al. (1998)) with standard errors given in brackets (GPP_{max} units are µmol CO_2 m^{-2} s^{-1}).

Year	∝ (± s.e.)	GPP_{max} (µmol m^{-2} s^{-1} ± s.e.)
2016	0.016 (0.0005)	-11.4 (0.21)
2017	0.034 (0.0008)	-14.4 (0.14)
2018	0.021 (0.0007)	-11.8 (0.18)
2019	0.017 (0.0005)	-12.8 (0.21)
2020	0.020 (0.0004)	-16.7 (0.23)

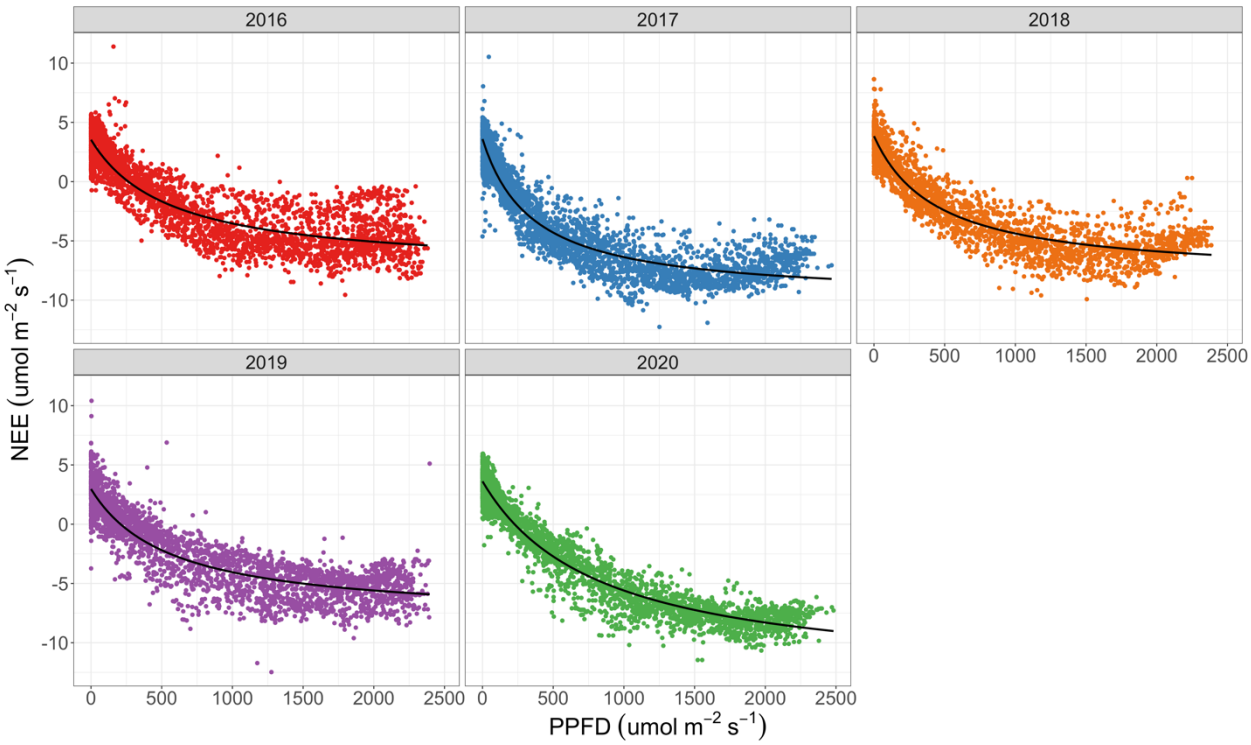

Figure 2.8: Light response relationship between half-hourly NEE (µmol m^{-2} s^{-1}) and PPFD (µmol m^{-2} s^{-1}) using Frolking et al. (1998) equation for summer (JJA). Colours indicate year as follows: 2016 – red, 2017 – blue, 2018 – orange, 2019 – purple, 2020 – green.

2.5 Discussion

We expected the response of wet and dry conditions in the boreal shield peatlands to be amplified due to limited water storage on this fill and spill landscape and the generally shallower peat depth, which is reflected in the growing season CO_2 fluxes, summer CO_2 budget, and connection to climatic interannual variability. This multi-year dataset is the first for peatlands in the boreal shield region and outlines the connection between interannual variability in summer CO_2 flux and water availability in the ecosystem. However, despite the expected greater sensitivity of boreal shield peatlands to wet and dry conditions, our daily and summer budget CO_2 fluxes were of similar magnitude to recent studies of deeper peatlands in the boreal regions, including Helbig et al. (2019), Humphreys et al. (2006), Lund et al. (2010), and Piechl et al. (2014). Nevertheless, we also found there is a strong water table control on CO_2 uptake by the peatland, similar to Strachan et al. (2016) and Sonnentag et al. (2010), where wet years have greater CO_2 uptake than drier years. We also have found there is a connection between late winter and early spring temperatures with ecosystem respiration, similar to Piechl et al. (2014). This study shows the important connection between interannual climate patterns and CO_2 uptake during the growing season by peatlands in the EGB and the boreal shield region.

2.5.1 Eddy covariance CO_2 uptake

Our results show late winter and early spring environmental conditions may play a role in the timing of growing season start and the start of water table dynamics following winter freezing. We found a significant relationship between cumulative ER and winter air temperatures, warmer winter air temperatures have also been associated with an earlier start to the growing season (Kross et al., 2014) and connected to snow melt timing (Aurela et al., 2004). The combination of mild

winter air temperatures and earlier growing season start have been found to stimulate greater daily GPP and ER (Peichl et al., 2014), and greater peak summer NEE (Kross et al., 2014). Years with lower mean winter air temperatures (2016, 2019) had the latest start to the growing season (May 17 (DOY 138) and May 3 (DOY 123) for 2016 and 2019, respectively) and transitioned from daily CO_2 sink to source earlier than other years (July 8 (DOY 190) and August 14 (DOY 226), respectively). However, these years also had the longest growing season lengths and were on the lower end of cumulative NEE range for the summer season. Years with a mild winter had earlier growing season start and greater total summer CO_2 uptake. An earlier start to the growing season and early snowmelt from warmer winter and early spring air temperatures allows for melt water contributions from the watershed to initiate an earlier fill and spill hydrological connectivity between the peatlands, ephemeral wetlands, upland bedrock and forested areas (Spence and Woo, 2003). Hydrological connectivity between landscape units earlier in the spring results in earlier water table activity in the basin peatlands (Spence and Woo, 2003), and increasing water availability may allow spring vegetation productivity to commence earlier (Kreyling, 2010), shown in the observed greater daily GPP and ER for May and June. Years with a mild winter also coincided with growing seasons with no summer drought period, as the water table was maintained in the top of the peat profile throughout the growing season (2017 and 2020). Rainfall and temperature anomalies in southern Canada may be influenced by teleconnections, such as the Southern Oscillation, bringing milder and drier winters during El Niño events (Shabbar, 2006; Shabbar et al., 1997) and decreased temperatures in the summer of the El Niño year (Hu et al., 2019). Although 2015-2016 and 2018-2019 were El Niño years, the winter and early spring air temperatures (JFMA months) of 2016 and 2019 were colder than other years of the study. Similarly, late growing season (September and October) of the 2018 El Niño experienced colder

than average temperatures, while the rest of the growing season of 2018 was warmer than average (Figure 2.2).

The transition day from net CO_2 uptake to net CO_2 emission, or end of the carbon uptake period, at this site occurred earlier (August 10 ± 29 days) than the well-studied Mer Bleue peatland, which is located at similar latitude although farther east and transitioned from CO_2 sink to CO_2 source around October 3 (Lafleur et al., 2003; Roulet et al., 2007). For all five years in this study, rainfall in September was greater than the long-term average, and all years experienced colder than average temperatures with the exception of 2016 (Figure 2.2). Although the variability of temperature and rainfall anomalies in October was greater than September, the colder and wetter environmental conditions in September may have triggered an early fall vegetation senescence, slowing the photosynthetic activity of vegetation in the ecosystem and enhancing ecosystem respiration leading to a shift from negative NEE to positive (Järveoja et al., 2018; Piao et al., 2008). Similar to Lafleur et al. (2003), we found years with a drier growing season to transition from net CO_2 sink to net CO_2 source earlier than other years of the study period. The earlier transition to a net CO_2 source compared to other studies may also be a result of geographic location and the potential influence of eastern Georgian Bay on weather patterns in this region of the boreal shield.

The interannual variability in meteorological variables did not considerably affect daily and cumulative ER between years, it appears the differences in summer NEE are more attributable to changes in summer GPP between years. There is also limited evidence of changes in ER as a result of WTD, considering the stronger relationship between winter air temperatures with cumulative summer ER. We found winter and early spring air temperatures to be an important

predictor of summer ER, where 2020 experienced the warmest pre-growing season air temperature and 2019 the coldest. The warm winter and spring of 2020, 2018 and 2017 may have induced an early snowmelt, allowing for the start of hydrological connectivity from water the rock barrens landscape and into the peatlands thereby increasing soil moisture, triggering the start of vegetation phenology (Kreyling, 2010). Warmer winters may also stimulate and earlier ramp up of ER as vegetation phenology progresses, through the inherent exponential relationship between temperature and ER (Lloyd & Taylor, 1994), where the warm winter allowed for greater total ER CO_2 emission for the summer as these years had an earlier start to the growing season and the vegetation community may be in slightly different phenological stages.

2.5.2 Water storage as control on CO_2 fluxes

Fill and spill hydrological dynamics are important in the boreal shield as peatlands on the rock barrens landscape are positioned in shallow bedrock basins, relying on precipitation and overland flow from upland areas to fill the peatland (Spence and Woo, 2003). This hydrological connectivity between landscape units usually decreases or ceases completely during periods of the growing season, leaving the ecosystem vulnerable to drought conditions. Throughout the growing season, water table dynamics follow similar trends in all study years, where the water table experiences small scale fluctuations in response to rain events while remaining in the top 30 cm of peat until the beginning of June and maintaining daily net CO_2 uptake. Summer drought periods were experienced in 2016, 2018, and 2019, with the water table falling below 40 cm in the peat profile for a period of time in the summer season. In 2017 and 2020, the water table was maintained in the top of the peat profile throughout the summer because of large rain events throughout the summer. The occurrence of a summer drought period in two years of this study has shown there is

a significant relationship between water table depth and total summer NEE and GPP. The response of GPP to changes in water table depth have been varied. For example, Ratcliffe et al. (2019) observed no change in GPP to water table fluctuations, while there have been several occurrences of changes in GPP with changes in WT where lower WT would decrease GPP (*e.g.* Humphreys et al., 2014; Strachan et al., 2016; Sulman et al., 2010), and limited GPP at WT extremes (*e.g.* Peichl et al., 2014; Ratcliffe et al., 2019; Sonnentag et al., 2010). At our study site there was greater diurnal daytime CO_2 uptake and cumulative summer GPP in non-drought years, while years with a summer drought had lower CO_2 uptake in comparison to other studies (Sonnentag et al., 2010; Strachan et al., 2016). The relationship between CO_2 exchange and WTD was more important at the seasonal scale than the daily scale for this study, similar to Bubier et al. (1998). Although there is greater cumulative ER in years with a wet summer, the relationship was not statistically significant with mean summer water table depth. Dry summers may also be associated with greater DOC export (Jager et al., 2009), and this area of research would be valuable to expand on in the boreal shield region.

Vegetation productivity was more efficient in years with wet summers, as evidenced by a shift in the light response relationship in 2017 and 2020 (Figure 2.8), which also may have led to greater autotrophic respiration contribution to total respiration (Moore et al., 2002; Strachan et al., 2016). Light response parameters for the summer season of each year demonstrate that vegetation communities are utilizing light for photosynthesis similarly to other peatland sites (Bubier et al., 2003; Frolking et al., 1998; Humphreys et al., 2006; Ratcliffe et al., 2019; Sonnentag et al., 2010). Combining the results of the light response relationship with the diurnal cycle of PPFD (Figure 2.3, 2.8), we did find evidence of enhanced light availability in the wet years that may be driving

differences in the light response relationship parameters. Differences in the interannual variability in light response parameters have been attributed to water availability in the ecosystem as a limiting factor for photosynthesis and similar to our results, warmer and drier years have been found to have lower alpha and GPP_{max} (Aurela et al., 2007). A water table closer to the surface of the peatland, and more specifically in the top 30 cm of peat provides optimal growing conditions for *Sphagnum* (Peichl et al., 2014; Rydin and McDonald, 1985), thus contributing to greater daytime uptake as the vegetation community has more efficient photosynthesis, and larger cumulative GPP during the summers where the water table did not fall below 30 cm depth.

2.5.3 Implications for future climate change

Boreal shield peatlands are unique in that they are shallower than other regions of the boreal and the hydrology of the ecosystem is highly connected to the surrounding landscape. Peatlands in the boreal shield may be more sensitive to climate interannual variability due to those characteristics, where peat depth plays an important role in the autogenic feedbacks of peatland ecosystems and thinner peat may be more susceptible to drought (Moore et al., 2021; Waddington et al., 2015). The responsiveness of boreal shield peatlands to climate may have important consequences for the ecosystem and landscape as a whole with a changing climate.

Given that future climate change is expected to result in an increase in air temperature and precipitation, there is likely a greater potential to affect carbon cycling in peatland ecosystems (D'Orgeville et al., 2014; Mortsch and Quinn, 1996; Notaro et al., 2015; Tarnocai, 2006). These changes to the climate regime will contribute cascading effects on C cycling through changes in

growing season length, natural disturbance regimes, and vegetation community changes (Fenner et al., 2007).

Increased temperatures may promote an earlier start to the growing season and extend the length of the growing season, and increase GPP but also be regulated by other environmental variables such as water and light availability thereby affecting net CO_2 exchange (Aurela et al., 2007; Nijp et al., 2015; Roulet et al., 2007). There have been observed increases in ER rates as a result of increased temperatures and changes in the vegetation community (Ward et al., 2013), and which may occur as a result of changes in climatic regimes in the future (Breeuwer et al., 2009; Walker et al., 2015). Increased winter air temperatures may increase the magnitude of total summer ER, as soils may not be subject to seasonal freezing and have a greater influence on total NEE than at present.

Changes to the moss and vascular vegetation community composition are expected if there are long-term changes in the water table regime (Breeuwer et al., 2009; Moore et al., 2002; Strack et al., 2006). This would have direct effects on above and below ground biomass and productivity, thereby changing the total C flux and storage of the ecosystem (Moore et al., 2002). A shift in *Sphagnum* community composition may occur with climate change, to *Sphagnum* species dominating that are more tolerant to deeper water tables and drier surface conditions (Dieleman et al., 2015; McCarter and Price, 2014; Moore et al., 2021) and a greater proportion of vascular vegetation (Breeuwer et al., 2009; Fenner et al., 2007). A persistently low water table may have different effects across microform types, where hummocks may experience a reduction of *Sphagnum* moss cover and surface moisture as well as enhanced respiration, while the lowering of

the water table at hollows increased *Sphagnum* and vascular vegetation cover at hollows (Strack et al., 2006).

Although there is a predicted increase in precipitation, greater evaporative water loss from peatlands is expected under a warming climate across the boreal region (Helbig et al., 2020) creating decreasing water availability for peatland ecosystems. This may leave the C stocks of peatlands vulnerable to release to the atmosphere naturally from limited photosynthesis, stimulated ecosystem respiration (Riutta et al., 2007), or due to natural disturbance, such as wildfire (Turetsky et al., 2002, 2015). This study provides an understanding of how the rock barrens peatland ecosystem may respond under a changing climate with a deeper water table regime. Moisture stress may decrease the productivity of the peatland vegetation community (Breeuwer et al., 2009; Moore et al., 2021). A deep water table leaves peatlands with an increased likelihood of ignition as a result of the disruption of hydroclimatic feedbacks in peat (Turetsky et al., 2015; Waddington et al., 2015). Drier peat is more susceptible to deep burning (Wilkinson et al., 2020), and may experience increased fire severity (Nelson et al., 2021). The recovery of vegetation following wildfire will promote CO_2 uptake by the vegetation community, although the return to a carbon sink is not expected until more than 10 years post-wildfire (Wieder et al., 2009).

Conclusion

The relationship between CO_2 exchange and water table depth is important in this landscape as peatlands throughout the rock barrens landscape are located in shallow bedrock basins, in that they are separated from regional groundwater and mainly rely on precipitation inputs and overland flow to maintain water storage function. This connection between CO_2 exchange processes and peatland water availability suggests that peatlands in the Canadian boreal shield region may be vulnerable to losing their CO_2 uptake capacity with climate change due to changes in precipitation frequency, greater increases in air temperature, and water loss through greater evapotranspiration. Further research on the full annual C budget of a boreal shield peatland would be important to characterize the sensitivity of different components of the C budget to meteorological interannual variability in Eastern Georgian Bay.

2.6 Literature cited

Aurela, M., Riutta, T., Laurila, T., Tuovinen, J., Vesala, T., Tuittila, E., Rinne, J., Haapanala, S., & Laine, J. (2007). CO_2 exchange of a sedge fen in southern Finland-the impact of a drought period. *Tellus B: Chemical and Physical Meteorology*, 59:5, 826-837. https://doi.org/10.1111/j.1600-0889.2007.00309.x.

Aurela, M., Laurila, T., & Tuovinen, J. (2004). The timing of snow melt controls the annual Co2 balance in a subarctic fen. *Geophysical Research Letters,* 31, L16119, 1-4. https://doi.org/10.1029/2004GL020315.

Benscoter, B. W., Vitt, D. H., & Wieder, R. K. (2005). Association of postfire peat accumulation and microtopography in boreal bogs. *Canadian Journal of Forest Research*, 35, 2188-2193. https://doi.org/10.1139/x05-115.

Blodau, C., Basiliko, N., & Moore, T. R. (2004). Carbon turnover in peatland mesocosms exposed to different water table levels. *Biogeochemistry,* 67, 331-351. https://doi.org/10.1023/B:BIOG.0000015788.30164.e2.

Breeuwer, A., Robroek, B. J. M., Limpens, J., Heijmans, M. M. P. D., Schouten, M. G. C., & Berendse, F. (2009). Decreased summer water table depth affects peatland vegetation. *Basic and Applied Ecology*, 10(4), 330-339. https://doi.org/10.1016/j.baae.2008.05.005.

Bubier, J. L., Bhatia, G., Moore, T. R., Roulet, N. T., & Lafleur, P. M. (2003). Spatial and Temporal Variability in Growing-Season Net Ecosystem Carbon Dioxide Exchange at a Large Peatland in Ontario, Canada. *Ecosystems*, 6, 353-367. https://doi.org/10.1007/s10021-003-0125-0.

Bubier, J. L., Crill, P. M., Moore, T. R., Savage, K., & Varner, R. K. (1998). Seasonal patterns and controls on net ecosystem CO_2 exchange in a boreal peatland complex. *Global Biogeochem. Cycles*, 12(4), 703-714. https://doi.org/10.1029/98GB02426.

Catling, P. M., & Brownell, V. R. (1999). The Flora and Ecology of Southern Ontario Granite Barrens. In R. C. Anderson, J. S. Fralish, & J. M. Baskin (Eds.) *Savannas, Barrens, and Rock Outcrop Plant Communities of North America* (pp. 392-405). Cambridge University Press.

Chimner, R. A., Pypker, T. G., Hribljan, J. A., Moore, P. A., & Waddington, J. M. (2017). Multi-decadal Changes in Water Table Levels Alter Peatland Carbon Cycling. *Ecosystems*, 20(5), 1042-1057. https://doi.org/10.1007/s10021-016-0092-x.

Clymo, R. S. (1987). The ecology of peatlands. *Science Progress (1933-)*, 71, 593-614.

Clymo, R. S. (1984). The Limits to Peat Bog Growth. *Philosophical Transactions of the Royal Society B: Biological Sciences,* 303 (1117), 605-654. https://doi.org/10.1098/rstb.1984.0002.

Devito, K. J., Dillon, P. J., & Lazerte, B. D. (1989). Phosphorus and nitrogen retention in five Precambrian shield wetlands. *Biogeochemistry*, 8, 185-204. https://doi.org/10.1007/BF00002888.

Dieleman, C. M., Branfireun, B. A., McLaughlin, J. W., & Lindo, Z. (2015). Climate change drives a shift in peatland ecosystem plant community: Implications for ecosystem function and stability. *Global Change Biology,* 21(1), 388-395. https://doi.org/10.1111/gcb.12643.

Dixon, S. J., Kettridge, N., Moore, P. A., Devito, K. J., Tilak, A. S., Petrone, R. M., Mendoza, C. A., & Waddington, J. M. (2017). Peat depth as a control on moss water availability under evaporative stress. *Hydrological Processes,* 31(23), 4107-4121. https://doi.org/10.1002/hyp.11307.

d'Orgeville, M., Peltier, W. R., Erler, A., & Gula, J. (2014). Climate change impacts on Great Lakes Basin precipitation extremes. *JGR: Atmospheres*, 119, 10799-10812. https://doi.org/10.1002/2014JD021855.

Drever, C. R., Cook-Patton, S. C., Akhter, F., Badiou, P. H., Chmura, G. L., Davidson, S. J., Desjardins, R. L., et al. (2021). Natural climate solutions for Canada. *Science Advances*, 7, 1-14.

Environment Canada. (2021). Daily Data Report for Parry Sound CCG. [Data file]. Retrieved from https://climate.weather.gc.ca/climate_data/daily_data_e.html?StationID=32128.

Falge, E., Baldocchi, D., Olsen, R., Anthoni, P., Aubinet, M., Bernhofer, C., Burba, G., Ceulemans, R., Clement, R., Dolman, H., Cranier, A., Gross, P., Grünwald, Hollinger, D., Jensen, N.-O., Katul, G., Keronen, P., Kowalski, A., Lai, C., … Wofsy, S. (2001). Gap filling strategies for defensible annual sums of net ecosystem exchange. *Agricultural and Forest Meteorology,* 107(1), 43-69. https://doi.org/10.1016/S0168-1923(00)00225-2.

Fenner, N., Ostle, N. J., McNamara, N., Sparks, T., Harmens, H., Reynolds, B., & Freeman, C. (2007). Elevated CO_2 Effects on Peatland Plant Community Carbon Dynamics and DOC Production. *Ecosystems*, 10(4), 635-657. https://doi.org/10.1007/s10021-007-9051-x.

Flannigan, M., Stocks, B., Turetsky, M., & Wotton, B. (2009). Impacts of climate change on fire activity and fire management in the circumboreal forest. *Global Change Biology,* 15(3), 549-560. https://doi.org/10.1111/j.1365-2486.2008.01660.x.

Fortuniak, K., Pawlak, W., Siedlecki, M., Chambers, S., & Bednorz, L. (2021). Temperate mire fluctuations from carbon sink to carbon source following changes in water table. *Science of the Total Environment*, 756, 144071. https://doi.org/10.1016/j.scitotenv.2020.144071.

Frolking, S. E., Bubier, J. L., Moore, T. R., Ball, T., Bellisario, L. M., Bhardwaj, A., Carroll, P., Crill, P. M., Lafleur, P. M., McCaughey, J. H., Roulet, N. T., Suyker, A. E., Verma, S. B., Waddington, J. M., & Whiting, G. J. (1998). Relationship between ecosystem productivity and photosynthetically active radiation for northern peatlands. *Global Biogeochem. Cycles,* 12(1), 115-126. https://doi.org/10.1029/97GB03367.

Fu, Z., Stoy, P. C., Luo, Y., Chen, J., Sun, J., Montagnani, L., Wohlfahrt, G., Rahman, A. F., Rambal, S., Bernhofer, C., Wang, J., Shirkey, G., & Niu, S. (2017). Climate controls over the net carbon uptake period and amplitude of net ecosystem production in temperate and boreal ecosystems. *Agricultural and Forest Meteorology,* 243, 9-18. https://doi.org/10.1016/j.agrformet.2017.05.009.

Gorham, E. (1991). Northern Peatlands: Role in the Carbon Cycle and Probably Response to Climatic Warming. *Ecological Applications,* 1(2), 182-195.

Helbig, M., Humphreys, E. R., & Todd, A. (2019). Contrasting Temperature Sensitivities of CO_2 Exchange in Peatlands of the Hudson Bay Lowlands, Canada. *JGR: Biogeosciences,* 124, 2126-2143. https://doi.org/10.1029/2019JG005090.

Helbig, M., Waddington, J. M., Alekseychik, P., Amiro, B. D., Aurela, M., Barr, A. G., Black, T. A., Blanken, P. D., Carey, S. K., et al. (2020). Increasing contribution of peatlands to boreal evapotranspiration in a warming climate. *Nature Climate Change,* 10(6), 555-560. https://doi.org/10.1038/s41558-020-0763-7.

Hu, L., Andrews, A. E., Thoning, K. W., Sweeney, C., Miller, J. B., Michalak, A. M., Dlugokencky, E., Tans, P. P., et al. (2019). Enhanced North American carbon uptake associated with El Nino. *Science Advances,* 5(6), 1-11. https://doi.org/10.1126/sciadv.aaw0076.

Humphreys, E. R., Lafleur, P. M., Flanagan, L. B., Hedstrom, N., Syed, K. H., Glenn, A. J., & Granger, R. (2006). Summer carbon dioxide and water vapour fluxes across a range of northern peatlands. *Journal of Geophysical Research,* 111, G04011. https://doi.org/10.1029/2005JG000111.

Jager, D. F., Wilmking, M., & Kukkonen, J. V. K. (2009). The influence of summer seasonal extremes on dissolved organic carbon export from a boreal peatland catchment: Evidence from one dry and one wet growing season. *Science of the Total Environment*, 407(4), 1373-1382. https://doi.org/10.1016/j.scitotenv.2008.10.005.

Järveoja, J., Nilsson, M. B., Gažovič, M., Crill, P. M., & Peichl, M. (2018). Partitioning of net CO_2 exchange using an automated chamber system reveals plant phenology as key control of production and respiration fluxes in a boreal peatland. *Global Change Biology*, 24, 3436-3451. https://doi.org/10.1111/gcb.14292.

Kljun, N., Calanca, P., Rotach, M. W., & Schmid, H. P. (2015). A simple two-dimensional parameterisation for Flux Footprint Prediction (FFP). *Geoscientific Model Development*, 8(11), 3695-3713. https://doi.org/10.5194/gmd-8-3695-2015.

Kreyling, J. (2010). Winter climate change: a critical factor for temperate vegetation performance. *Ecology,* 91(7), 1939-1948.

Kross, A. S. E., Roulet, N. T., Moore, T. R., Lafleur, P. M., Humphreys, E. R., Seaquist, J. W., Flanagan, L. B., & Aurela, M. (2014). Phenology and its role in carbon dioxide exchange processes in northern peatlands. *JGR: Biogeosciences*, 119, 1370-1384. https://doi.org/10.1002/ 2014JG002666.

Lafleur, P. M., Roulet, N. T., Bubier, J. L., Frolking, S., & Moore, T. R. (2003). Interannual variability in the peatland-atmosphere carbon dioxide exchange at an ombrotrophic bog. *Global Biogeochemical Cycles,* 17(2), 1-14. https://doi.org/10.1029/2002gb001983.

Lasslop, G., Reichstein, M., Papale, D., Richardson, A. D., Arneth, A., Barr, A., Stoy, P., & Wohlfahrt, G. (2010). Separation of net ecosystem exchange into assimilation and respiration using a light response curve approach: critical issues and global evaluation. *Global Change Biology,* 16(1), 187-208.

Liu, M., He, H., Yu, G., Luo, Y., Sun, X., & Wang, H. (2009). Uncertainty analysis of CO_2 flux components in sub-tropical evergreen coniferous plantation. *Science in China Series D: Earth Sciences,* 52(2), 257-268. https://doi.org/10.1007/s11430-009-0010-6.

Lloyd, J., & Taylor, J. A. (1994). On the Temperature Dependence of Soil Respiration. *Functional Ecology,* 8(3), 315-323.

Lund, M., Lafleur, P. M., Roulet, N. T., Lindroth, A., Christensen, T. R., Aurela, M., Chojnicki, B. H., et al. (2010). Variability in exchange of CO_2 across 12 northern peatland and tundra sites. *Global Change Biology*, 16, 2436-2448. https://doi.org/10.1111/j.1365-2486.2009.02104.x.

Lund, M., Christensen, T. R., Lindroth, A., & Schubert, P. (2012). Effects of drought conditions on the carbon dioxide dynamics in a temperate peatland. *Environmental Research Letters,* 7(4), 045704, https://doi.org/10.1088/1748-9326/7/4/045704.

Markle, C. E., North, T. D., Harris, L. I., Moore, P. A., & Waddington, J. M. (2020a). Spatial Heterogeneity of Surface Topography in Peatlands: Assessing Overwintering Habitat Availability for the Eastern Massasauga Rattlesnake. *Wetlands*, 40, 2337-2349. https://doi.org/10.1007/s13157-020-01378-2.

Markle, C. E., Wilkinson, S. L., & Waddington, J. M. (2020b). Initial Effects of Wildfire on Freshwater Turtle Nesting Habitat. *Journal of Wildlife Management,* 84(7), 1373-1383. https://doi.org/10.1002/jwmg.21921.

McCarter, C. P. R., & Price, J. S. (2014). Ecohydrology of Sphagnum moss hummocks: mechanisms of capitula water supply and simulated effects of evaporation. *Ecohydrology*, 7(1), 33-44. https://doi.org/10.1002/eco.1313.

Moncrieff, J. B., Malhi, Y., & Leuning, R. (1996). The propagation of errors in long-term measurements of land-atmosphere fluxes of carbon and water. *Global Change Biology*, 2(3), 231-240. https://doi.org/10.1111/j.1365-2486.1996.tb00075.x.

Moore, T. R., Bubier, J. L., Frolking, S. E., Lafleur, P. M., & Roulet, N. T. (2002). Plant biomass and production and CO_2 exchange in an ombrotrophic bog. *Journal of Ecology,* 90(1), 25-36. https://doi.org/10.1046/j.0022-0477.2001.00633.x.

Moore, T. R., & Knowles, R. (1989). The influence of water table levels on methane and carbon dioxide emissions from peatland soils. *Canadian Journal of Soil Science,* 69(1), 33-38. https://doi.org/10.4141/cjss89-004.

Moore, P. A., Didemus, B. D., Furukawa, A. K., & Waddington, J. M. (2021). Peat depth as a control on Sphagnum moisture stress during seasonal drought. *Hydrological Processes*, 35, e14117. https://doi.org/10.1002/hyp.14117.

Moore, P. A., Smolarz, A. G., Markle, C. E., & Waddington, J. M. (2019). Hydrological and thermal properties of moss and lichen species on rock barrens: Implications for turtle nesting habitat. *Ecohydrology,* 12, e2057. https://doi.org/10.1002/eco.2057.

Mortsch, L. D., & Quinn, F. H. (1996). Climate change scenarios for Great Lakes Basin ecosystem studies. *Limnology and Oceanography,* 41(5), 903-911. https://doi.org/10.4319/lo.1996.41.5.0903.

Murphy, M. T., & Moore, T. R. (2010). Linking root production to aboveground plant characteristics and water table in a temperate bog. *Plant and Soil,* 336(1), 219-231. https://doi.org/10.1007/s11104-010-0468-1.

Nelson, K., Thompson, D., Hopkinson, C., Petrone, R., & Chasmer, L. (2021). Peatland-fire interactions: A review of wildland fire feedbacks and interactions in Canadian boreal peatlands. *Science of the Total Environment*, 769, 145212. https://doi.org/10.1016/j.scitotenv.2021.145212.

Nichols, J. E, & Peteet, D. M. (2019). Rapid expansion of northern peatlands and doubled estimate of carbon storage. *Nature Geoscience,* 12(11), 917-921. https://doi.org/10.1038/s41561-019-0454-z

Nijp, J. J., Limpens, J., Metselaar, K., Peichl, M., Nilsson, M. B., van der Zee, S. E. A. T. M., & Berendse, F. (2015). Rain events decrease boreal peatland net CO_2 uptake through reduced light availability. *Global Change Biology*, 21, 2309-2320. https://doi.org/10.1111/gcb.12864.

Notaro, M., Bennington, V., & Vavrus, S. (2015). Dynamically Downscaled Projections of Lake-Effect Snow in the Great Lakes Basin. *Journal of Climate,* 28(4). 1661-1684. https://doi.org/10.1175/JCLI-D-14-00467.1.

Papale, D., Reichstein, M., Aubinet, M., Canfora, E., Bernhofer, C., Kutsch, W., Longdoz, B., Rambal, S., Valentini, R., Vesala, T., & Yakir, D. (2006). Towards a standardized processing of Net Ecosystem Exchange measured with eddy covariance technique: algorithms and uncertainty estimation. *Biogeosciences,* 3(4), 571-583. https://doi.org/10.5194/bg-3-571-2006.

Peichl, M., Öquist, M., Löfvenius, M. O., Ilstedt, U., Sagerfors, J., Grelle, A., Lindroth, A., & Nilsson, M. B. (2014). A 12-year record reveals pre-growing season temperature and water table level threshold effects on the net carbon dioxide exchange in a boreal fen. *Environmental Research Letters,* 9(5). https://doi.org/10.1088/1748-9326/9/5/055006.

Piao, S., Ciais, P., Friedlingstein, P., Peylin, P., Reichstein, M., Luyssaert, S., Margolis, H., Fang, J., Barr, A., Chen, A., et al. (2008). Net carbon dioxide losses of northern ecosystems in response to autumn warming. *Nature,* 451(7174), 49-52. https://doi.org/10.1038/nature06444.

R Core Team (2020). R: A language and environment for statistical computing. R Foundation for Statistical Computing, Vienna, Austria. URL https://www.R-project.org/.

Ratcliffe, J. L., Campbell, D. I., Clarkson, B. R., Wall, A. M., & Schipper, L. A. (2019). Water table fluctuations control CO_2 exchange in wet and dry bogs through different mechanisms. *Science of the Total Environment*, 655, 1037-1046. https://doi.org/10.1016/j.scitotenv.2018.11.151.

Reichstein, M., Falge, E., Baldocchi, D., Papale, D., Aubinet, M., Berbigier, P., Bernhofer, C., Buchmann, N., Gilmanov, T., Granier A., Grünwald, T., Kavránková, K., Ilvesniemi, H., Janous, D., Knohl, A., Laurila, T., Lohila, A., Loustau, D., Matteucci, G., … Valentini, R. (2005). On the separation of net ecosystem exchange into assimilation and ecosystem respiration: review and improved algorithm. *Global Change Biology*, 11(9), 1424-1439. https://doi.org/10.1111/j.1365-2486.2005.001002.x.

Richardson, A. D., Aubinet, M., Barr, A. G., Hollinger, D. Y., Ibrom, A., Lasslop, G., & Reichstein, M. (2012). Uncertainty quantification. In *Eddy covariance* (pp. 173-209). Springer, Dordrecht.

Riutta, T., Laine, J., Aurela, M., Rinne, J., Vesala, T., Laurila, T., Haapanala, S., Pihlatie, M., & Tuittila, E. S. (2007). Spatial variation in plant community functions regulates carbon gas dynamics in a boreal fen ecosystem. *Tellus B: Chemical and Physical Meteorology*, 59(5), 838-852. https://doi.org/10.1111/j.1600-0889.2007.00302.x.

Robroek, B. J .M., van Ruijven, J., Schouten, M. G. C., Breeuwer, A., Crushell, P. H., Berendse, F., & Limpens, J. (2009). Sphagnum re-introduction in degraded peatlands: The effects of aggregation, species identity and water table. *Basic and Applied Ecology,* 10(8), 697-706. https://doi.org/10.1016/j.baae.2009.04.005.

Roulet, N. T., Lafleur, P. M., Richard, P. J. H., Moore, T. R., Humphreys, E. R., & Bubier, J. (2007). Contemporary carbon balance and late Holocene carbon accumulation in a northern peatland. *Global Change Biology*, 13(2), 397-411. https://doi.org/10.1111/j.1365-2486.2006.01292.x.

Rydin, H., & McDonald, A. J. S. (1985). Tolerance of Sphagnum to water level. *Journal of Bryology,* 13, 572-578. https://doi.org/10.1179/jbr.1985.13.4.571.

Shabbar, A. (2006). The impact of El Niño-Southern Oscillation on the Canadian climate. *Advances in Geosciences,* 6, 149-153. https://doi.org/10.5194/adgeo-6-149-2006.

Shabbar, A., Bonsal, B., & Khandekar, M. (1997). Canadian precipitation patterns associated with the Southern Oscillation. *Journal of Climate,* 10(12), 3016-3027. https:// 10.1175/1520-0442(1997)010<3016:CPPAWT>2.0.CO;2.

Smolarz, A. G., Moore, P. A., Markle, C. E., & Waddington, J. M. (2018). Identifying resilient Eastern Massasauga Rattlesnake (Sistrurus catenatus) peatland hummock hibernacula. *Canadian Journal of Zoology,* 96(6), 1024-1031. https://doi.org/10.1139/cjz-2017-0334.

Spence, C., & Woo, M. (2003). Hydrology of subarctic Canadian shield: soil-filled valleys. *Journal of Hydrology*, 279, 151-166. https://doi.org/10.1016/S0022-1694(03)00175-6.

Sonnentag, O., van der Kamp, G., Barr, A. G., & Chen, J. M. (2010). On the relationship between water table depth and water vapour and carbon dioxide fluxes in a minerotrophic fen. *Global Change Biology*, 16(6), 1762-1776. https://doi.org/10.1111/j.1365-2486.2009.02032.x.

Strachan, I. B., Pelletier, L., & Bonneville, M. (2016). Inter-annual variability in water table depth controls net ecosystem carbon dioxide exchange in a boreal bog. *Biogeochemistry,* 127, 99-111. https://doi.org/10.1007/s10533-015-0170-8.

Strack, M., & Price, J. S. (2009). Moisture controls on carbon dioxide dynamics of peat-Sphagnum monoliths. *Ecohydrology,* 2, 34-41. https://doi.org/10.1002/eco.36.

Strack, M., Waddington, J. M., Rochefort, L., & Tuitilla, E.-S. (2006). Response of vegetation and net ecosystem carbon dioxide exchange at different peatland microforms following water table drawdown. *Journal of Geophysical Research*, 111, G02006. https://doi.org/10.1029/2005JG000145.

Tarnocai, C. (2006). The effect of climate change on carbon in Canadian peatlands. *Global and Planetary Change,* 53(4), 222-232. https://doi.org/10.1016/j.gloplacha.2006.03.012.

Turetsky, M., Wieder, K., Halsey, L., & Vitt, D. (2002). Current disturbance and the diminishing peatland carbon sink. *Geophysical Research Letters,* 29(11). https://doi.org/10.1029/2001GL014000.

Turetsky, M. R., Benscoter, B., Page, S., Rein, G., van der Werf, G. R., & Watts, A. (2015). Global vulnerability of peatlands to fire and carbon loss. *Nature Geoscience,* 8(1), 11-14. https://doi.org/10.1038/ngeo2325.

Waddington, J. M., Morris, P. J., Kettridge, N., Granath, G., Thompson, D. K., & Moore, P. A. (2015). Hydrological feedbacks in northern peatlands. *Ecohydrology*, 8, 113-127. https://doi.org/10.1002/eco.1493.

Walker, T. N., Ward, S. E., Ostle, N. J., & Bardgett, R. D. (2015). Contrasting growth responses of dominant peatland plants to warming and vegetation composition. *Oecologia,* 178, 141-151. https://doi.org/10.1007/s00442-015-3254-1.

Ward, S. E., Ostle, N. J., Oakley, S., Quirk, H., Henrys, P. A., & Bardgett, R. D. (2013). Warming effects on greenhouse gas fluxes in peatlands are modulated by vegetation composition. *Ecology Letters,* 16(10), 1285-1293. https://doi.org/10.1111/ele.12167.

Webb, E. K., Pearman, G. I., & Leuning, R. (1980). Correction of flux measurements for density effects due to heat and water vapour transfer. *Quarterly Journal of the Royal Meteorological Society*, *106*(447), 85-100.

Wieder, R. K., Scott, K. D., Kamminga, K., Vile, M. A., Vitt, D. H., Bone, T., Xu, B., Benscoter, B. W., & Bhatti, J. S. (2009). Postfire carbon balance in boreal bogs of Alberta, Canada. *Global Change Biology,* 25(1), 63-81. https://doi.org/10.1111/j.1365-2486.2008.01756.x.

Wilkinson, S. L., Tekatch, A. M., Markle, C. E., Moore, P. A., & Waddington, J. M. (2020). Shallow peat is most vulnerable to high peat burn severity during wildfire. *Environmental Research Letters,* 15(10), 104032. https://doi.org/10.1088/1748-9326/aba7e8.

Wutzler, T., Lucas-Moffat, A., Migliavacca, M., Knauer, J., Sickel, K., Šigut, L., Menzer, O., & Reichstein, M. (2018). Basic and extensible post-processing of eddy covariance flux data with REddyProc. *Biogeosciences,* 15, 5015-5030. https://doi.org/10.5194/bg-2018-56.

Xu, J., Morris, P. J., Liu, J., & Holden, J. (2018). PEATMAP: Refining estimates of global peatland distribution based on a meta-analysis. *Catena*, 160, 134-140. https://doi.org/10.1016/j.catena.2017.09.010.

Yu, Z., Loisel, J., Brosseau, D. P., Beilman, D. W., & Hunt, S. J. (2010). Global peatland dynamics since the Last Glacial Maximum. *Geophysical Research Letters,* 37, LI3402. https://doi.org/10.1029/2010GL043584.

Chapter 3 – Post-wildfire CO_2 exchange from a boreal shield peatland, Ontario, Canada

3.1 Abstract

Peatlands are globally significant carbon storage reservoirs, at risk of losing this long term carbon store due to a changing climate and increased natural disturbance, such as wildfire. Within the boreal biome, drier environmental conditions may lead to a cascade of effects including increased vulnerability to combustion and a loss of water table leading to the loss of CO_2 uptake capacity from limited photosynthesis. Carbon cycling in a post-wildfire ecosystem may be altered due to the recovery of lost vegetation communities, and the potential for limited water availability and storage on the landscape. Rapid recovery of vegetation within boreal plains peatlands has been found to be essential for the recovery of C uptake capacity of the ecosystem, however post-wildfire recovery through CO_2 exchange measurements have not been previously studied in the boreal shield region. In an effort to fill this knowledge gap, we quantify ecosystem- and plot-scale CO_2 exchange from and around a recently burned peatland within a >11,000 ha wildfire footprint on Eastern Georgian Bay. We used the eddy covariance technique to capture growing season CO_2 fluxes 1- and 2- years post-wildfire, and the chamber technique to measure plot-scale CO_2 fluxes toward the end of the summer of the 2nd year post-wildfire. Within the two years post-wildfire, the burned site was a net CO_2 sink, and the year with more frequent and greater rainfall had greater CO_2 uptake and photosynthetic efficiency at both the burned and unburned control site. The responsiveness of boreal shield peatlands to wet and dry events, and the capacity to turn on and

off in response to water availability, indicates the sensitivity of these ecosystems to future climate change and the possibility of net CO_2 loss during the summer depending on presence and severity of summer drought.

3.2 Introduction

Peatlands in northern regions have been accumulating carbon throughout the Holocene and are important ecosystems for long term carbon storage (Blodau et al., 2004; Clymo, 1987; Loisel et al., 2014). Peatlands store approximately one third of the global soil organic carbon pool, while covering only 2.8% of the global land area (Gorham, 1991; Xu et al., 2018). Climate change induced changes in temperature (Mortsch and Quinn, 1996), precipitation (D'Orgeville et al., 2014; Notaro et al., 2015), increases in evapotranspiration (Helbig et al., 2020), and frequency of disturbance, such as wildfire, are expected to affect several processes within the ecosystem CO_2 budget (Morison et al., 2021, 2020; Turetsky et al., 2002). Drier environmental conditions may lead to the loss of the capacity of the ecosystem to act as a carbon sink through decreased primary productivity (Aurela et al., 2007; Strachan et al., 2016), increased ecosystem respiration (Cai et al., 2010; Lund et al., 2010; Riutta et al., 2007), and increased likelihood of combustion (Thompson et al., 2019; Wilkinson et al., 2020).

Wildland fire is a significant natural disturbance in the boreal region affecting northern peatlands (Turetsky et al., 2002). Increased frequency of wildland fire frequency, intensity, and extent of affected areas are expected with future climate change (Bergeron and Flannigan, 1995; Flannigan et al., 2005; Kasischke and Turetsky, 2006). Wildfire affects several ecosystem processes in peatlands including altering peat properties (Sherwood et al., 2013; Thompson and Waddington, 2013), essential for the ecosystem's resilience and self-regulating ecohydrological

feedbacks (Waddington et al., 2015). There is evidence peatlands are resilient ecosystems capable of returning to a net carbon sink in approximately 13 years post-wildfire (Wieder et al., 2009). However, the loss of surface vegetation coupled with deep combustion of the peat profile and changes in water availability may leave peatland ecosystems at risk of transitioning from a carbon sink to a carbon source in the future through a change in the vegetation community (Kettridge et al., 2015; Turetsky et al., 2002, 2015).

Wildfire affects C-cycling in peatlands through the instantaneous loss of C through combustion, the loss of above ground vegetation affecting primary production following fire (Turetsky et al., 2002), and below-ground changes to the peat structure and decomposition rates (Gray et al., 2020). In the boreal region, peatlands in Canada's boreal plains have been estimated to recover after wildfire from carbon source back to carbon sink over 10 years post-fire (Weider et al. 2009). Rapid vegetation recovery post-fire is an important process to re-initiate carbon uptake for a recently burned peatland, and vegetation may re-colonize more rapidly following low severity fires (Gray et al., 2020). *Sphagnum* communities would be less affected by low severity fires due to their moisture-retaining function, thereby contributing to post-fire carbon uptake and recolonization of the ecosystem (Grau-Andrés et al., 2017). While water availability is important for peatland ecosystem function, specifically moss photosynthesis and peat formation, severe burning can increase evaporative loss from burned areas with the possibility of further limiting ecosystem productivity (Kettridge et al. 2019, Waddington et al. 2015).

In the Canadian boreal shield region where the landscape is composed of heterogeneous rock barrens, peatlands formed in bedrock depressions on the landscape and are present at varying

spatial scales interspersed within upland forest areas (Catling and Brownell, 1999). These ecosystems are highly sensitive to water availability due to hydrological connectivity between landscape units primarily through the fill and spill process (Spence and Woo, 2003), relying on precipitation events to maintain the water table. Years with lower frequency and depth of precipitation events will not only leave these ecosystems with decreased carbon uptake capacity through lower primary production (Nijp et al., 2015; Strachan et al., 2016), but also may leave peat vulnerable to ignition and combustion from wildfire (Thompson et al., 2019). On the other hand, peatlands in the boreal shield have the potential for post-wildfire recovery faster than peatlands in the boreal plains considering the liberal water availability throughout early fall and spring (see *Chapter 2*). Although, there are no studies focused on the CO_2 exchange in a boreal shield peatland immediately following wildfire.

To fill this research gap, we quantify and compare the ecosystem-scale and plot-scale CO_2 fluxes 1- and 2- years post-fire in a burned and unburned a boreal shield peatland. To account for heterogeneity in the rock barrens landscape and peatland biogeochemistry, we use plot-scale CO_2 fluxes to identify key environmental controls over net ecosystem exchange and the component fluxes. We hypothesized primary production and ecosystem respiration would be lower at the burned peatland compared to the unburned peatland. Within the burned peatland, we hypothesize that differences in vegetation recovery post-fire due to a range of burn severity within the peatland will be reflected in a greater primary production and respiration in the middle, deep peat and lower burn severity areas. While in the shallow burned peatland margins, we hypothesize lower primary production and increased respiration will lead to positive NEE or net release.

3.3 Methods

3.3.1 Study Area

The two sites used in this study are located ~20 km (unburned) and ~80 km (burned) north of Parry Sound, ON, within the Georgian Bay Biosphere Mnidoo Gamii, a UNESCO Biosphere, situated within the Robinson-Huron Treaty of 1850 and the Williams Treaty of 1923, and located on Anishinabek territory. Ontario's Eastern Georgian Bay (EGB) region, located in the Ontario shield ecozone, consists of a mosaic of moss cushions and lichen mats, moss-dominated ephemeral wetlands, *Sphagnum*-dominated peatlands, and forested uplands of exposed granitic bedrock on the Canadian Boreal Shield (Hudson et al., 2021; Markle et al., 2020b; Moore et al., 2019; Wilkinson et al., 2020). The burned site is located within the footprint of the Parry Sound 33 wildfire which burned over 11,000 ha of the EGB rock barrens from July 18 to October 31, 2018. The eddy covariance tower at the burned site was set up in July 2019, and the unburned site was setup in June 2015. Regional 19-year (2002-2019) mean (± s.d.) annual temperature is 6.6 ± 11.3 ^{o}C, with mean monthly air temperature in January of -8.5 ^{o}C and a mean monthly air temperature in July of 20.5 ^{o}C. Long-term annual cumulative precipitation totals 853 ± 251 mm, and the growing season rainfall long-term mean is 452 ± 148 mm.

Vegetation community of the peatlands is comprised of a variety of shrubs (*Rhododendrom groenlandicum, Chamaedaphne calyculata, Kalmia angustifolia)*, graminoid species (Cotton grass, *Maianthemum trifolium)*, mosses *(Polytrichum strictum, Sphagnum palustre, Sphagnum fallax, Sphagnum cuspidatum)*, and jack pine *(Pinus banksiana)*. Tree species present in the upland forest area include tamararck *(Larix laricina),* black spruce *(Picea mariana)*, white pine (*Pinus strobus)*, and jack pine (*Pinus banksiana*). There is characteristic hummock-hollow

microtopography in the middle of the burned peatland, where hummock height ranges from 20 cm to 41 cm above the surrounding peat surface, with a mean hummock height of 31 cm (North 2021, *unpublished).*

3.3.2 Ecosystem-scale measurements

Eddy covariance CO_2 exchange

In accordance with the standard eddy covariance technique, 30-min CO_2 fluxes were calculated throughout the summer growing season (May to October) in 2019 and 2020 at the unburned and burned sites. Continuous fluxes of CO_2 were measured with wind velocity by an integrated three-dimensional sonic anemometer and open-path infrared gas analyzer (IRGASON, Campbell Scientific, Canada), along with fine wire thermocouple (FW10 Type E, OMEGA, Canada). Instruments were mounted 7.8 m above the land surface and oriented at 285^o at unburned, and 11.25 m above the land surface at 300^o at burned. Wind direction measurements were corrected to align with cardinal directions. All measurements were recorded on a CR5000 datalogger at the unburned and on a CR1000 at the burned site (Campbell Scientific, Canada).

Environmental variables

Environmental variables were measured simultaneously at the unburned tower, and a smaller meteorological tower was used to measure environmental variables at the burned site. Incoming solar radiation was measured by a pyranometer (SP-Lite2, Kipp & Zonen, Netherlands), and net radiation was recorded by a net radiometer (CNR1, Kipp & Zonen, Netherlands). Photosynthetic photon flux density (PPFD) was calculated from incoming shortwave radiation using a conversion factor of 2.3, the product of the fraction of incoming radiation that is

photosynthetically active radiation (approx. 0.5) and a unit conversion factor. Air temperature and relative humidity were measured with a temperature and relative humidity probe (HMP60, Vaisala, Finland). Precipitation was measured using a tipping bucket rain gauge (TE525M, Texus Electronics Inc., USA). Precipitation measurements for the burned area were taken from a site adjacent to the eddy covariance tower in 2019 and 2020. Water table depth (WTD) was measured every 15 minutes in the deepest part of the peatland to bedrock using Solinst levelogger pressure transducer (Solinst, Georgetown, ON) in 0.05 m diameter PVC wells.

Eddy covariance data analysis

Using the eddy covariance technique, NEE data were collected from two peatlands, one burned and one unburned, over the growing season (May to October) for 2019 and 2020. Net ecosystem exchange (NEE) of CO_2 was derived from the sum of turbulent CO_2 flux and the storage term at 10 Hz. Coordinate rotation, frequency response correction, density correction for temperature and humidity compensation (Webb et al., 1980), spike removal, and calculation of half-hourly fluxes were completed in an in-house Matlab script (Mathworks, USA).

Flux data were then processed using the *REddyProc* package in R for gap-filling, u* filtering, and flux partitioning (Wutzler et al., 2018). Prior to processing, vapour pressure deficit (VPD) is calculated from relative humidity and air temperature. Calculated NEE was filtered by a friction velocity threshold of 0.14 m s^{-1}, identified following Papale et al. (2006), representing the limit of turbulent conditions whereby below the threshold flux data may have large uncertainties due to low surface wind speed (Wutzler et al., 2018). This threshold was selected as this was the minimal velocity when the correlation with temperature from nighttime data, selected when the

global radiation is below 20 W m^{-2}, became weak or absent (Reichstein et al., 2005). Calculated NEE was gap filled using the marginal distribution sampling method and look up tables for incoming solar radiation (R_g), VPD, T_{air}, and mean diurnal course, and the number of days used in the algorithm increases until a window of more than 2 existing datapoints is identified (Reichstein et al., 2005; Wutzler et al., 2018). Proportion of each site and year's dataset identified as gap prior to filling were 43% (Unburned 2019), 45% (Unburned 2020), 61% (Burned 2019), 38% (Burned 2020). Marginal distribution sampling method was then used to gap fill environmental conditions: R_g, T_{air}, and VPD.

Flux partitioning was completed using daytime-based methods, a modified light-response curve that incorporates the temperature-respiration relationship is used to model NEE (Falge et al., 2001; Lasslop et al., 2010). NEE is the difference between gross primary productivity (GPP) and ecosystem respiration (ER) (Eq 3.1).

$$NEE = GPP - ER \quad (3.1)$$

A detailed flux footprint analysis was completed using the Kljun et al. (2015) flux footprint prediction model in R and a land classification scheme for each study site. A simple linear regression analysis was completed to determine if percent of the peat land cover class within each half-hour footprint is a significant predictor of flux.

Daily fluxes were calculated by converting the units of each half hourly measurement from μmol CO_2 m^{-2} s^{-1} to g C m^{-2} d^{-1}, fluxes were then summed for each day. Cumulative fluxes were calculated by adding successive daily flux together for a continuous period of time. For all measurements a negative flux indicates uptake by the ecosystem, and positive measurements

indicate exchange from ecosystem to atmosphere. Uncertainty estimates from half hour and daily gap-filled data were used to quantify uncertainty in the cumulative flux estimates for the summer season (Liu et al., 2009; Moncrieff et al., 1996; Richardson et al., 2012). For this analysis, growing season is from May 1 to October 31, and the summer season is classified as June 1 to August 31.

3.3.3 Plot-scale measurements

Static chamber CO_2 measurements

CO_2 exchange at the plot scale were measured using the static chamber approach. At the unburned peatland, five circular collars (20.5 cm diameter) were permanently placed in areas of the peatland characterized with 'shallow' peat depth, and five collars were placed areas of the peatland with 'deep' peat depth. Locations were selected to have varied microtopography and vegetation cover. In the burned peatland, six identical collars were placed in three paired hummock-hollow locations in the middle of the peatland. Four collars were placed in the margin, where there is minimal microtopography. Collars were inserted into the peat one week prior to sampling.

For each measurement, a clear plastic chamber (40.5 cm height, 20.5 cm diameter) was placed over each collar. Using a syringe, water was placed within the collar groove in order to create a seal with the chamber. A portable infrared gas analyzer (EGM-5, PP Systems) was used to measure CO_2 concentration every 10 seconds for a total sample time of 2 minutes. To help regulate temperature changes inside the chamber, cold water was pumped through the spiral copper coil inside the chamber every three to five measurements and a battery-operated fan was located at the top of the chamber for air circulation. Three measurements were taken at each collar, representing full light, half light using a sheer shroud, and dark condition using an opaque shroud

for respiration. PAR was recorded using a handheld sensor (Apogee Instruments) simultaneously with CO_2 concentration. Between each measurement, the chamber was removed from the collar to allow concentrations to return to ambient conditions.

Peat temperature at 10 cm depth was measured prior to every CO_2 measurement using a handheld temperature probe (Temp JKT Thermocouple Thermometer, Oakton Instruments), and volumetric water content was measured for the upper 6 cm depth using a handheld moisture probe (ML3 ThetaProbe Soil Moisture Sensor, Delta-T Devices).

Chamber CO_2 fluxes were calculated from the slope of the change in concentration over time. Fluxes with an $R^2 < 0.5$ were flagged and assessed manually for uncharacteristic behaviour over the sample time and subsequently removed, resulting in the removal of 1% of data points.

Vegetation surveys

Vegetation surveys were conducted 2 years post-fire, in July of 2020. Within the middle and margin areas of the burned site, plots were selected based on previously conducted depth of burn surveys (Wilkinson et al., 2020). Surveys were completed in 5 plots in the peatland middle and 5 plots in the peatland margin. Using a 1 m x 1 m quadrat, the total percent cover of bare peat, bare rock, litter, moss/lichen, and vascular plants were recorded. The percent cover of each species of moss, lichen, and vascular plants were also recorded. The dominant microform within each quadrat was classified (*i.e.* hummock, hollow, intermediate). Pre-fire peat depth data for each plot was previously recorded, and survey sites were selected at the unburned site using the range of pre-fire peat depth for margin and middle from the burned site.

Identical vegetation surveys were conducted within each CO_2 collar after installation. Leaf area index (LAI) was quantified at each collar by counting total vascular leaves within the collar area for each month of flux measurements, similar to Strack et al. (2006). For each vascular species present in the collars, three individuals outside of the collars were selected, all leaves were counted and length and width dimensions were measured to calculate average surface area of the leaves using standard geometric shape of the leaf (*e.g.* ellipse) (Wilson et al., 2007). The average surface area was multiplied by the number of leaves in each collar, and divided by collar area to determine LAI (Strack et al., 2006).

3.3.4 Analyses

Analyses were completed in R, version 4.0.3 (R Core Team, 2020). Ecosystem-scale growing season daily CO_2 fluxes were compared between sites and years using a Wilcoxon rank sum test, as the flux datasets for both sites did not meet the assumption of normality. The ecosystem-scale fluxes capture the general growing season from May 1 to October 31. When specified, portions of the analysis are focused only on the summer season, classified as the months of June, July, and August. At the plot-scale, to compare differences in CO_2 fluxes and environmental variables, Kruskal-Wallis analysis of variance tests were completed on the data grouped by (1) site (burned/unburned) and (2) peat depth zone (shallow/deep). Statistical tests were deemed statistically significant to the $p < 0.01$ level.

Light response

Light response curves were estimated from the relationship between measured NEE (μmol m^{-2} s^{-1}) and incoming PPFD (μmol m^{-2} s^{-1}) using the nonlinear least squares analysis in R. The light response relationship was evaluated based on the rectangular hyperbola equation from Frolking et al. (1998) (Eq 3.2):

$$NEE = \frac{\propto PPFD\ GPP_{max}}{\propto PPFD + GPP_{max}} + R \quad (3.2)$$

where ∝ represents the quantum yield (initial slope), R is the y-intercept (representing ecosystem respiration when there is no available light; μmol m^{-2} s^{-1}), GPP_{max} is the maximum gross photosynthesis (μmol m^{-2} s^{-1}). The initial conditions for ∝ and GPP_{max} specified within the *nls* function were 0.001 and 0.3, respectively, for plot-scale relationships and 0.01 and 5, respectively, for the ecosystem-scale relationships.

Ecohydrological controls on plot-scale CO_2 exchange

Generalized linear mixed effects models (GLMM, *lme4,* Bates et al., 2015) were used to determine the effects of ecohydrological variables on plot-scale fluxes (NEE, GPP, ER). The NEE data was normally distributed, and while GPP and ER followed a gamma distribution (fit with gamma distribution and log link using *glmer*). We tested models with a combination of peat temperature, VWC, mean PPFD, and LAI, with plot number as a random effect to account for non-independence of samples from the same plot. The models were compared using ANOVA, and model selection was based on Akaike's Information Criterion, likelihood ratio test. Variance inflation factor indicating multicollinearity, correlation of fixed effects, and estimate size were also considered following model comparison and selection.

3.4 Results

3.4.1 Environmental variables

Mean air temperatures were lower in 2019 than 2020 for both sites. At the unburned site growing season (May to October) daily air temperature ranged from 2.8 to 24.6 ºC in 2019, and -1.34 to 25.3 ºC in 2020, with mean daily air temperatures of 14.9 and 16.3 ºC in 2019 and 2020, respectively. At the burned site, mean growing season air temperature was 15.8 and 16.9 ºC in 2019 and 2020, respectively. In comparison to the climate normal from the nearest Environment Canada weather station (Parry Sound Station, 79 km from burned site), mean daily air temperatures for the whole growing season were greater than the 19-year long-term average, with the exception of 2019 at the unburned site (Environment Canada, 2021). At both sites, all months experienced colder than monthly average temperatures, with the exception of June and July of 2020 which were warmer than average.

Rainfall during the study period exceeded the long-term total growing season rainfall at the burned site for both years. At the burned site, total growing season rainfall was 508 mm for 2019, and 449 mm for 2020. Total growing season rainfall was greater at the unburned site than at the burned site for both years, where the unburned site accumulated 543 mm in 2019 and 481 mm in 2020. The summer season, June to August, in 2019 was drier than 2020, where there are more frequent rain events in the summer of 2020 (Figure 3.1). In September, both years experienced colder than average temperatures.

Water table dynamics closely followed daily rainfall throughout the growing season (Figure 3.1). The trends in water table depth were also similar between sites, although mean water table was deeper in 2019 than 2020 at both sites. Mean water table depth at the unburned site was

0.16 m and 0.10 m in 2019 and 2020, respectively. While at the burned site mean water table depth was 0.19 m and 0.12 m in 2019 and 2020, respectively. 2019 experienced a dry summer for the region, where water table depth fell below 0.4 m in August at both sites. In 2020, water table depth during the growing season was sustained by larger and more frequent rain events, markedly throughout the end of the summer season in July and August. These events kept the water table closer to the surface, in the top 20 cm of peat at the unburned site and in the top 40 cm of peat at the burned peatland.

The daily diurnal cycle of PPFD follows a characteristic trend, and for both sites maximum PPFD occurred in July in 2019 and June in 2020. Mean growing season PPFD at the unburned site was greater in 2019 than 2020, while at the burned site mean growing season PPFD was similar between years (Table 3.1).

Table 3.1: Environmental variables for unburned and burned sites for 2019 and 2020, including daily CO_2 fluxes from the eddy covariance towers. Winter air temperature data are missing for 2020 at the unburned site, and winter of 2019 at the burned site.

	Unburned		Burned	
	2019	2020	2019	2020
T_{air} (°C)	14.9	16.3	14.4	16.8
January mean T_{air} (°C)	-11.5			-5.0
July mean T_{air} (°C)	20.7	21.5	19.4	22.4
Mean WTD (m)	0.16	0.10	0.19	0.12
Total rainfall (mm)	531	481	368	380
Mean $PPFD_{GS}$ (umol m^{-2} s^{-1})	1106	1020	1123	1125
Mean NEE_{GS} (g C m^{-2} d^{-1})	-0.27	-0.54	-0.09	-0.79
GS NEE_{max} (g C m^{-2} d^{-1})	-2.54	-2.91	-1.69	-2.33

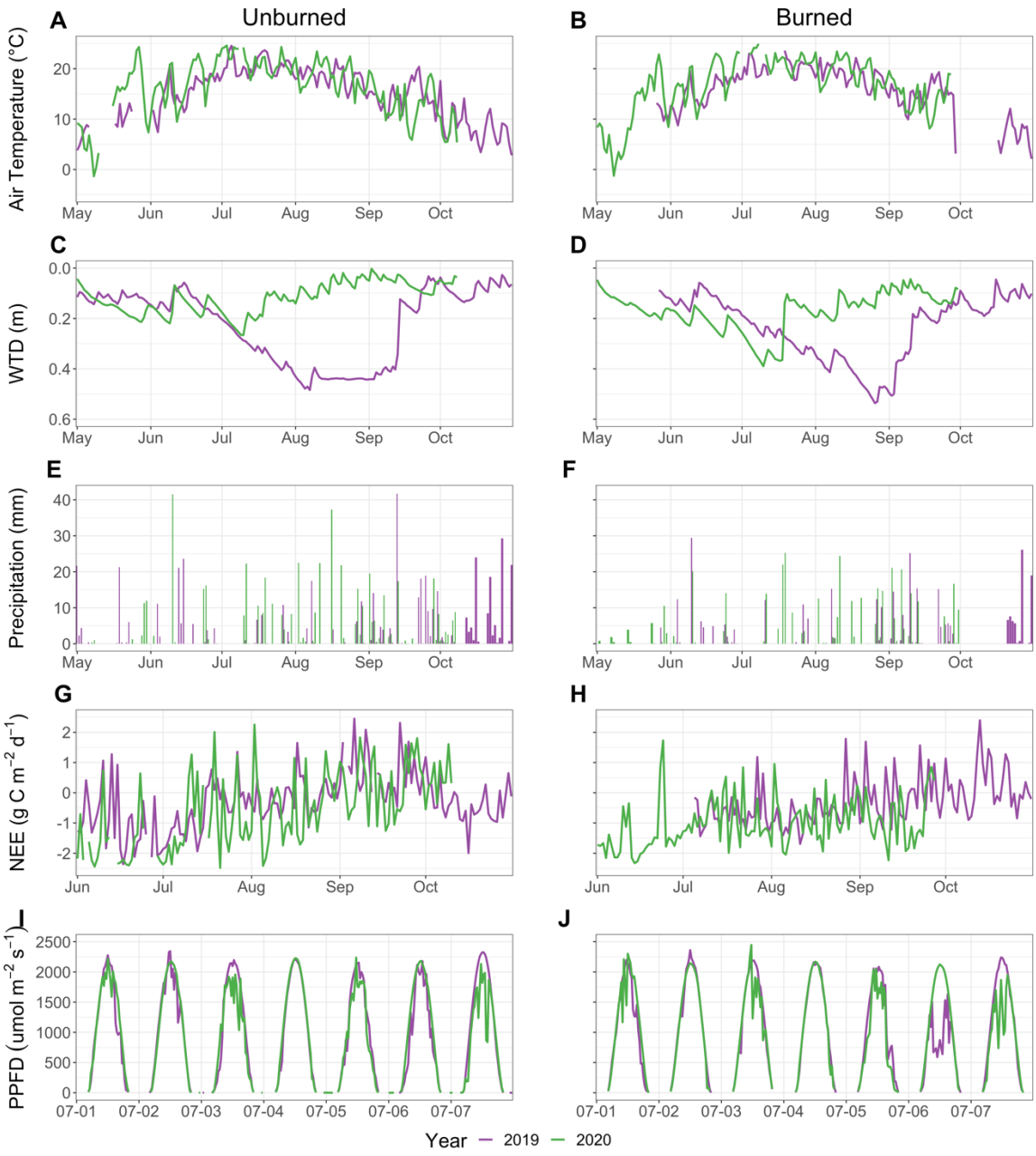

Figure 3.1: (A, B) Mean growing season daily air temperature (ºC), (C, D) mean growing season daily water table depth (m), (E, F) daily rainfall (mm), (G, H) daily NEE (g C m^{-2} d^{-1}), and (I, J) daily diurnal cycle of photosynthetic photon flux density (PPFD, µmol m^{-2} s^{-1}) for a typical week of the growing season (July 1-7). Left column shows unburned site, right column shows burned site. Years are represented by colours: 2019 - *purple*, 2020 – *green*.

3.4.2 Vegetation composition

Flux plots and general vegetation surveys were separated by peat depth into shallow and deep zones, and shallow zones were more severely burned and located in the margin of the peatlands (Wilkinson et al., 2020).

In the flux collars, mean peat depth for both categories was greater at the burned site than the unburned site (Table 3.2). Peat depth at the unburned peatland ranged from 35.5 – 45.5 cm in the shallow zone and 57.2 – 87.0 cm in the deep zone. At the burned peatland, peat depth ranged from 43.1 cm to 115 cm across both shallow and deep zones. Moss, lichen, and vascular plants dominated the composition of flux plots at the unburned site, litter covered less than 5% of the plots, and no bare peat was present at the time of sampling. At the burned peatland, bare peat was more prevalent in the deep zone than the shallow zone, however more moss and litter was present in the shallow zones (Figure 3.3). There was a similar mean percent cover of vascular plants in the shallow and deep zones.

In the flux collars, moss species at the unburned site was composed of *Sphagnum fallax* and *Sphagnum palustre*, and vascular plants in the flux collars was dominated by *Chamaedaphne calyculata.* In the burned peatland, moss species present included *Sphagnum fallax* and *Sphagnum palustre,* as well as *Polytrichum strictum*, *Sphagnum papillosum,* and singed *Sphagnum* at the deep flux plots only. The vascular species present at the burned site included *Chamaedaphne calyculata* in all plots, *Epilobium angustifolium, Kalmia angustifolia, Kalmia polifolia, Maianthemum trifolium* and *Rhododendron groenlandicum.*

Table 3.2: Mean vegetation characteristics (s.d.) for unburned and burned flux plots, separated by peat depth categories (shallow, deep).

	Unburned		Burned	
	Shallow	Deep	Shallow	Deep
Peat depth (cm)	39.6 (4)	70.8 (12)	53.7 (10)	93.0 (22)
Peat depth range (cm)	35.5 – 45.5	57.2 – 87.0	43.1 – 66.6	64.3 – 115.0
% Bare peat	0 (0)	0 (0)	5.8 (7)	29.5 (27)
% Moss/Lichen cover	78.9 (18)	79.5 (20)	52.8 (25)	34.5 (29)
% Litter	2.1 (2)	3.5 (1)	17.7 (21)	10.1 (7)
% Vascular	19.0 (18)	17.0 (19)	23.8 (31)	25.8 (11)
LAI	0.64 (0.3)	0.90 (0.5)	0.51 (0.5)	1.17 (0.9)

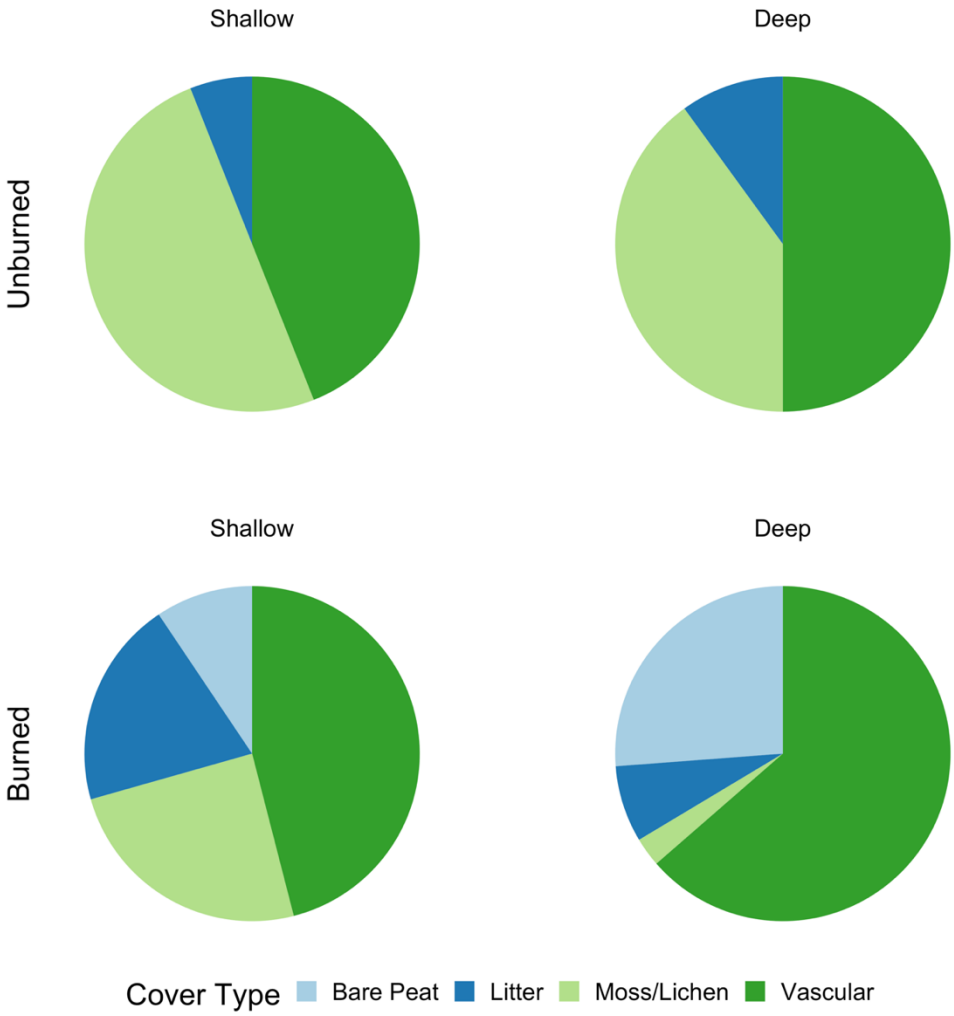

Figure 3.2: Vegetation community composition from general vegetation surveys and flux plots, indicating the proportional cover of bare peat (light blue), litter (dark blue), moss and lichen (light green), and vascular species (dark green). Surveys were completed in July and August 2020.

3.4.3 Ecosystem-scale CO_2 exchange

Growing season NEE at the unburned site ranged from -2.53 g C m^{-2} d^{-1} to 3.05 g C m^{-2} d^{-1} in 2019, and -2.91 g C m^{-2} d^{-1} to 2.84 g C m^{-2} d^{-1} in 2020. At the burned site in 2019 and 2020 growing season daily NEE ranged from -1.69 g C m^{-2} d^{-1} to 2.40 g C m^{-2} d^{-1}, and -2.33 g C m^{-2} d^{-1} to 1.73 g C m^{-2} d^{-1}, respectively. The magnitude of growing season mean daily NEE, GPP, and ER were greater at the unburned site than the burned site, and greater in 2020 than 2019 at the unburned site (Table 3.3, Figure 3.3). There were significant differences between the burned and unburned daily GPP in both years (2019: *p = 1.10e-11,* Wilcoxon V = 12259, n=153; 2020: p = 6.68e-06, Wilcoxon V = 15180, n=153). The unburned site switches from net CO_2 sink to source, end of carbon dioxide uptake period, earlier than at the burned site in both years of the study period. Unburned NEE changed from negative (uptake) to positive (emission) on August 14 in 2019 and August 27 in 2020. At the burned site, NEE changed from negative to positive on September 20 in 2019 and September 27 in 2020.

Table 3.3: Growing season (May to October) mean daily net ecosystem exchange (NEE, g C m^{-2} d^{-1}), gross primary productivity (GPP, g C m^{-2} d^{-1}), ecosystem respiration (ER, g C m^{-2} d^{-1}) and summer maximum daily NEE, GPP, ER (g C m^{-2} d^{-1}) for 1- and 2- years post-fire (2019 and 2020, respectively) for the unburned and burned sites.

	Unburned		Burned	
Growing season	2019	2020	2019	2020
NEE_{mean}	-0.27 (1.01)	-0.54 (1.25)	-0.09 (1.08)	-0.79 (0.84)
GPP_{mean}	-3.28 (1.37)	-3.45 (2.00)	-2.05 (1.37)	-2.60 (1.66)
ER_{mean}	2.53 (1.01)	2.82 (1.65)	2.53 (2.84)	1.82 (1.22)
Summer (JJA)				
NEE_{max}	-2.54	-2.91	-1.69	-2.33
GPP_{max}	-6.64	-7.25	-6.36	-5.74
ER_{max}	5.91	6.78	18.	4.50

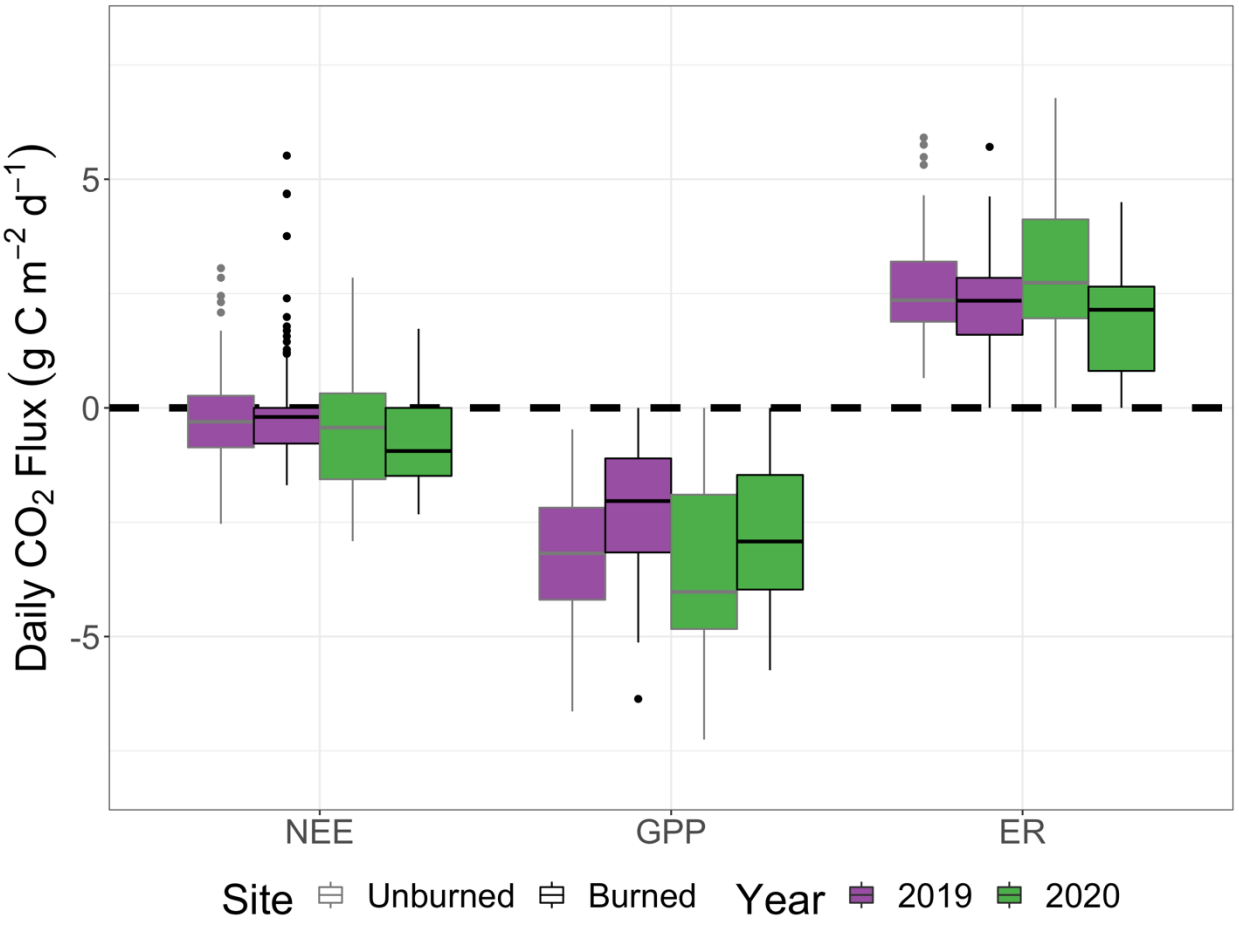

Figure 3.3: Growing season daily net ecosystem exchange (NEE), gross primary production (GPP), and ecosystem respiration (ER) in 2019 (purple) and 2020 (green) sites, for the unburned (light grey) and burned sites (black). Data included is from summed half hourly fluxes for May 1 to October 31 of each year (Data starts July 2019 for the burned site).

Table 3.4: Results of paired Wilcox Rank sum test for daily NEE, GPP, ER by year between sites (n=153).

Year	Flux	Statistic (W)	*p-value*
2019	NEE	12259	4.74e-01
2020	NEE	10315	7.18e-02
2019	GPP	16960	1.10e-11
2020	GPP	15180	6.68e-06
2019	ER	10679	1.85e-01
2020	ER	7573	8.62e-08

3.4.4 Burned cumulative fluxes for full year

Cumulative NEE from July 2019 to October 2020 at the burned site decreases (greater uptake) from July throughout the summer months (Figure 3.4). The site carbon uptake period ends in October, indicated by the local minimum in September of 2019. The site resumes CO_2 accumulation in March, where following the local maximum in March cumulative NEE transitions to a declining slope indicative of the change from a net emission to net uptake of CO_2 until the end of the study period in October 2020. ER continues at a similar rate throughout the winter months, showing the dominance of ER in NEE over the winter as GPP. Rate of GPP uptake slows around October/November, influencing the transition from negative NEE (net uptake) to positive NEE (net emission) at this time. Cumulative GPP slows to a proportion of peak summer GPP but continues to increase over fall and winter. The rate of CO_2 uptake from GPP ramps up in the spring around April, and the increased slope in June is an indication of the transition from spring green-up to summer photosynthesis.

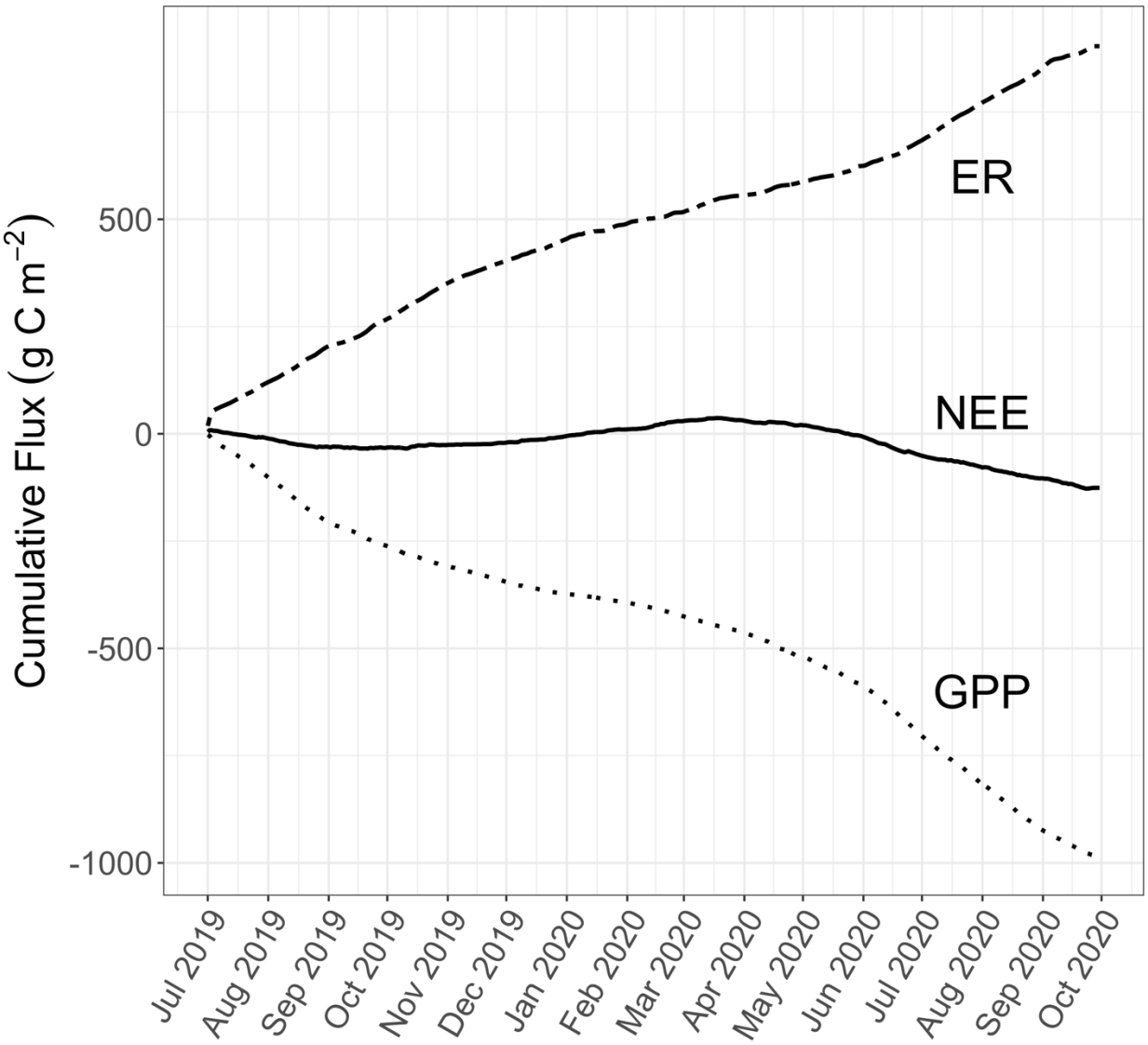

Figure 3.4: Cumulative CO_2 flux (g C m^{-2}) from July 2019 to October 2020 for the burned site using daily flux data. Line type shows CO_2 flux type: *solid* - NEE, *dotted* - GPP, *dashed* - ER.

3.4.5 Light response relationship

The initial slope of the summer (JJA) light response relationship, quantum yield (∝), was greater for the unburned sites in both years of the study. For both sites, quantum yield was greater in 2020 than 2019 (Figure 3.5). Quantum yield was 0.017 (± 0.0005) in 2019 and 0.020 (± 0.0004) in 2020 at the unburned site, and 0.013 (± 0.0008) in 2019 and 0.013 (± 0.0002) in 2020 at the burned site. There is a greater magnitude of NEE and greater GPP_{max} at both sites in 2020 resulting in greater quantum yield, thereby shifting the light response relationship in comparison to 2019. At the unburned site, GPP_{max} was -12.8 (± 0.2) g C m^{-2} d^{-1} in 2019 and -16.7 (± 0.2) g C m^{-2} d^{-1} in 2020. At the burned site, GPP_{max} was -12.8 (± 0.6) g C m^{-2} d^{-1} in 2019 and -13.9 (± 0.2) g C m^{-2} d^{-1} in 2020.

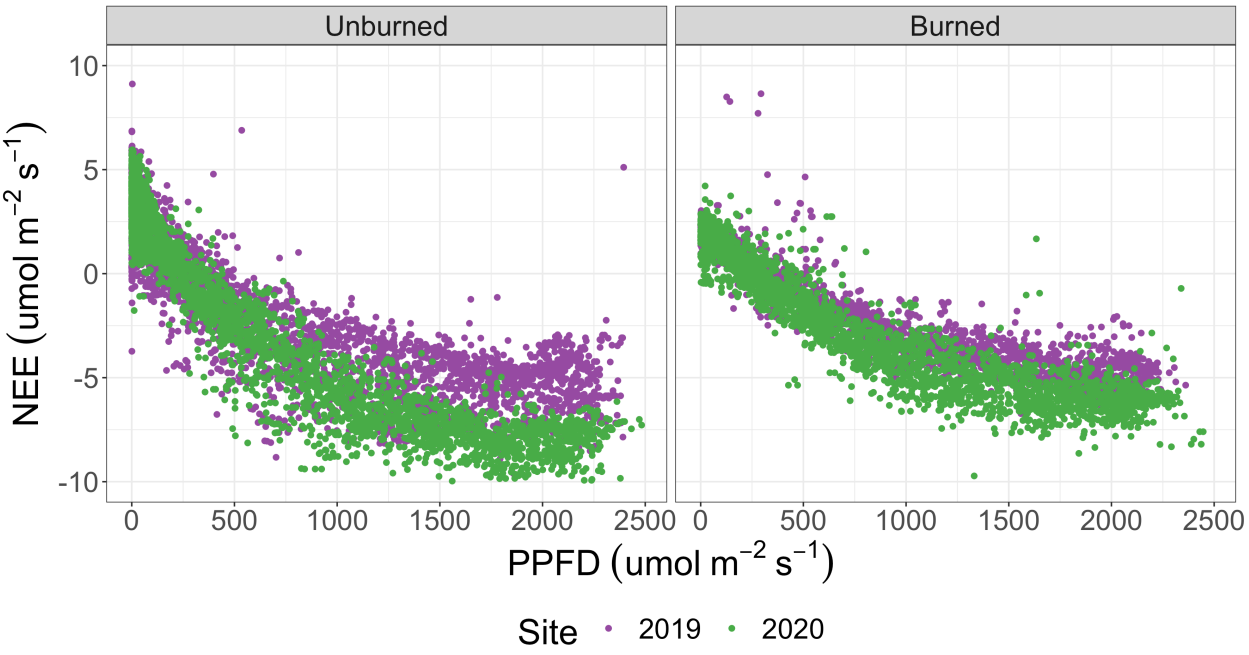

Figure 3.5: Ecosystem-scale light response relationship between half-hourly summer (months: JJA) net ecosystem exchange (NEE, µmol m^{-2} s^{-1}) and photosynthetic photon flux density (PPFD, µmol m^{-2} s^{-1}) for each site (left – unburned, right – burned) and year (*purple* - 2019, *green* - 2020).

3.4.5 Plot-scale variables

Peat temperatures were significantly greater at the unburned peatland, within both the deep and shallow peatland zones compared to the burned peatland (Kruskal-Wallis, $p < 0.01$; Table 3.6). In both peatlands, VWC was significantly greater in the shallow margins of the peatlands than the deep middle regions ($p < 0.01$; Table 3.5). In contrast, LAI was significantly lower in the shallow margins than the deep regions of both the unburned and burned peatlands ($p < 0.01$; Table 3.5), with greater moss, lichen, and litter cover than the deep region of the burned peatland (Figure 3.2).

Table 3.5: Mean environmental variables and CO_2 fluxes for plot-scale measurements and results from the Kruskal-Wallis analysis of variance test for significant differences between sites.

	Unburned	Burned	KW test (H-statistic, p=value)
Mean LAI	0.79 (0.4)	0.84 (0.8)	0.52, p=0.47
Mean peat temperature (°C)	17.2 (3.8)	14.0 (3.1)	**45.23, p<0.01**
Mean VWC (m^3 m^{-3})	0.86 (0.2)	0.80 (0.3)	0.63, p=0.43
Mean PPFD (µmol m^{-2} s^{-1})	756 (420)	811 (353)	1.6, p=0.2
Mean NEE (g C m^{-2} d^{-1})	-0.11 (0.1)	-0.03 (0.2)	**9.9, p<0.01**
Mean GPP (g C m^{-2} d^{-1})	-0.29 (0.2)	-0.32 (0.3)	0.13, p=0.7
Mean ER (g C m^{-2} d^{-1})	0.19 (0.1)	0.28 (0.2)	**17.0, p<0.01**

Plot-scale CO_2 exchange

At the unburned site at the plot-scale, NEE ranged from net uptake of -0.52 g C m^{-2} d^{-1} to net emission of 0.23 g C m^{-2} d^{-1}. All mean fluxes (NEE, GPP, and ER) were greater at in the deep peat areas of the unburned peatland than the shallow margin areas, however only mean NEE in the deep zone was significantly different to NEE in the shallow zone (Kruskal-Wallis, $p < 0.01$; Figure 3.6). Deep peat areas in the middle of the unburned peatland had a mean NEE of -0.14 g C m^{-2} d^{-1} and shallow margin areas mean NEE of -0.08 g C m^{-2} d^{-1} (Figure 3.6).

At the burned site, NEE ranged from net uptake of -0.79 g C m^{-2} d^{-1} in the shallow margin to net emission of 0.64 g C m^{-2} d^{-1} in the deep middle. Shallow areas of the burned peatland margins had greater mean NEE (-0.06 g C m^{-2} d^{-1}) compared to the deep peat areas (NEE: -0.02 g C m^{-2} d^{-1}), and similar GPP across zones. Mean ER at the burned peatland was similar between zones and maximum ER fluxes were measured in the deep peat in the peatland middle (Table 3.5; Figure 3.6). None of the fluxes were significantly different between shallow and deep zones of the burned peatland.

Mean NEE and ER at the unburned peatland were significantly different to the burned peatland, with greater net uptake at the unburned site (more negative NEE) and significantly greater ER at the burned peatland (Table 3.5; $p < 0.01$).

Table 3.6: Summary data for plot-scale (± s.d.) measurements collected in August and September 2020 at flux plots.

	Unburned		Burned	
	Shallow	Deep	Shallow	Deep
Mean LAI	0.64 (0.3)	0.90 (0.5)	0.51 (0.5)	1.17 (0.9)
Mean peat temperature (°C)	17.0 (3.5)	17.3 (4.1)	14.4 (2.9)	13.7 (3.1)
Mean VWC (m^3 m^{-3})	0.96 (0.1)	0.76 (0.3)	1.00 (0)	0.64 (0.4)
Mean NEE (g C m^{-2} d^{-1})	-0.08 (0.1)	-0.14 (0.1)	-0.06 (0.3)	-0.02 (0.2)
Mean GPP (g C m^{-2} d^{-1})	-0.25 (0.1)	-0.33 (0.2)	-0.33 (0.3)	-0.32 (0.3)
Mean ER (g C m^{-2} d^{-1})	0.18 (0.1)	0.19 (0.1)	0.27 (0.1)	0.29 (0.2)

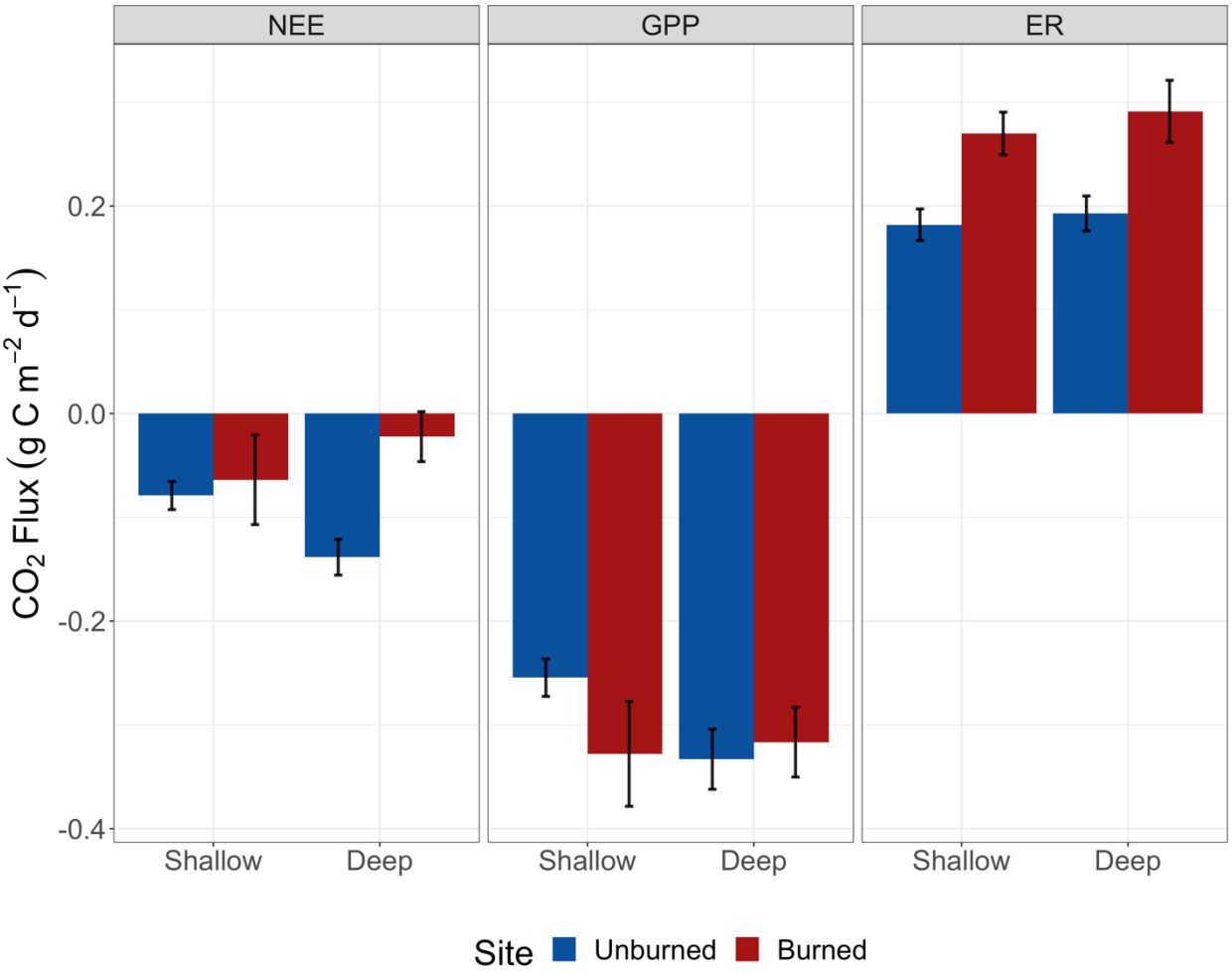

Figure 3.6: Plot-scale mean CO_2 flux (g C m^{-2} d^{-1}) by peat depth category: shallow peat within the peatland margins and deep peat in the middle of the unburned and burned peatland. Colours representing sites: *blue* – unburned, *red* – burned. Error bars showing ± standard error.

Light response relationship

At the plot-scale, the slope of the light response relationship, the quantum yield, is greater for the burned plots than the unburned (Table 3.7). However GPP_{max} is greater at the unburned site. The differences in quantum yield between sites is the opposite at the plot-scale than the ecosystem-scale light response relationship. The light response relationship shows a similar relationship to the ecosystem-scale, where the curve is positioned lower (higher) at the burned site indicating the flux at saturation light levels is lower at the burned site than the unburned site (Figure 3.7). When examining at the light response relationship with GPP, the relationship between sites is similar however GPP at the burned site has a greater range and variability at different light levels (Figure 3.7). There appears to be a difference in the ability to photosynthesize at low PAR levels. A lower asymptote with similar slope would indicate saturation occurs at lower light levels for the burned site than the unburned site.

Table 3.7: Parameters for plot-scale light response curve using Frolking et al. (1998) rectangular hyperbola relationship for peatland ecosystems.

	Quantum yield ($\propto$)	GPP_{max} (g C m^{-2} d^{-1})
Unburned	0.002 (± 0.0004)	-0.42 (± 0.04)
Burned	0.003 (±0.0016)	-0.39 (± 0.06)

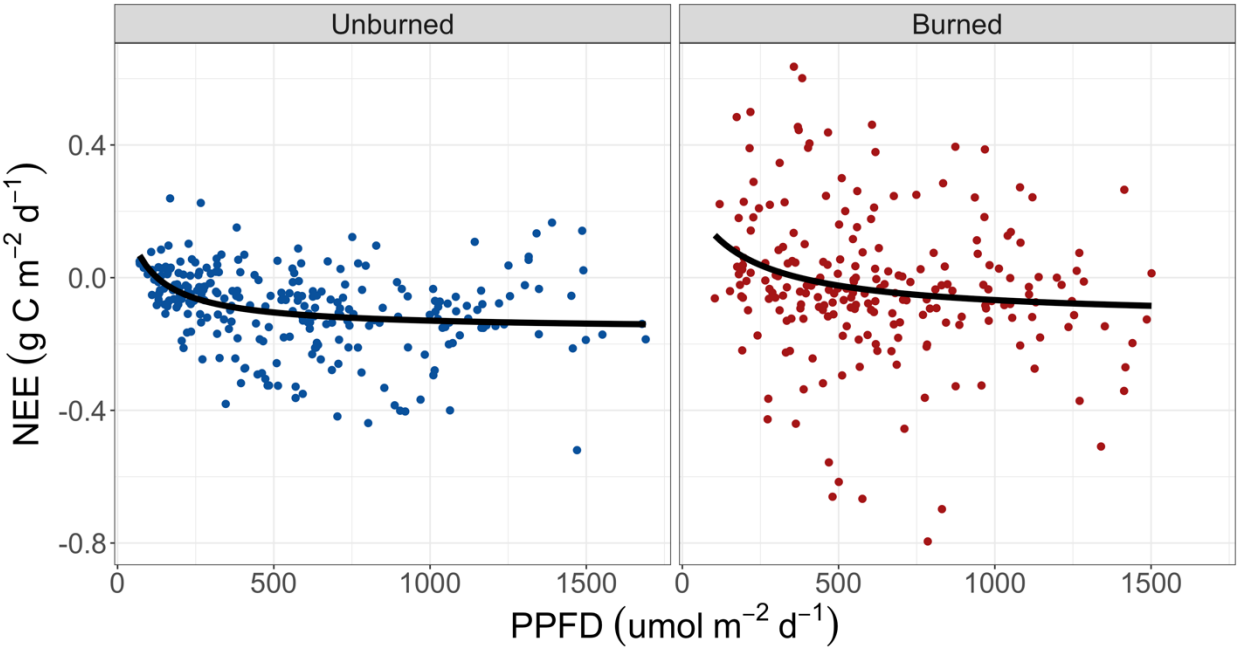

Figure 3.7: Plot-scale light response relationship from chamber-based flux measurements, showing the relationship between net ecosystem exchange (NEE, g C m^{-2} d^{-1}) and photosynthetic photon flux density (PPFD, µmol m^{-2} s^{-1}) for the (left, blue) unburned and (right, red) burned sites in August and September 2020.

3.4.6 Ecohydrological controls on plot-scale CO_2 exchange

Generalized linear mixed effects models with the three variables LAI, peat temperature, and mean PPFD were selected to predict NEE and GPP fluxes, as this model had the lowest AIC in both cases and the addition of variables passed the likelihood ratio test. Results from generalized linear mixed effects modelling suggest LAI is a significant control on NEE and GPP at the plot-scale in the unburned site, showing the largest effect size (NEE: *est* = -0.18, *stat* = -4.47, $p < 0.001$; GPP: *est* = 0.59, *stat* = 2.71, $p = 0.007$) (Table 3.8). Temperature and PPFD (light availability) were also identified as having a significant effect on unburned NEE and GPP. The combination of these three predictor variables and the inclusion of plot number as a random effect explained most of the variation in GPP ($R^2_{cond} = 0.95$, $n = 128$). Temperature was the main control on ER in the unburned peatland (*est* = 0.10, *stat* = 11.43, $p < 0.001$), and most of the variation in ER was explained by this variable and plot number ($R^2_{cond} = 0.97$, $n = 128$, Figure 3.8).

Results from the generalized linear mixed effects modelling suggest that at the burned peatland peat temperature was a significant control on NEE, GPP, and ER at the plot-scale (Table 3.9). For burned NEE and GPP, peat temperature had the greatest coefficient (NEE: *est* = -0.02, *stat* = -4.10, $p < 0.001$; GPP: *est* = 0.14, *stat* = 15.68, $p < 0.001$), and for ER LAI exhibited the largest effect (*est* = 0.38, *stat* = 2.56, $p = 0.010$). The combination of temperature, PPFD, and plot number as a random effect explained a large portion of the variation in GPP ($R^2_{cond} = 0.95$, $n = 104$). For ER, the combination of temperature, LAI, and a random effect of plot number explained a significant portion of the variance in ER ($R^2_{cond} = 0.93$, $n = 112$).

Table 3.8: Generalized linear mixed effects model parameters for unburned NEE, GPP, and ER from plot-scale flux measurements.

	Variable	Estimate	Std. error	Statistic	p-value
NEE	Intercept	-0.03	0.04	-0.58	0.5610
	LAI	-0.18	0.04	-4.47	< 0.0001
	Temperature	0.01	0.00	2.78	0.0054
	PPFD	-0.00	0.00	-2.84	0.0045
GPP	Intercept	-2.83	0.17	-16.55	< 0.0001
	LAI	0.59	0.22	2.71	0.0068
	Temperature	0.03	0.01	4.62	< 0.0001
	PPFD	0.00	0.00	7.56	< 0.0001
ER	Intercept	-3.68	0.23	-16.01	< 0.0001
	Temperature	0.10	0.01	11.43	< 0.0001

Table 3.9: Generalized linear mixed effects model parameters for burned NEE, GPP, and ER from plot-scale flux measurements.

	Variable	Estimate	Std. error	Statistic	p-value
NEE	Intercept	0.44	0.12	3.81	0.0002
	Temperature	-0.02	0.01	-4.10	< 0.0001
	PPFD	-0.00	0.00	-3.80	0.0001
GPP	Intercept	-4.59	0.41	-11.16	< 0.0001
	Temperature	0.14	0.01	15.68	< 0.0001
	PPFD	0.00	0.00	9.12	< 0.0001
ER	Intercept	-2.55	0.25	-10.05	< 0.0001
	LAI	0.04	0.01	2.98	0.0029

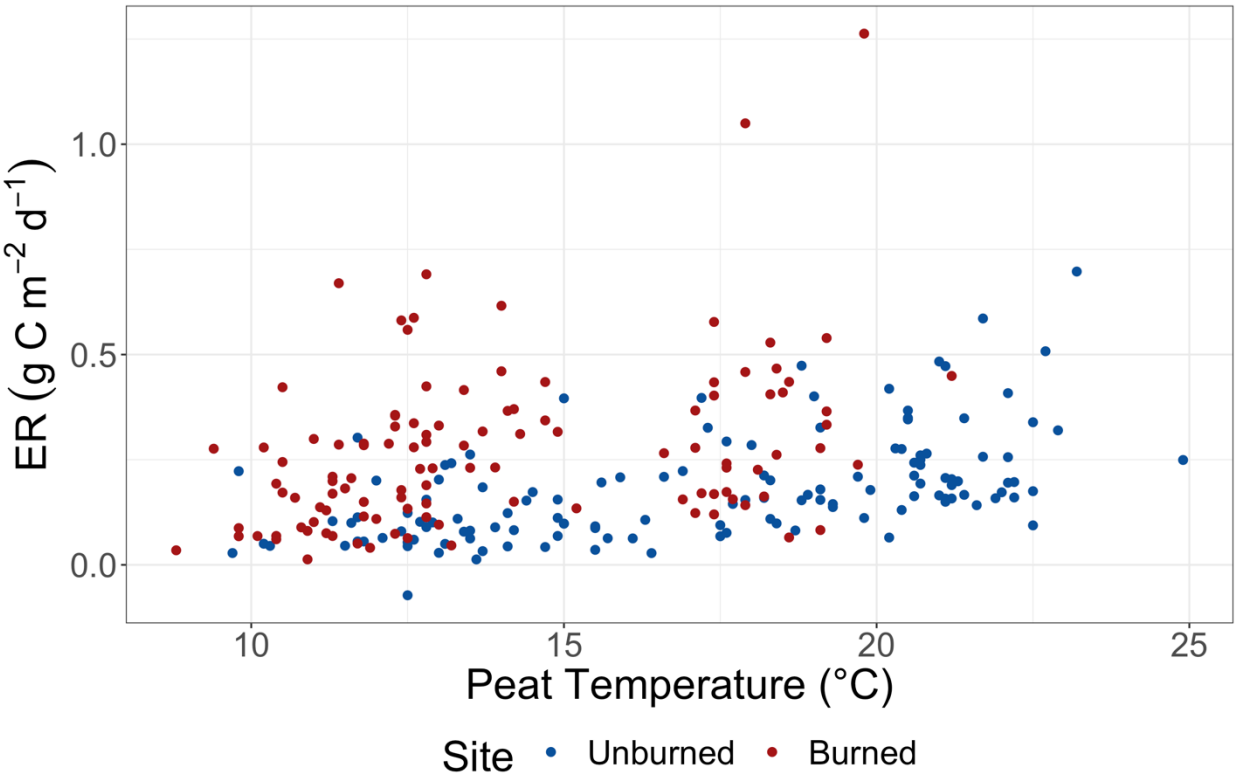

Figure 3.8: Plot-scale relationship between ecosystem respiration (ER, g C m^{-2} d^{-1}) and peat temperature (°C), from chamber-based flux measurements in August and September 2020. Colours represent sites (unburned, *blue*; burned, *red).*

3.5 Discussion

3.5.1 Post-wildfire CO_2 exchange

With almost two years of growing season CO_2 exchange measurements at an unburned and burned site in the Canadian Shield rock barrens region, we can quantify post-wildfire recovery of CO_2 exchange processes and assess the role of interannual variability in climatic variables on CO_2 exchange trends throughout the summer season. Water table dynamics throughout the growing season closely followed rainfall events, owing to the natural fill and spill hydrological dynamics and connectivity of the landscape (Spence and Woo, 2003). The similar diurnal cycle of PPFD and no discernable differences in VPD between sites indicates the two sites in this study are experiencing similar air masses (Figure 3.1). During the summer season (June, July, August) of 2019, there was a considerable summer drying period at both sites, where the water table falls below 30 cm for more than a week (Figure 3.1). In 2020, more frequent and greater rainfall events throughout the summer season maintained the water table in the top 30 cm of the peat surface at the unburned peatland and top 40 cm of peat at the burned peatland. We have considered 2020 as a wet summer year and 2019 as a dry summer year when compared to the temperature and rainfall trends from the past five years at the unburned site, 2016 to 2020 (*Chapter 2*).

Ecosystem-scale NEE fluxes were similar to the unburned and post-wildfire sites of Morison et al. (2020). Interannual variability in NEE and GPP fluxes followed similar trends between sites. At the unburned site, growing season mean NEE was not significantly different between years (Figure 3.3). In the dry summer year (2019) there was lower mean GPP and ER compared to the wet summer year at the unburned site. While drought in peatlands has been shown to affect either of the component fluxes, GPP and ER (Adkinson et al., 2011; Aurela et al., 2007;

Cai et al., 2010; Lund et al., 2010; Sonnentag et al., 2010; Strachan et al., 2016), in this region of the boreal shield there is evidence from interannual variability in CO_2 exchange and climatic variables that GPP is more strongly affected by changes in water availability than other climatic factors (see Chapter 2*)*. Greater photosynthetic efficiency in the wet summer of 2020 at the unburned site, indicated by the shift in light response relationship compared to 2019 (Figure 3.5), may have contributed to the increase in ER under wet conditions due to greater autotrophic respiration (Moore et al., 2002). Some areas of the burned peatland may experience greater light availability, due to the loss of canopy cover from the wildfire, however further research with greater spatial variability across the burned peatland and burned landscape would be helpful to investigate this further.

At the plot-scale, burned NEE and GPP were slightly reduced compared to the unburned fluxes in both the shallow and deep zones of the peatland, similar to Morison et al. (2021). At the unburned site there was a significant change in LAI across the peatland zones, which was identified as a significant control on NEE. Although greater vascular cover was found in the deep middle of the burned peatland and mosses cover in the shallow margins, this relationship with LAI and NEE was not obvious in the burned peatland but was present for LAI and ER. Temperature was identified as having a significant control on all burned CO_2 fluxes (NEE, GPP, and ER) and may be due to a shift in the nonlinear relationship between ER and temperature (Lloyd, Taylor, 1994), where at a given temperature ER at the unburned site is lower than the burned (Figure 3.8). There was also significantly greater ER at the burned site than the unburned site, which may be a result of greater autotrophic respiration and nutrient addition to the burned peatland following wildfire (Moore et al., 2002; Morison et al., 2021; van Beest et al., 2019).

The recovery of net C uptake post-wildfire in boreal peatlands has been shown to change from net source of C back to net sink of C about 13 to 20 years following wildfire (Wieder et al., 2009), however some peatlands in this region will not recover the carbon lost before the next fire (Ingram et al., 2018). The growing season ecosystem-scale CO_2 fluxes and short snapshot of late summer plot-scale processes from this study have shown the burned landscape to be a net CO_2 sink for the growing season and summer period 1- and 2- years post-wildfire. Considering the C loss from the PS33 wildfire (1.61 ± 0.97 kg C m^{-2}, Wilkinson et al., 2020) and the total annual of C uptake from NEE of -50 g C m^{-2} (from July 2019 to June 2020), we can estimate the amount of C lost from peatlands in the wildfire has the potential to recover in about 32 years when accounting for only CO_2 exchange, provided the burned peatlands stay wet.

This rapid recovery to a CO_2 sink, compared to the boreal plains, throughout the growing season may be a result of the unique structure and function of boreal shield peatlands. Peatlands in the boreal shield may be smaller and thinner than those in the boreal plains and are likely to be more responsive to wetting and drying throughout the growing season. These peatlands effectively turn on and off in response to water availability, reflected in decreased moss productivity during drought (Moore et al., 2021) and differences in total GPP rates in wet and dry summers (Chapter 2). Uniquely, these boreal shield peatlands also hydrologically reset in the fall and spring, where winter conditions and snowmelt commence water movement on the landscape in the spring, keeping the water table closer to the peat surface into the start of the growing season. While this study has shown the vegetation recovery has progressed successfully in the first two years post-wildfire, contributing to a net CO_2 sink for a full year post-wildfire (July 2019 to 2020), a full

analysis of the post-wildfire C budget would be valuable given the role of water availability on peatland ecohydrological processes in this landscape.

Plot-scale fluxes from this study are lower than other literature using a similar measurement design, however plot-scale measurements were completed towards the onset of fall senescence (late August, September) and were similar to Bubier et al. (1998). Temporal resolution of plot-scale sampling was limited due to the COVID-19 pandemic restrictions; therefore, it would be valuable to continue this study design over the whole growing season.

3.5.2 Environmental changes post-wildfire contributing to CO_2 flux patterns

Peat depth has been identified as a control on peat burn severity from the PS33 wildfire, with areas of deep peat experiencing lower severity burning than shallow peat areas (Wilkinson et al., 2020). These shallow peat areas which underwent severe burning were predominantly in the margins of the peatland, closest to upland open bedrock and forest areas. Hummock-hollow microtopography was not present in the margin of the burned peatland, however microtopography was identified in the middle of the burned peatland. Despite these differences in burn severity and microtopography, vegetation productivity (GPP) did not vary significantly across the peatland shallow (margin) and deep (middle) zones. At the ecosystem-scale, GPP followed similar trends with climatic variability observed at the unburned site across 1- and 2- years post-fire, and may be attributed to the rapid recolonization of the burned landscape by early successional bryophytes and vascular species across the range of burn severity observed.

Recolonization of the plant community post-wildfire resembled the observed differences in burn severity across the peatland. Margins with deep burning had greater *Polytrichum* sp. regrowth, which has been characterized as a pioneer species in peatlands post-wildfire (Grau-Andrés et al., 2019; Maltby et al., 1990), than *Sphagnum* sp. The rhizoids of *Polytrichum* rigidly attach into peat soils, providing an important stabilization function for post-wildfire soils (Groeneveld and Rochefort, 2005). *Polytrichum* sp. have also been found to facilitate the growth of later successional vegetation, including *Sphagnum* sp. (Groeneveld et al., 2007), and we found *Sphagnum* shoots were interspersed within the *Polytrichum* cover in some of the flux plots in the 2nd year post-fire. Continuous monitoring of *Sphagnum* recovery in the years following wildfire in this landscape is important as *Sphagnum* recovery is essential to return the peatland to a C sink following disturbance, such as mined peatland restoration (Waddington et al., 2010; Waddington and Warner, 2001).

Intact, but singed, *Sphagnum* were present in the peatland middle, as well as a few fully intact hummocks that did not appear to be subjected to burning, however these intact hummocks were not monitored. The rapid recolonization of the burned peatland within the first two years post-fire may have been a result of the presence of areas of potential wildfire refugia, which has been described as areas where vegetation survives within the fire footprint at various spatial scales and thus allowing for vegetation dispersal into disturbed areas (Hylander and Johnson, 2010; Meddens et al., 2018; Robinson et al., 2013). The presence of wildfire refugia has been connected to wildfire intensity and is intrinsically heterogeneous (Hylander and Johnson, 2010).

Changes in the nutrient availability in a post-wildfire ecosystem may promote different rates of vegetation recolonization, as deeper burned areas have been associated with changes in nutrient availability, including increased phosphorus (P) and nitrogen (N) concentrations (Morison et al., 2021; van Beest et al., 2019). Increased P in the margins of wetlands within the PS33 wildfire footprint has been measured (Chow-Fraser, *personal communication)*, however further research is needed to examine connections between vegetation colonization and biogeochemical changes post-wildfire in the rock barrens landscape.

3.5.3 Implications for climate change

The predicted increase in air temperature and precipitation with climate change in the Eastern Georgian Bay region may have significant effects on C cycling in this boreal shield rock barrens ecosystem (D'Orgeville et al., 2014; Mortsch and Quinn, 1996; Notaro et al., 2015). The increase in air temperature is expected to lead to water loss from the ecosystem through increased evaporation and evapotranspiration (Helbig et al., 2020). Increased temperatures may also promote a longer growing season, lengthening the summer season, resulting in changes to the magnitude of CO_2 fluxes in the shoulder seasons (Lund et al., 2010). Under a warming climate, carbon in peatlands will be vulnerable to loss through changes in the proportion of GPP and ER contributing to NEE from interannual climatic variability (Wu and Roulet, 2014), through combustion loss (Turetsky et al., 2015; Wilkinson et al., 2020), and post-disturbance recovery (Morison et al., 2020; Wieder et al., 2009). Our results at the ecosystem-scale indicate these peatlands may be at risk of becoming net CO_2 sources during the summer depending on the presence and severity of drought conditions keeping the water table low in the peat profile (*Chapter 2*). Drying conditions also leave peatlands susceptible to increased likelihood of ignition and increased fire severity (Nelson et al.,

2021). The combination of drying and a change in the wildfire disturbance regime may aid in a shift in the vegetation composition of peatlands. Sphagnum species composition may shift to species that are more desiccant tolerant in response to periodic changes in water table depth (Breeuwer et al., 2009), and a full shift in the plant community composition to have greater variance and shrub or graminoid dominant over longer time scales of low water availability (Dieleman et al., 2015). As temperature exhibited a significant control on CO_2 fluxes at the burned site, post-wildfire recovery in a warming climate may elevate the contribution of ER to NEE as a function of temperature and greater vascular vegetation cover.

3.6 Literature cited

Adkinson, A. C., Syed, K. H., & Flanagan, L. B. (2011). Contrasting responses of growing season ecosystem CO2 exchange to variation in temperature and water table depth in two peatlands in northern Alberta. Canada, J. Geophys. Res., 116, G01004. https://doi.org/10.1029/2010JG001512.

Aurela, M., Riutta, T., Laurila, T., Tuovinen, J., Vesala, T., Tuittila, E., Rinne, J., Haapanala, S., & Laine, J. (2007). CO_2 exchange of a sedge fen in southern Finland-the impact of a drought period. *Tellus B: Chemical and Physical Meteorology*, 59:5, 826-837. https://doi.org/10.1111/j.1600-0889.2007.00309.x.

Bates, D., Mächler, M., Bolker, B., & Walker, S. (2015). lme4: Linear mixed-effects models using Eigen and S4. R package version 1.1–7. 2014.

Bergeron, Y., & Flannigan, M. D. (1995). Predicting the effects of climate change on fire frequency in the southeastern Canadian boreal forest. *Water, Air, & Soil Pollution,* 82, 437-444. https://doi.org/10.1007/BF01182853.

Blodau, C., Basiliko, N., & Moore, T. R. (2004). Carbon turnover in peatland mesocosms exposed to different water table levels. *Biogeochemistry,* 67, 331-351. https://doi.org/10.1023/B:BIOG.0000015788.30164.e2.

Breeuwer, A., Robroek, B. J. M., Limpens, J., Heijmans, M. M. P. D., Schouten, M. G. C., & Berendse, F. (2009). Decreased summer water table depth affects peatland vegetation. *Basic and Applied Ecology*, 10(4), 330-339. https://doi.org/10.1016/j.baae.2008.05.005.

Bubier, J. L., Crill, P. M., Moore, T. R., Savage, K., & Varner, R. K. (1998). Seasonal patterns and controls on net ecosystem CO_2 exchange in a boreal peatland complex. *Global Biogeochem. Cycles*, 12(4), 703-714. https://doi.org/10.1029/98GB02426.

Cai, T., Flanagan, L. B., & Syed, K. H. (2010). Warmer and drier conditions stimulate respiration more than photosynthesis in a boreal peatland ecosystem: Analysis of automatic chambers and eddy covariance measurements. *Plant, Cell and Environment*, 33, 394-407. https://doi.org/10.1111/j.1365-3040.2009.02089.x.

Catling, P. M., & Brownell, V. R. (1999). The Flora and Ecology of Southern Ontario Granite Barrens. In R. C. Anderson, J. S. Fralish, & J. M. Baskin (Eds.) *Savannas, Barrens, and Rock Outcrop Plant Communities of North America* (pp. 392-405). Cambridge University Press.

Clymo, R. S. (1987). The ecology of peatlands. *Science Progress (1933-)*, 71, 593-614.

Dieleman, C. M., Branfireun, B. A., McLaughlin, J. W., & Lindo, Z. (2015). Climate change drives a shift in peatland ecosystem plant community: Implications for ecosystem function and stability. *Global Change Biology,* 21(1), 388-395. https://doi.org/10.1111/gcb.12643.

d'Orgeville, M., Peltier, W. R., Erler, A., & Gula, J. (2014). Climate change impacts on Great Lakes Basin precipitation extremes. *JGR: Atmospheres*, 119, 10799-10812. https://doi.org/10.1002/2014JD021855.

Environment Canada. (2021). Daily Data Report for Parry Sound CCG. [Data file]. Retrieved from https://climate.weather.gc.ca/climate_data/daily_data_e.html?StationID=32128.

Falge, E., Baldocchi, D., Olsen, R., Anthoni, P., Aubinet, M., Bernhofer, C., Burba, G., Ceulemans, R., Clement, R., Dolman, H., Cranier, A., Gross, P., Grünwald, Hollinger, D., Jensen, N.-O., Katul, G., Keronen, P., Kowalski, A., Lai, C., … Wofsy, S. (2001). Gap filling strategies for defensible annual sums of net ecosystem exchange. *Agricultural and Forest Meteorology,* 107(1), 43-69. https://doi.org/10.1016/S0168-1923(00)00225-2.

Flannigan, M. D., Logan, K. A., Amiro, B. D., Skinner, W. R., & Stocks, B. J. (2005). Future area burned in Canada. *Climate Change,* 72, 1-16. https://doi.org/10.1007/s10584-005-5935-y.

Frolking, S. E., Bubier, J. L., Moore, T. R., Ball, T., Bellisario, L. M., Bhardwaj, A., Carroll, P., Crill, P. M., Lafleur, P. M., McCaughey, J. H., Roulet, N. T., Suyker, A. E., Verma, S. B., Waddington, J. M., & Whiting, G. J. (1998). Relationship between ecosystem productivity and photosynthetically active radiation for northern peatlands. *Global Biogeochem. Cycles,* 12(1), 115-126. https://doi.org/10.1029/97GB03367.

Gorham, E. (1991). Northern Peatlands: Role in the Carbon Cycle and Probably Response to Climatic Warming. *Ecological Applications,* 1(2), 182-195.

Grau-Andrés, R., Gray, A., & Davies, G. M. (2017). Sphagnum abundance and photosynthetic capacity show rapid short-term recovery following managed burning. *Plant Ecology & Diversity*, 10(4), 353-359. https://doi.org/10.1080/17550874.2017.1394394.

Gray, A., Davies, G. M., Domènech, R., Taylor, E., & Levy, P. E. (2021). Peatland Wildfire Severity & Post-fire Gaseous Carbon Fluxes. *Ecosystems,* 24, 713-725. https://doi.org/10.1007/s10021-020-00545-0.

Groenveld, E. V. G., & Rochefort, L. (2005). Polytrichum strictum as a solution to frost heaving in disturbed ecosystems: a case study with milled peatlands. *Restoration Ecology,* 13(1), 74-82. https://doi.org/10.1111/j.1526-100X.2005.00009.x.

Groenveld, E. V. G., Massé, A., & Rochefort, L. (2007). Polytrichum strictum as a nurse-plant in peatland restoration. *Restoration Ecology*, 15(4), 709-719. https://doi.org/10.1111/j.1526-100X.2007.00283.x.

Helbig, M., Waddington, J. M., Alekseychik, P., Amiro, B. D., Aurela, M., Barr, A. G., Black, T. A., Blanken, P. D., Carey, S. K., Chen, J., Chi, J., Desai, A. R., Dunn, A., Euskirchen E. S., Flannigan, L. B., Forbrich, I., Friborg, T., Grelle, A., Harder, S., … Zyrianov, V. (2020). Increasing contribution of peatlands to boreal evapotranspiration in a warming climate. *Nature Climate Change,* 10(6), 555-560. https://doi.org/10.1038/s41558-020-0763-7.

Hudson, D. T., Markle, C. E., Harris, L. I., Moore, P. A., & Waddington, J. M. (2021). Ecohydrological controls on lichen and moss CO_2 exchange in rock barrens turtle nesting habitat. *Ecohydrology*, 14, 1-11, https://doi.org/10.1002/eco.2255.

Hylander, K., & Johnson, S. (2010). In situ survival of forest bryophytes in small-scale refugia after an intense forest fire. *Journal of Vegetation Science,* 21, 1099-1109. https://doi.org/10.1111/j.1654-1103.2010.01220.x.

Ingram, R. C., Moore, P. A., Wilkinson, S., Petrone, R. M., & Waddington, J. M. (2019). Postfire soil carbon accumulation does not recover boreal peatland combustion loss in some hydrogeological settings. *Journal of Geophysical Research: Biogeosciences*, 124, 775–788. https://doi.org/10.1029/ 2018JG004716.

Kasischke, E. S., & Turetsky, M. R. (2006). Recent changes in the fire regime across the North American boreal region – Spatial and temporal patterns of burning across Canada and Alaska. *Geophysical Research Letters,* 33, L09703. https://doi.org/10.1029/2006GL025677.

Kettridge, N., Turetsky, M. R., Sherwood, J. H., Thompson, D. K., Miller, C. A., Benscoter, B. W., Flannigan, M. D., Wotton, B. M., & Waddington, J. M. (2015). Moderate drop in water table increases peatland vulnerability to post-fire regime shift. *Scientific Reports*, 5, 8063. https://doi.org/10.1038/srep08063.

Kettridge, N., Lukenbach, M. C., Hokanson, K. J., Devito, K. J., Petron, R. M., Mendoza, C. A., & Waddington, J. M. (2019). Severe wildfire exposes remnant peat carbon stocks to

increased post-fire drying. *Scientific Reports,* 9, 5-10. https://doi.org/10.1038/s41598-019-40033-7.

Kljun, N., Calanca, P., Rotach, M. W., & Schmid, H. P. (2015). A simple two-dimensional parameterisation for Flux Footprint Prediction (FFP). *Geoscientific Model Development*, 8(11), 3695-3713. https://doi.org/10.5194/gmd-8-3695-2015.

Lasslop, G., Reichstein, M., Papale, D., Richardson, A. D., Arneth, A., Barr, A., Stoy, P., & Wohlfahrt, G. (2010). Separation of net ecosystem exchange into assimilation and respiration using a light response curve approach: critical issues and global evaluation. *Global Change Biology,* 16(1), 187-208.

Liu, M., He, H., Yu, G., Luo, Y., Sun, X., & Wang, H. (2009). Uncertainty analysis of CO_2 flux components in sub-tropical evergreen coniferous plantation. *Science in China Series D: Earth Sciences,* 52(2), 257-268. https://doi.org/10.1007/s11430-009-0010-6.

Loisel, J., Yu, Z., Beilman, D. W., Camill, P., Alm, J., Amesbury, M. J., Anderson, D., Andersson, S., Bochicchio, C., Barber, K., Belyea, L. R., Bunbury, J., Chambers, F. M., Charman, D. J., De Vleeschouwer, F., Fialkieeqicz-Koziel, B., Finkelstein, S. A., Galka, M., Garneau, M., … Zhou, W. (2014). A database and synthesis of northern peatland soil properties and Holocene carbon and nitrogen accumulation. *The Holocene,* 24(9), 1028-1042. https://doi.org/10.1177/0959683614538073.

Lund, M., Lafleur, P. M., Roulet, N. T., Lindroth, A., Christensen, T. R., Aurela, M., Chojnicki, B. H., et al. (2010). Variability in exchange of CO_2 across 12 northern peatland and tundra sites. *Global Change Biology*, 16, 2436-2448. https://doi.org/10.1111/j.1365-2486.2009.02104.x.

Maltby, E., Legg, C. J., & Proctor, M. C. F. (1990). The Ecology of Severe Moorland Fire on the North York Moors: Effects of the 1976 Fires, and Subsequent Surface and Vegetation Development. *Journal of Ecology*, 78(2), 490-518. https:// 10.2307/2261126.

Markle, C. E., Wilkinson, S. L., & Waddington, J. M. (2020). Initial Effects of Wildfire on Freshwater Turtle Nesting Habitat. *Journal of Wildlife Management,* 84(7), 1373-1383. https://doi.org/10.1002/jwmg.21921.

Meddens, A. J. H., Kolden, C. A., Lutz, J. A., Smith, A. M. S., Cansler, C. A., Abatzoglou, J. T., Meigs, G. W., Downing, W. M., & Krawchuk, M. A. (2018). Fire Refugia: What Are They and Why Do They Matter for Global Change?. *Bioscience*, 68(12), 944-954. https://doi.org/10.1093/biosci/biy103.

Moncrieff, J. B., Malhi, Y., & Leuning, R. (1996). The propagation of errors in long-term measurements of land-atmosphere fluxes of carbon and water. *Global Change Biology*, 2(3), 231-240. https://doi.org/10.1111/j.1365-2486.1996.tb00075.x.

Moore, P. A., Smolarz, A. G., Markle, C. E., & Waddington, J. M. (2019). Hydrological and thermal properties of moss and lichen species on rock barrens: Implications for turtle nesting habitat. *Ecohydrology,* 12, e2057. https://doi.org/10.1002/eco.2057.

Moore, T. R., Bubier, J. L., Frolking, S. E., Lafleur, P. M., & Roulet, N. T. (2002). Plant biomass and production and CO_2 exchange in an ombrotrophic bog. *Journal of Ecology,* 90(1), 25-36. https://doi.org/10.1046/j.0022-0477.2001.00633.x.

Moore, P. A., Didemus, B. D., Furukawa, A. K., & Waddington, J. M. (2021). Peat depth as a control on Sphagnum moisture stress during seasonal drought. *Hydrological Processes*, 35, e14117. https://doi.org/10.1002/hyp.14117.

Morison, M., van Beest, C., Macrae, M., Nwaishi, F., & Petrone, R. (2021). Deeper burning in a boreal fen peatland 1-year post-wildfire accelerates recovery trajectory of carbon dioxide uptake. *Ecohydrology,* 14(3), e2277. https://doi.org/10.1002/eco.2277.

Morison, M. Q., Petrone, R. M., Wilkinson, S. L., Green, A., & Waddington, J. M. (2020). Ecosystem scale evapotranspiration and CO_2 exchange in burned and unburned peatlands: Implications for the ecohydrological resilience of carbon stocks to wildfire. *Ecohydrology,* 13(2), e2189. https://doi.org/10.1002/eco.2189.

Mortsch, L. D., & Quinn, F. H. (1996). Climate change scenarios for Great Lakes Basin ecosystem studies. *Limnology and Oceanography,* 41(5), 903-911. https://doi.org/10.4319/lo.1996.41.5.0903.

Nelson, K., Thompson, D., Hopkinson, C., Petrone, R., & Chasmer, L. (2021). Peatland-fire interactions: A review of wildland fire feedbacks and interactions in Canadian boreal peatlands. *Science of the Total Environment*, 769, 145212. https://doi.org/10.1016/j.scitotenv.2021.145212.

Nijp, J. J., Limpens, J., Metselaar, K., Peichl, M., Nilsson, M. B., van der Zee, S. E. A. T. M., & Berendse, F. (2015). Rain events decrease boreal peatland net CO_2 uptake through reduced light availability. *Global Change Biology*, 21, 2309-2320. https://doi.org/10.1111/gcb.12864.

Notaro, M., Bennington, V., & Vavrus, S. (2015). Dynamically Downscaled Projections of Lake-Effect Snow in the Great Lakes Basin. *Journal of Climate,* 28(4). 1661-1684. https://doi.org/10.1175/JCLI-D-14-00467.1.

Papale, D., Reichstein, M., Aubinet, M., Canfora, E., Bernhofer, C., Kutsch, W., Longdoz, B., Rambal, S., Valentini, R., Vesala, T., & Yakir, D. (2006). Towards a standardized processing of Net Ecosystem Exchange measured with eddy covariance technique: algorithms and uncertainty estimation. *Biogeosciences,* 3(4), 571-583. https://doi.org/10.5194/bg-3-571-2006.

Reichstein, M., Falge, E., Baldocchi, D., Papale, D., Aubinet, M., Berbigier, P., Bernhofer, C., Buchmann, N., Gilmanov, T., Granier A., Grünwald, T., Kavránková, K., Ilvesniemi, H., Janous, D., Knohl, A., Laurila, T., Lohila, A., Loustau, D., Matteucci, G., … Valentini, R. (2005). On the separation of net ecosystem exchange into assimilation and ecosystem respiration: review and improved algorithm. *Global Change Biology*, 11(9), 1424-1439. https://doi.org/10.1111/j.1365-2486.2005.001002.x.

Richardson, A. D., Aubinet, M., Barr, A. G., Hollinger, D. Y., Ibrom, A., Lasslop, G., & Reichstein, M. (2012). Uncertainty quantification. In *Eddy covariance* (pp. 173-209). Springer, Dordrecht.

Riutta, T., Laine, J., Aurela, M., Rinne, J., Vesala, T., Laurila, T., Haapanala, S., Pihlatie, M., & Tuittila, E. S. (2007). Spatial variation in plant community functions regulates carbon gas dynamics in a boreal fen ecosystem. *Tellus B: Chemical and Physical Meteorology*, 59(5), 838-852. https://doi.org/10.1111/j.1600-0889.2007.00302.x.

Robinson, N. M., Leonard, S. W. J., Ritchie, E. G., Bassett, M., Chia, E. K., Buckingham, S., Gibb, H., Bennett, A. F., & Clarke, M. F. (2013). Review: Refuges for fauna in fire-prone landscapes: their ecological function and importance. *Journal of Applied Ecology*, 50(6), 1321-1329. https://doi.org/10.1111/1365-2664.12153.

R Core Team (2020). R: A language and environment for statistical computing. R Foundation for Statistical Computing, Vienna, Austria. URL https://www.R-project.org/.

Sherwood, J. H., Kettridge, N., Thompson, D. K., Morris, P. J., Silins, U., & Waddington, J. M. (2013). Effect of drainage and wildfire on peat hydrophysical properties. *Hydrological Processes*, 27(13), 1866-1874. https://doi.org/10.1002/hyp.9820.

Spence, C., & Woo, M. (2003). Hydrology of subarctic Canadian shield: soil-filled valleys. *Journal of Hydrology*, 279, 151-166. https://doi.org/10.1016/S0022-1694(03)00175-6.

Sonnentag, O., van der Kamp, G., Barr, A. G., & Chen, J. M. (2010). On the relationship between water table depth and water vapour and carbon dioxide fluxes in a minerotrophic fen. *Global Change Biology*, 16(6), 1762-1776. https://doi.org/10.1111/j.1365-2486.2009.02032.x.

Strachan, I. B., Pelletier, L., & Bonneville, M. (2016). Inter-annual variability in water table depth controls net ecosystem carbon dioxide exchange in a boreal bog. *Biogeochemistry,* 127, 99-111. https://doi.org/10.1007/s10533-015-0170-8.

Strack, M., Waddington, J. M., Rochefort, L., & Tuitilla, E.-S. (2006). Response of vegetation and net ecosystem carbon dioxide exchange at different peatland microforms following water table drawdown. *Journal of Geophysical Research*, 111, G02006. https://doi.org/10.1029/2005JG000145.

Thompson, D. K., Simpson, B. N., Whitman, E., Barber, Q. E., & Parisien, M.-A. (2019). Peatland hydrological dynamics as a driver of landscape connectivity and fire activity in the boreal plain of Canada. *Forests*, 10(7), 534. https://doi.org/10.3390/f10070534.

Thompson, D. K., & Waddington, J. M. (2013). Peat properties and water retention in boreal forested peatlands subject to wildfire. *Water Resources Research,* 49(6), 3651-3658. https://doi.org/10.1002/wrcr.20278.

Turetsky, M., Wieder, K., Halsey, L., & Vitt, D. (2002). Current disturbance and the diminishing peatland carbon sink. *Geophysical Research Letters,* 29(11). https://doi.org/10.1029/2001GL014000.

Turetsky, M. R., Benscoter, B., Page, S., Rein, G., van der Werf, G. R., & Watts, A. (2015). Global vulnerability of peatlands to fire and carbon loss. *Nature Geoscience,* 8(1), 11-14. https://doi.org/10.1038/ngeo2325.

Van Beest, C., Petrone, R., Nwaishi, F., Waddington, J. M., & Macrae, M. (2019). Increased Peatland Nutrient Availability Following the Fort McMurray Horse River Wildfire. *Diversity*, 11(9), 1-17. https://doi.org/10.3390/d11090142.

Waddington, J .M., Morris, P. J., Kettridge, N., Granath, G., Thompson, D. K., & Moore, P. A. (2015). Hydrological feedbacks in northern peatlands. *Ecohydrology*, 8, 113-127. https://doi.org/10.1002/eco.1493.

Waddington, J. M., Strack, M., & Greenwood, M. J. (2010). Toward restoring the net carbon sink function of degraded peatlands: Short-term response in CO_2 exchange to ecosystem-scale restoration. *Journal of Geophysical Research,* 115, G01008. https://doi.org/10.1029/2009jg001090.

Waddington, J. M., & Warner, K. D. (2001). Atmospheric CO_2 sequestration in restored mined peatlands. *Ecoscience,* 8(3), 359-368. https://doi.org/10.1080/11956860.2001.11682664.

Webb, E. K., Pearman, G. I., & Leuning, R. (1980). Correction of flux measurements for density effects due to heat and water vapour transfer. *Quarterly Journal of the Royal Meteorological Society*, *106*(447), 85-100.

Wieder, R. K., Scott, K. D., Kamminga, K., Vile, M. A., Vitt, D. H., Bone, T., Xu, B., Benscoter, B. W., & Bhatti, J. S. (2009). Postfire carbon balance in boreal bogs of Alberta, Canada. *Global Change Biology,* 25(1), 63-81. https://doi.org/10.1111/j.1365-2486.2008.01756.x.

Wilkinson, S. L., Tekatch, A. M., Markle, C. E., Moore, P. A., & Waddington, J. M. (2020). Shallow peat is most vulnerable to high peat burn severity during wildfire. *Environmental Research Letters,* 15(10), 104032. https://doi.org/10.1088/1748-9326/aba7e8.

Wilson, D., Alm, J., Riutta, T., Laine, J., Byrne, K. A., Farrell, E. P., & Tuittila, E-S. (2007). A high resolution green area index for modelling the seasonal dynamics of CO_2 exchange in peatland vascular plant communities. *Plant Ecology*. 190(1), 37-51. https://doi.org/10.1007/s11258-006-9189-1.

Wutzler, T., Lucas-Moffat, A., Migliavacca, M., Knauer, J., Sickel, K., Šigut, L., Menzer, O., & Reichstein, M. (2018). Basic and extensible post-processing of eddy covariance flux data with REddyProc. *Biogeosciences,* 15, 5015-5030. https://doi.org/10.5194/bg-2018-56.

Wu, J., & Roulet, N. T. (2014). Climate change reduces the capacity of northern peatlands to absorb the atmospheric carbon dioxide: The different responses of bogs and fens. *Global Biogeochemical Cycles,* 27, 1005-1024. https://doi.org/10.1111/1462-2920.13280.

Xu, J., Morris, P. J., Liu, J., & Holden, J. (2018). PEATMAP: Refining estimates of global peatland distribution based on a meta-analysis. *Catena*, 160, 134-140. https://doi.org/10.1016/j.catena.2017.09.010.

Chapter 4 - General Conclusions

Peatlands are present at varying spatial scales in the EGB rock barrens region of the eastern boreal shield ecozone and are important carbon sinks in northern landscapes. In the rock barrens of EGB, peat depths are thinner and peatlands may be smaller than other areas of the boreal biome. However, ecohydrological processes regulating peatland carbon uptake have shown to be similar. Peatlands on this landscape rely on fill and spill hydrological connectivity dynamics, in turn regulating water table dynamics through overland flow following rain events (Spence and Woo, 2003). As such, the peatlands are highly responsive to changes in water availability, or wet and dry periods, and may also be shallow enough to lose their water table out of the peat profile during drought, reducing moss productivity (Moore et al., 2021) and leaving the ecosystem vulnerable to wildfire (Wilkinson et al., 2020). Climate change and drought may leave these peatlands unprotected from the loss of the significant C stocks in peat due to changes in water availability across this landscape. An understanding of interannual variability of CO_2 exchange in boreal shield peatlands is fundamental research to evaluate the role of regional climate patterns on C uptake capacity of peatland ecosystems and has shown how these ecosystems resume ecohydrological processes following wildfire disturbance.

In chapter 2, we present the first long-term CO_2 dataset for a peatland in the boreal shield and EGB rock barrens region. We use 5-years of data for the growing season, from May to October inclusive, to elucidate the main climatic drivers of variability in summer CO_2 exchange budgets. Using multiple linear regression modelling, we found total summer NEE and GPP to be strongly controlled by summer mean water table depth. The relationship between CO_2 exchange and water table depth is important on this landscape as the peatlands are positioned in shallow bedrock basins,

largely separated from regional groundwater, and rely on precipitation and overland flow for maintaining water availability to vegetation and wildlife that inhabit these wetlands, including reptilian species at risk (Markle et al., 2020). We found summer total ER to be strongly influenced by the preceding winter and spring (January to April, inclusive) air temperature, indicating snowmelt in the spring increases water availability flowing between landscape units, stimulating vegetation productivity, autotrophic respiration, and warmer summer air temperatures. This connection between CO_2 exchange processes and the water availability may leave peatlands in the boreal shield region vulnerable to losing the CO_2 uptake capacity with climate change induced changes in precipitation frequency, greater increases in air temperature, and water loss through greater evapotranspiration (D'Orgeville et al., 2014; Helbig et al., 2021; Mortsch and Quinn, 1996; Notaro et al., 2015). Long-term changes to water availability may also promote changes to the vegetation community of the peatland, including a shift in *Sphagnum* spp. distribution and an increased proportion of vascular spp. (Breeuwer et al., 2009; Fenner et al., 2007). We suggest that further research on the full carbon balance of a boreal shield peatland would be important to characterize the sensitivity of different components of the C budget to meteorological interannual variability in Eastern Georgian Bay.

In chapter 3, we monitored CO_2 exchange in a wildfire-disturbed area 1- and 2- years post-fire at the ecosystem- and plot-scale. We found the burned site to be a net CO_2 sink for the growing season, at both the ecosystem- and plot-scale. A snapshot of more than one continuous year of measurements, from July 2019 to October 2020, showed the burned site to also act as a net CO_2 sink from 1 to 2 years post-fire. Using what we learned from chapter 2, we could evaluate if interannual meteorological patterns affect the burned landscape similarly to the unburned site. We

found greater CO_2 uptake in the summer deemed a "wet summer" (2020), and greater photosynthetic efficiency in the wet summer year at both the unburned and burned site. This analysis indicates the processes necessary for C uptake and subsequent storage of C in the peatland may commence in a recently burned peatland given adequate water availability and rapid vegetation recovery (Gray et al., 2020; Morison et al., 2021; Waddington et al., 2015). There was evidence of effective vegetation recovery of both vascular and moss spp. throughout the burned peatland, and may have been due to the presence of fire refugia and sufficient water availability on the landscape post-fire (Hylander and Johnson, 2010; Meddens et al., 2018). The vegetation functional groups varied by peat depth and burn severity, contributing to different rates of CO_2 exchange between the shallow and deep zones of the burned peatland. We would expect peatlands on this landscape to recover the amount of carbon lost by the wildfire within approximately 30 years, given the rates of net CO_2 uptake by the peatlands within the first 2 years post-wildfire. The connections to interannual climate variability and wildfire recovery have implications for a warming world, where we would expect greater temperatures and rainfall (D'Orgeville et al., 2014; Mortsch and Quinn, 1996; Notaro et al, 2015) and pronounced evapotranspiration (Helbig et al., 2021), leading to decreased water availability. Drier peatlands are more vulnerable to combustion, and eventually may release more C to the atmosphere if vegetation recolonization and photosynthesis cannot commence to recover the C lost from the wildfire.

In summary, this research expands the existing literature surrounding environmental controls on interannual variability in peatland CO_2 exchange dynamics with a dataset from a new geographic range, as well as following disturbance. We found summer water table depth to be a limiting factor in total summer CO_2 uptake, indicating if the water table is lower in the peat profile there is a disconnect between vegetation and water supply, thus limiting photosynthesis. This was

expanded further by considering this relationship in a recently burned peatland, and found the influence of water table and water availability still holds. The rapid recolonization of vegetation into the burned peatland advanced the CO_2 uptake capacity of the ecosystem within the first two years post-wildfire. Our findings show water availability is a key element for peatlands on EGB rock barrens to sustain carbon uptake and storage, and vegetation recovery is an essential process for returning the burned peatland into a CO_2 sink. For future research, an analysis of the full C budget of a Canadian shield peatland and in a post-wildfire setting would be useful for expanding this interannual climate variability analysis to other components of the C budget. Furthermore, the expansion of plot-scale flux measurements to the whole growing season would be useful to elucidate connections between environmental conditions, phenology, and C cycling in shield peatlands.

4.1 Literature cited

Breeuwer, A., Robroek, B. J. M., Limpens, J., Heijmans, M. M. P. D., Schouten, M. G. C., & Berendse, F. (2009). Decreased summer water table depth affects peatland vegetation. *Basic and Applied Ecology*, 10(4), 330-339. https://doi.org/10.1016/j.baae.2008.05.005.

d'Orgeville, M., Peltier, W. R., Erler, A., & Gula, J. (2014). Climate change impacts on Great Lakes Basin precipitation extremes. *JGR: Atmospheres*, 119, 10799-10812. https://doi.org/10.1002/2014JD021855.

Fenner, N., Ostle, N. J., McNamara, N., Sparks, T., Harmens, H., Reynolds, B., & Freeman, C. (2007). Elevated CO_2 Effects on Peatland Plant Community Carbon Dynamics and DOC Production. *Ecosystems*, 10(4), 635-657. https://doi.org/10.1007/s10021-007-9051-x.

Gray, A., Davies, G. M., Domènech, R., Taylor, E., & Levy, P. E. (2021). Peatland Wildfire Severity & Post-fire Gaseous Carbon Fluxes. *Ecosystems,* 24, 713-725. https://doi.org/10.1007/s10021-020-00545-0.

Helbig, M., Waddington, J. M., Alekseychik, P., Amiro, B. D., Aurela, M., Barr, A. G., Black, T. A., Blanken, P. D., Carey, S. K., Chen, J., Chi, J., Desai, A. R., Dunn, A., Euskirchen E. S., Flannigan, L. B., Forbrich, I., Friborg, T., Grelle, A., Harder, S., … Zyrianov, V. (2020). Increasing contribution of peatlands to boreal evapotranspiration in a warming climate. *Nature Climate Change,* 10(6), 555-560. https://doi.org/10.1038/s41558-020-0763-7.

Hylander, K., & Johnson, S. (2010). In situ survival of forest bryophytes in small-scale refugia after an intense forest fire. *Journal of Vegetation Science,* 21, 1099-1109. https://doi.org/10.1111/j.1654-1103.2010.01220.x.

Markle, C. E., North, T. D., Harris, L. I., Moore, P. A., & Waddington, J. M. (2020). Spatial Heterogeneity of Surface Topography in Peatlands: Assessing Overwintering Habitat Availability for the Eastern Massasauga Rattlesnake. *Wetlands*, 40, 2337-2349. https://doi.org/10.1007/s13157-020-01378-2.

Meddens, A. J. H., Kolden, C. A., Lutz, J. A., Smith, A. M. S., Cansler, C. A., Abatzoglou, J. T., Meigs, G. W., Downing, W. M., & Krawchuk, M. A. (2018). Fire Refugia: What Are They and Why Do They Matter for Global Change?. *Bioscience*, 68(12), 944-954. https://doi.org/10.1093/biosci/biy103.

Moore, P. A., Didemus, B. D., Furukawa, A. K., & Waddington, J. M. (2021). Peat depth as a control on Sphagnum moisture stress during seasonal drought. *Hydrological Processes*, 35, e14117. https://doi.org/10.1002/hyp.14117.

Morison, M., van Beest, C., Macrae, M., Nwaishi, F., & Petrone, R. (2021). Deeper burning in a boreal fen peatland 1-year post-wildfire accelerates recovery trajectory of carbon dioxide uptake. *Ecohydrology,* 14(3), e2277. https://doi.org/10.1002/eco.2277.

Mortsch, L. D., & Quinn, F. H. (1996). Climate change scenarios for Great Lakes Basin ecosystem studies. *Limnology and Oceanography,* 41(5), 903-911. https://doi.org/10.4319/lo.1996.41.5.0903.

Notaro, M., Bennington, V., & Vavrus, S. (2015). Dynamically Downscaled Projections of Lake-Effect Snow in the Great Lakes Basin. *Journal of Climate,* 28(4). 1661-1684. https://doi.org/10.1175/JCLI-D-14-00467.1.

Spence, C., & Woo, M. (2003). Hydrology of subarctic Canadian shield: soil-filled valleys. *Journal of Hydrology*, 279, 151-166. https://doi.org/10.1016/S0022-1694(03)00175-6.

Waddington, J .M., Morris, P. J., Kettridge, N., Granath, G., Thompson, D. K., & Moore, P. A. (2015). Hydrological feedbacks in northern peatlands. *Ecohydrology*, 8, 113-127. https://doi.org/10.1002/eco.1493.

Wilkinson, S. L., Tekatch, A. M., Markle, C. E., Moore, P. A., & Waddington, J. M. (2020). Shallow peat is most vulnerable to high peat burn severity during wildfire. *Environmental Research Letters,* 15(10), 104032. https://doi.org/10.1088/1748-9326/aba7e8.

4.2 Appendix

Photo of peatland study site used in Chapter 2 and "unburned" site in Chapter 3, taken August 2020.

Photo of peatland study site used in Chapter 2 and "unburned" site in Chapter 3, taken August 2020.

Photo of "burned" peatland study site from Chapter 3, with the shallow peatland margin on the right side of the photo. Photo taken August 2020.

Photo overlooking "burned" peatland study site in Chapter 3 study, photo taken August 2020.